Study on Linking a SuperCritical Water-Cooled Nuclear Reactor to a Hydrogen Production Facility

By

Andrew John Lukomski

A Thesis Submitted in Partial Fulfillment

of the Requirements for the Degree of

Master of Applied Science

Nuclear Engineering

The Faculty of Energy Systems and Nuclear Science

University of Ontario Institute of Technology

July 2011

ABSTRACT

The SuperCritical Water-cooled nuclear Reactor (SCWR) is one of six Generation-IV nuclear-reactor concepts currently being designed. It will operate at pressures of 25 MPa and temperatures up to 625°C. These operating conditions make a SuperCritical Water (SCW) Nuclear Power Plant (NPP) suitable to support thermochemical-based hydrogen production via co-generation. The Copper-Chlorine (Cu–Cl) cycle is a prospective thermochemical cycle with a maximum temperature requirement of ~530°C and could be linked to an SCW NPP through a piping network. An intermediate Heat eXchanger (HX) is considered as a medium for heat transfer with operating fluids selected to be SCW and SuperHeated Steam (SHS). Thermalhydraulic calculations based on an iterative energy balance procedure are performed for counter-flow double-pipe design concept HXs integrated at several locations on an SCW NPP coolant loop. Using various test cases, design and operating parameters are recommended for detailed future research. In addition, predicted effects of heat transfer enhancement on HX parameters are evaluated considering theoretical improvements from helically-corrugated HX piping. The effects of operating fluid pressure drop are briefly discussed for applicability in future studies.

Keywords: Hydrogen Production, Thermochemical Cycles, Copper-Chlorine Cycle, Generation IV Reactor, SuperCritical Water-cooled nuclear Reactor, Heat Exchanger

ACKNOWLEDGEMENTS

Many individuals enabled me to carry out this research and complete my academic studies. I would like to thank my whole family, especially my parents, Janina and Mieczyslaw, who were a source of continuous support and advice. Their faith provided encouragement to move forward, especially during periods of struggle. I would like to extend thanks to friends who supported me throughout this work and to fellow students and researchers who helped overcome challenges during these studies, your support was always appreciated: Lisa Grande, Wargha Peiman, Dr. Zhaolin Wang, Dr. Venkata Daggupati, Harwinder Thind, Sarah Mokry and Eugene Saltanov. Thank you to past professors, teachers and others who have shared their knowledge and experiences over the years. To all of the support staff at UOIT who assisted with this thesis, I am appreciative of your efforts and the time you dedicated to support its completion. Finally, to my supervisors, Dr. Kamiel Gabriel and Dr. Igor Pioro, I sincerely thank you for the guidance you provided throughout my studies. Your support extended beyond the academic and contributed to my personal development.

Generous financial support from NSERC/NRCan/AECL Generation IV Energy Technologies Program, ORF and NSERC Discovery Grants are gratefully acknowledged in support of this work.

SUMMARY

Various alternatives for hydrogen production are being considered to reduce the demand on fossil fuel-based production methods. Thermochemical cycles are one alternative which generate hydrogen through the decomposition of water using reactions of intermediate materials and the input of thermal energy. The Copper-Chlorine (Cu–Cl) cycle requires temperatures of approximately 530°C to enable hydrogen production. There are several variations of this cycle, however, discussion is limited to the 5 and 4-step cycles. The 4-step cycle was primarily considered in this investigation based on ongoing research at the hydrogen research facility at the University of Ontario Institute of Technology (UOIT). By providing a source of non-fossil fuel-based thermal energy to the Cu–Cl cycle, a more environmentally sustainable method of hydrogen production can be achieved.

One of the energy sources considered for the Cu–Cl cycle is the SuperCritical Water-cooled nuclear Reactor (SCWR). The SCWR is a Generation IV nuclear reactor concept that would operate with SuperCritical light Water (SCW) coolant at pressures of 25 MPa and reactor outlet temperatures up to 625°C. There are several Nuclear Power Plant (NPP) cycles which an SCWR could be designed to, two of which are discussed in this investigation: the no-reheat and single reheat cycles. In theory, the SCWR could provide the thermal energy requirements for the Cu–Cl cycle via a Heat eXchanger (HX) linking the two facilities. An intermediate loop of SuperHeated Steam (SHS) would be heated in the HX and deliver the thermal energy to the Cu–Cl reactors.

The objective of this research is to provide a review of recent development in the Cu–Cl cycle and SCW NPP concepts, identify preliminary design and operating parameters for an interfacing HX and perform thermalhydraulic calculations to determine suitable designs for future development. A counter-flow double-pipe HX design is selected as the choice HX due to the feasibility of performing iterative calculations across individual HX pipes. An HX integrated downstream of the SCWR (termed “HX A”) in the no-reheat cycle layout would have SCW flow in the inner pipe and SHS in the annulus gap. In the

single reheat cycle, one HX could be located identically as in the no-reheat layout or in a different location, downstream of the SCWR reheat channels (termed "HX B"). This second HX would operate with SHS flowing in both the inner pipe (High Pressure fluid – HP) and annulus gap (Low Pressure fluid – LP).

A multi-purpose MATLAB script was developed to perform thermalhydraulic calculations based on iterative energy balances for the HXs at locations on the two NPP cycles. The code allows thermal approximations to be tested based on the Log Mean Temperature Difference (LMTD) method. In addition, frictional pressure losses for both flows can be calculated across the HX pipe lengths. User input parameters include SHS (for HX A)/LP SHS (for HX B) operating pressure and pipe mass flow rates, SCW (for HX A)/HP SHS (for HX B) pipe mass fluxes, and inner and outer piping dimensions.

Three piping materials (Inconel–600, Inconel–718 and Stainless Steel 304) were evaluated for mechanical properties including burst pressure and thermal conductivity to assess the feasibility of their use in the topic HXs. A lower bounding analysis was selected using SS–304 as the piping material. A number of combinations were developed based on the user inputs and then evaluated for heat transfer characteristics, thermophysical properties and other parameters such as flow velocity. For HX A, 26 suitable combinations were identified for further development. For HX B, 5 suitable combinations were determined with operating parameters documented. Profiles of thermophysical properties, fluid temperature and pressure drop were prepared for a select number of combinations. The effects of theoretical heat transfer enhancement were evaluated and concluded that significant reductions in HX heat transfer area may be realized with 75% increase in local Heat Transfer Coefficients (HTC). Results obtained from the MATLAB code were verified through a reproduction of the code in Microsoft Excel with a comparison between sample results.

The study concludes that an HX at either of the locations investigated may supply the thermal energy requirements of the Cu–Cl cycle. Furthermore, in terms of HX A, none of the proposed operating conditions permitted the SCW temperature to exit the HX

below the *pseudocritical* temperature at 25 MPa. This will require a suitable SCW re-entry point to the NPP coolant loop to be established. More detailed pressure loss calculations will be required in future work which will further refine suitable operating and design parameter combinations.

TABLE OF CONTENTS

LIST OF FIGURES

LIST OF TABLES

NOMENCLATURE

A: Area, m^2

c_p: Specific Heat, J/kg K

$\bar{c_p}$, $c_{p,avg}$: Average Specific Heat, J/kg K; $\left(\frac{H_w - H_b}{T_w - T_b}\right)$

D, d: Diameter, m

f: Friction factor

G: Mass Flux, kg/m^2s; $\frac{\dot{m}}{A}$

H: Specific Enthalpy, J/kg

h: Heat Transfer Coefficient, W/m^2K

k: Thermal Conductivity, W/m K

L: Length, m

$\dot{m}$: Mass Flow Rate, kg/s

N: Number of Pipes in an HX

P: Pressure, Pa

p: Perimeter, m

Q: Thermal Energy, J

$\dot{Q}$: Heat Transfer Rate, W

q'': Heat Flux, W/m^2; $\frac{\dot{Q}}{A}$

R: Thermal Resistance, K m^2/W

S: Tensile Strength, MPa

T: Temperature, °C, K

U: Overall Heat Transfer Coefficient, W/m^2K

u: Velocity, m/s; $\frac{\dot{m}}{\rho A}$

V: Electrical Energy, J

x: Axial Position, m

Greek symbols

Δ: Difference

ρ: Density, kg/m^3

μ: Viscosity, Pa·s

δ: Wall Thickness, m

Dimensionless Numbers

Nu: Nusselt Number $\left(\frac{hd_i}{k}\right)$ Inner Pipe; $\left(\frac{hD_{hy}}{k}\right)$ Annulus Gap

Pr: Prandtl Number $\left(\frac{\mu c_p}{k}\right)$

$\overline{\mathbf{Pr}}$: Average Prandtl Number $\left(\frac{\mu \overline{c_p}}{k}\right)$

Re: Reynolds Number $\left(\frac{G_{SCW} d_i}{\mu_i}\right)$ Inner Pipe; $\left(\frac{G_{SHS} D_{hy}}{\mu_o}\right)$ Annulus Gap

Subscripts

avg: average

b: bulk

c: cross section

cr: critical

el: electrical

hy: hydraulic

i: inner

inc: increment

lm: log mean

o: outer

pc: pseudocritical

s:	surface
sat:	saturation
x:	increment position
w:	wall
wet:	wetted

Acronyms

ACR	Advanced CANDU Reactor
AECL	Atomic Energy of Canada Limited
ANL	Argonne National Laboratory
BWR	Boiling Water Reactor
CANDU	CANada Deuterium Uranium
Cu–Cl	Copper Chlorine
cv	Control Volume
FHR	Fluoride-cooled High temperature Reactor
GE	General Electric
GFR	Gas-cooled Fast Reactor
GIF	Generation IV International Forum
HP	High Pressure
HTC	Heat Transfer Coefficient
HTE	High-Temperature Electrolysis
HX	Heat eXchanger
IP	Intermediate Pressure
JAERI	Japan Atomic Energy Research Institute
LFR	Lead-cooled Fast Reactor
LMTD	Log Mean Temperature Difference

LP	Low Pressure
MATLAB	MATrix LABoratory
MSR	Molten Salt Reactor
MSFR	Molten Salt Fast Reactor
MOX	Mixed OXide
NHI	Nuclear Hydrogen Initiative
NIST	National Institute of Standards and Technology
NPP	Nuclear Power Plant
PHWR	Pressurized Heavy Water Reactor
PT	Pressure Tube
PV	Pressure Vessel
PWR	Pressurized Water Reactor
REFPROP	REference Fluid thermodynamic and transport PROPerties
RMS	Root Mean Square
SCW	SuperCritical Water
SCWR	SuperCritical Water Reactor
SFR	Sodium-cooled Fast Reactor
SHS	SuperHeated Steam
SI	Sulphur Iodine
SMR	Steam Methane Reforming
STP	Standard Temperature - Pressure
UO	University of Ottawa
UOIT	University of Ontario Institute of Technology
VHTR	Very High-Temperature Reactor

GLOSSARY

Definitions of select terms related to *supercritical* and *near-critical* fluids and are provided to support discussion on SuperCritical Water-cooled nuclear Reactors (Pioro and Duffey, 2007). Figure i1 may also assist to provide a better understanding of the terms that have been defined.

Compressed fluid is a fluid at a pressure above the *critical* pressure but at a temperature below the *critical* temperature.

Critical point (also called a *critical state*) is the point where the distinction between the liquid and gas (or vapour) phases disappears, i.e. both phases have the same temperature, pressure and volume. The *critical point* is characterized by the phase state parameters T_{cr}, P_{cr} and V_{cr}, which have unique values for each pure substance.

Deteriorated heat transfer is characterized with lower values of the wall heat transfer coefficient compared to those at the normal heat transfer; and hence has higher values of wall temperature within some part of a test section or within the entire test section.

Improved heat transfer is characterized with higher values of the wall heat transfer coefficient compared to those at the normal heat transfer; and hence lower values of wall temperature within some part of a test section or within the entire test section.

Near-critical point is a narrow region around the *critical point* where all the thermophysical properties of a pure fluid exhibit rapid variations.

Normal heat transfer can be characterized in general with wall heat transfer coefficients similar to those of subcritical convective heat transfer far from the *critical* or *pseudocritical* regions, when calculated according to the conventional single-phase Dittus-Boelter type correlations.

Pseudocritical point (characterized with p_{pc} and t_{pc}) is a point at a pressure above the *critical* pressure and at a temperature ($t_{pc} > t_{cr}$) corresponding to the maximum value of the specific heat for this particular pressure.

Pseudocritical line is a line consisting of *pseudocritical* points.

Pseudocritical region is the region of temperatures, typically listed as ±25°C from the *pseudocritical* temperature for a given pressure where thermophysical properties of a pure fluid exhibit rapid changes - this analogous to the *near-critical point*.

Supercritical fluid is a fluid at pressures and temperature that are higher than the *critical* pressure and *critical* temperature.

Supercritical steam is actually *supercritical* water because at *supercritical* pressures there is no difference between phases. However, this term is widely and incorrectly used in the literature in relation to *supercritical* steam generators and turbines.

Superheated steam is steam at a pressure below the *critical* pressure but at temperatures above the *critical* temperature.

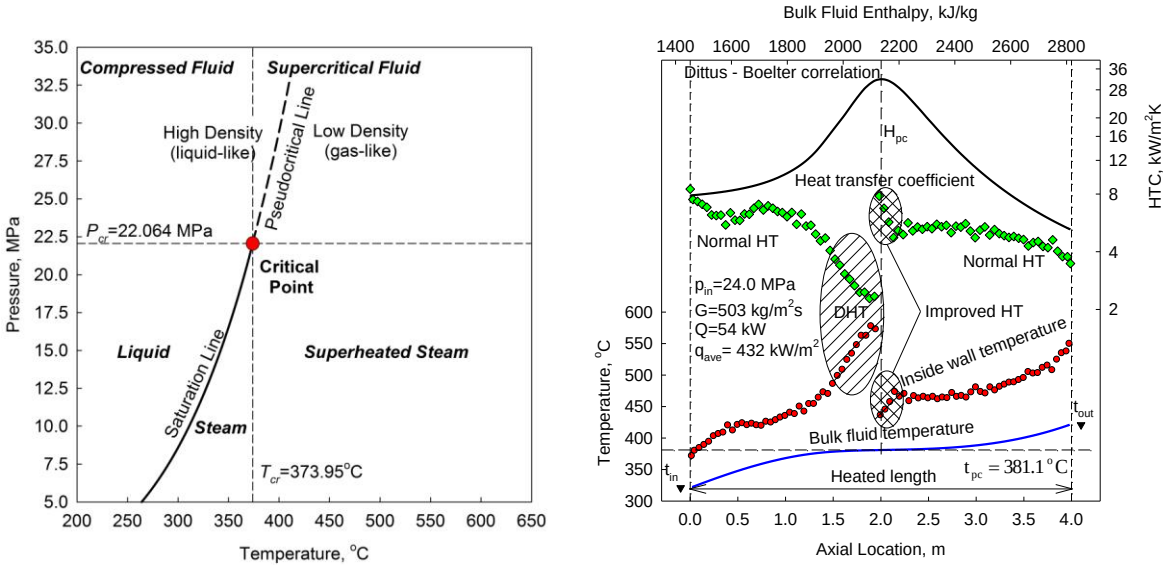

(a) (b)

Figure i1. (a) Pressure-Temperature Diagram for Water; (b) Temperature and Heat Transfer Coefficient Profiles Along the Heated Length of a Vertical Circular Tube: Water, *D*=10 mm and *L*=4 m. (Pioro et al., 2011).

INTRODUCTION

Hydrogen, as an energy carrier, could develop to have a significant role in the future energy supply of industrialized nations. Although carbon based fuel sources such as oil and gas will continue to dominate the energy landscape in the near future it is unlikely that they will be capable of fulfilling the entire energy requirements of the global economy as more nations industrialize while sources continue to be depleted. For other traditional energy sources such as coal, more stringent environmental restrictions on carbon emissions may lead to reduced consumption levels. Such projections warrant a need for an alternative energy source to offset a fraction of the energy consumed via oil, gas and coal sources.

Hydrogen, produced through non-carbon based methods may increase penetration with time into the automotive, food and agricultural industry as a shift in energy sources is realized. Thermochemical hydrogen production is one of several methods being researched that could provide a large supply of hydrogen through centralized generation facilities. Using water and external thermal energy (for hybrid cycles - thermal *and* electrical energy) as inputs, a thermochemical cycle decomposes water into hydrogen and oxygen while continuously recycling a number of intermediate compounds. Various thermal energy sources may be integrated with thermochemical cycles to supply reaction heat, including nuclear and solar power plant facilities.

The intent of this research was to conduct an evaluation of the feasibility for linking a Generation IV nuclear reactor, the SuperCritical Water-cooled nuclear Reactor (SCWR) concept, and a hydrogen production facility operating on the Copper Chlorine (Cu–Cl) thermochemical cycle through a Heat eXchanger (HX) transferring thermal energy between the facilities. The research scope involved performing a literature survey of recent developments in Cu–Cl cycle research, Generation IV nuclear reactor designs, specifically the SCWR, and applicable heat transfer correlations to be considered followed by analysis to determine suitable design and operating conditions for an HX linking the two facilities. The original work involved thermalhydraulic calculations

based on an iterative energy balance procedure for HXs with various design parameters and operating conditions. Certain inputs were based on existing design information for the SCWR concept and known operating conditions of the 4-step Cu–Cl cycle. In addition, operating experience from the Russian steam generator industry was incorporated to define acceptable HX piping dimensions. Theoretical enhancement of local Heat Transfer Coefficients (HTC) was considered through the use of helically corrugated pipes to reduce the physical size of the HX.

Chapter 1 provides a background and discussion on several hydrogen production methods that are used today such as Steam Methane Reforming (SMR) and gasification technology. Emerging processes such as High-Temperature Electrolysis (HTE) and thermochemical cycles are also described with specific focus on the Cu–Cl cycle. The reaction steps within the cycle are briefly discussed and the external thermal energy requirements are outlined. Chapter 2 provides insight into the six Generation IV reactor concepts currently under development. Chapter 3 discusses SuperCritical Water (SCW) and relevant heat transfer correlations considered in this analysis. Chapter 4 describes the Nuclear Power Plant (NPP) cycle layouts considered suitable for linking the facilities: i) no-reheat cycle; and ii) single reheat cycle. It also contains discussion on HX design options and use of the Log Mean Temperature Difference (LMTD) method for select HX analysis. The methodology employed to conduct thermalhydraulic calculations is outlined in Chapter 5. Chapter 6 is dedicated to results and the discussion of research findings. Conclusions are presented in Chapter 7 and recommendations for future work are listed in Chapter 8. Appendix A contains a summary of all results obtained from the thermalhydraulic analyses. Tables documenting the verification of results are contained in Appendix B. A summary of the calculations involved in this work are contained in Appendix C. The MATLAB script, used as the primary calculation tool is documented in Appendix D. Finally, publications by the author and a list of presentations at conferences are presented in Appendices E and F, respectively.

CHAPTER 1 – HYDROGEN PRODUCTION

Hydrogen is the most abundant element in the universe. However, it is not readily available in its molecular form and must be extracted from water or hydrocarbons for commercial and industrial applications. Currently, the most popular and least expensive method of hydrogen production is through steam reforming of fossil fuels (i.e. Steam Methane Reforming (SMR)) accounting for approximately 50% of world hydrogen production (Press et al., 2009). Jones and Thomas (2008) quote the fraction as high as 90% of the world's supply. If hydrogen is to become a sustainable energy carrier source in the future global economy, reliance on fossil fuels for its production must be significantly reduced.

Gasification and SMR are the most common fossil fuel-based hydrogen production methods. Gasification involves the net-exothermic reaction of carbon-based materials such as coal, methane or other petrochemical by-products with steam and oxygen under reducing conditions. Required reaction chamber operating temperatures and pressures of gasifiers are on the order of 1,250 to 1,575°C and 2 MPa (Jones and Thomas, 2008). The resulting products, a mix of carbon monoxide and hydrogen gases, generically known as synthetic (syn) gas, are separated for various applications. The H_2/CO ratio of the product varies depending on the gasifier type, the oxygen concentration, reactant feed rate, and the carbon feedstock composition; for example, natural gas typically has a H_2/CO ratio of 1.75 whereas coal has a ratio of 0.80 (Jones and Thomas, 2008). The CO gas component of syngas can be further reacted with steam at high temperatures under the water gas shift reaction to generate more hydrogen gas and carbon dioxide.

In SMR, fossil fuels such as methane gas are reacted with steam over a nickel-based catalyst at high temperatures producing syngas. The reaction involving methane is endothermic requiring 252 kJ per mole of methane at standard temperature-pressure (STP) conditions. Addition of oxygen into this reaction creates an autothermal reformer, where the exothermic methane/oxygen reaction, known as a partial oxidation reaction, assists in providing heat for the primary reaction (Rand and Dell, 2008).

Nuclear-based hydrogen production may be achieved through water electrolysis or steam electrolysis, which requires a combination of high temperatures and electrical energy input. The latter process involves directing steam from an NPP to a solid-oxide electrolyte. Efficiencies for HTE can reach up to 50 – 60%, as documented by Jones and Thomas (2008), due to the lower electrical overpotentials required, improved gas diffusivity and the thermal energy by-product (Ryland et al., 2006). Ryland et al. (2006) investigated the linkage of the Advanced CANDU (CANada Deuterium Uranium) Reactor (ACR-1000) design concept developed by Atomic Energy of Canada Limited (AECL) to an HTE facility, which predicted efficiencies of approximately 35%.

The Sulphur Iodine (SI) thermochemical cycle is a 3-Step reaction process, which has been widely investigated in several countries under laboratory-scale test loops. A research facility operated by the Japan Atomic Energy Research Institute (JAERI) has produced a hydrogen output up to 30 L/h (Jones and Thomas, 2008). The process involves the decomposition of sulfuric acid at temperatures above 800°C, processing of intermediate liquid and gas materials and further decomposition of hydrogen iodide to produce hydrogen. Efficiencies as high as 50% have been predicted for this cycle (Jones and Thomas, 2008). Due to the extreme reaction temperatures of the SI cycle, only certain technologies can meet this requirement, including the modular helium reactor which is characterized by reactor outlet temperatures up to 850°C (Richards et al., 2006).

Hydrogen production via thermochemical cycles has become a leading alternative to fossil-based production methods. Thermochemical cycles are desirable over traditional electrolysis methods given the higher production efficiency. Over 200 thermochemical cycles have been identified in literature, however, the vast majority have not progressed beyond theoretical calculations due to various limitations including high temperature requirements and/or low efficiencies (Naterer et al., 2008). Efforts by Argonne National Laboratory (ANL) in the US and by researchers in other universities in Europe, Japan, South Africa and the US are undergoing through the Nuclear Hydrogen Initiative (NHI) to evaluate thermochemical cycles identifying those most suitable for development. The

following factors have been considered: chemical viability (no significant competing reactions/high yields), engineering feasibility (simulated operation) and efficiency. The cycles under evaluation were: cerium-chlorine (Ce–Cl), copper chlorine (Cu–Cl), iron-chlorine (Fe–Cl), vanadium-chlorine (V–Cl), copper sulphate (Cu–SO_4), magnesium-iodine (Mg–I), hybrid chlorine and a metal alloy cycle potassium-bismuth (K–Bi) (Lewis and Masin, 2009). The majority of these cycles are characterized by low efficiencies, undesirable by-products, poor chemical kinetics or high-temperature requirements. From eight contending cycles, the Cu–Cl cycle was selected as the most promising cycle warranting continued research and development (Lewis and Masin, 2009). Research into thermochemical cycles such as the Cu–Cl cycle will advance the objective of the NHI to develop a cost effective nuclear based hydrogen production facility by 2019 (Lewis and Masin, 2009).

Teams at several institutions including the University of Ontario Institute of Technology (UOIT), AECL and ANL are currently advancing the research efforts on the 4-Step hybrid Cu–Cl cycle. Research involves scaling up and integrating a proof of principle experimental set-up to engineering scale assemblies capable of producing up to 3 kg of hydrogen per day (Wang et al., 2009).

1.1 COPPER-CHLORINE CYCLE

The Cu–Cl cycle has been selected as the most suitable thermochemical cycle to be interlinked with an SCWR (Naidin et al., 2009c). Several favourable characteristics of the Cu–Cl cycle make it an attractive process for hydrogen production. These include a relatively low maximum temperature requirement (~530°C), favourable reaction kinetics for the oxygen and hydrogen-production steps and the availability to utilize waste heat to supply endothermic processes (Naterer et al., 2009). Various forms of the Cu–Cl cycle exist, including a 2-Step process proposed by Dokiya and Kotera (1976), 3-Step, 4-Step and 5-Step processes documented by Naterer et al. (2008) and Wang et al. (2009).

The 5-Step Cu–Cl cycle is comprised of an exothermic hydrogen production step, three endothermic processes and an electrolysis step as shown Figure 1. The 4-Step variation combines the hydrogen production and electrolysis steps of the 5-Step process into a single electrochemical reaction which is shown in Figure 2. This step is analogous to that proposed by Dokiya and Kotera (1976). The associated reactions for both cycles are shown in Table 1 and described below in more detail.

In Step 1 of the 5-Step cycle, solid copper particles react with high-temperature hydrogen chloride gas resulting in the production of hydrogen gas and liquid cuprous chloride. Although the reaction is exothermic, reactants must initially be heated to the threshold temperature of approximately 475°C. Step 1 provides one of the advantages of the 5-Step cycle which is the by-product of high-temperature thermal energy as up to 139.8 MJ can be recycled for every kilogram of hydrogen produced stemming from cooling of products and recovery of reaction heat. A major disadvantage of the 5-Step cycle is the production and handling of solid copper compounds, which requires an additional drying process thus increasing heat demand and complexity of the cycle.

The second reaction in the 5-Step cycle would involve an electrochemical reaction using a feed of solid CuCl undergoing oxidation at ambient temperature to produce an aqueous solution of $CuCl_2$ and solid copper particles which would be routed to the hydrogen production reactor (Step 1). Chemical kinetics would be dependent on the operating temperature and pressure of the reactor and the composition of the reactants (Naterer et al., 2009b). Naterer et al. (2008) outlined the electrical energy requirements to be approximately 31 MJ per kilogram of hydrogen produced. Giving rise to the 4-Step cycle, the combination of the first two reactions into a new electrolysis reaction occurring at temperatures of approximately up to 100°C would produce hydrogen and copper chloride electrolytically. Such a reaction would avoid the production of solid copper and the required drying facilities simplifying the processes of the cycle. Research focus in literature has gradually shifted towards the 4-Step cycle, due in part to the less complex design requirements associated with the cycle.

Table 1. Reactions Involved in the 4-Step and 5-Step Cu–Cl Cycles (Naterer et al., 2010).

Step	Reaction		Temp. Range (°C)	Feed/Output	
1*	$2CuCl_{(aq)} + 2HCl_{(aq)} \rightarrow H_{2\,(g)} + 2CuCl_{2\,(aq)}$	Electrolysis (Hydrogen Production)	~100	Feed	Aqueous CuCl and HCl + *V* + *Q* Electrolytic Cu + dry HCl + *Q*
				Output	$H_2 + CuCl_{2\,(aq)}$
2	$CuCl_{2\,(aq)} \rightarrow CuCl_{2\,(s)}$	Drying	<100	Feed	Slurry containing HCl and $CuCl_2$ + *Q*
				Output	Granular $CuCl_2$ + H_2O/HCl vapours
3	$2CuCl_{2\,(s)} + H_2O_{(g)} \rightarrow CuO*CuCl_{2\,(s)} + 2HCl_{(g)}$	Hydrolysis	375–400	Feed	Powder/granular $CuCl_2$ + $H_2O_{(g)}$ + *Q*
				Output	Powder/granular $CuO*CuCl_2 + 2HCl_{(g)}$
4	$CuO*CuCl_{2\,(s)} \rightarrow 2CuCl_{(l)} + 1/2O_{2\,(g)}$	Oxygen Production	530–550	Feed	Powder/granular $CuO*CuCl_{2\,(s)}$ + *Q*
				Output	Molten CuCl salt + oxygen

Q, thermal energy; *V*, electrical energy

* 5-Step Cycle Reaction 1: a) $2Cu_{(s)} + 2HCl_{(g)} \rightarrow 2CuCl_{(l)} + H_{2\,(g)}$ at 450°C

b) $2CuCl_{(aq)} = Cu_{(s)} + CuCl_{2\,(aq)}$ in HCl solution at 30-80°C

In Step 3 of the cycle, solid cupric chloride is obtained from the drying of a slurry or solution of $HCl/CuCl_2$ in preparation for the hydrolysis reaction. Naterer et al. (2008) determined that drying a solution rather than a slurry precipitate would be the most heat-intensive step in the cycle increasing the overall heat requirement of the facility by a factor of 2.5. For the 5-Step cycle, with a slurry drying process, the overall thermal energy requirement of the 5-Step cycle (endothermic reactions, heating of reactants and drying processes) would be approximately 277 MJ per kilogram of hydrogen produced while the heat released (heat of reaction, cooling of reaction products and solidification of materials) would be approximately 116 MJ per kilogram of hydrogen (Naterer et al., 2008). Low grade waste heat could be utilized for this reaction given the temperature requirements are much lower compared to the other endothermic reactions in the cycle.

For the purposes of this research, the thermal energy requirements of this step were included into the overall energy demand of the cycle.

The hydrolysis reaction of the Cu–Cl cycle involves $CuCl_2$ and *SuperHeated Steam* (SHS) undergoing an endothermic reaction at temperatures of approximately 375°C (Naterer et al., 2009a). Solid particles of $CuCl_2$ obtained from Step 3 are fed into a steam stream to produce copper oxychloride ($CuO*CuCl_2$) and hydrochloric gas. Copper oxychloride is important in the downstream oxygen production reactor while cuprous chloride is required in the hydrogen production step (5-Step cycle) and the electrochemical reaction (4-Step cycle).

The final reaction in the Cu–Cl cycle leads to the production of oxygen through the decomposition of the copper oxychloride obtained in Step 4. This high-temperature reaction occurs at approximately 530°C and produces oxygen gas and liquid cuprous chloride which is fed to the electrolysis reaction after being converted to a solid. Developing a heat exchange network to enable this reaction has been considered by Naterer et al. (2008). One method, further discussed in Chapter 4, would use a circulating loop of molten CuCl heated in a nuclear or solar power plant based HX and delivered directly into the reaction vessel to provide reaction heat. Alternatively, a molten salt would be heated through an HX by external heat sources and then pass through a shell around the reaction vessel providing indirect heating of the reactants. In this research, the SHS flowing between the NPP and hydrogen production facility can be viewed as the molten salt equivalent supplying external thermal energy to the cycle.

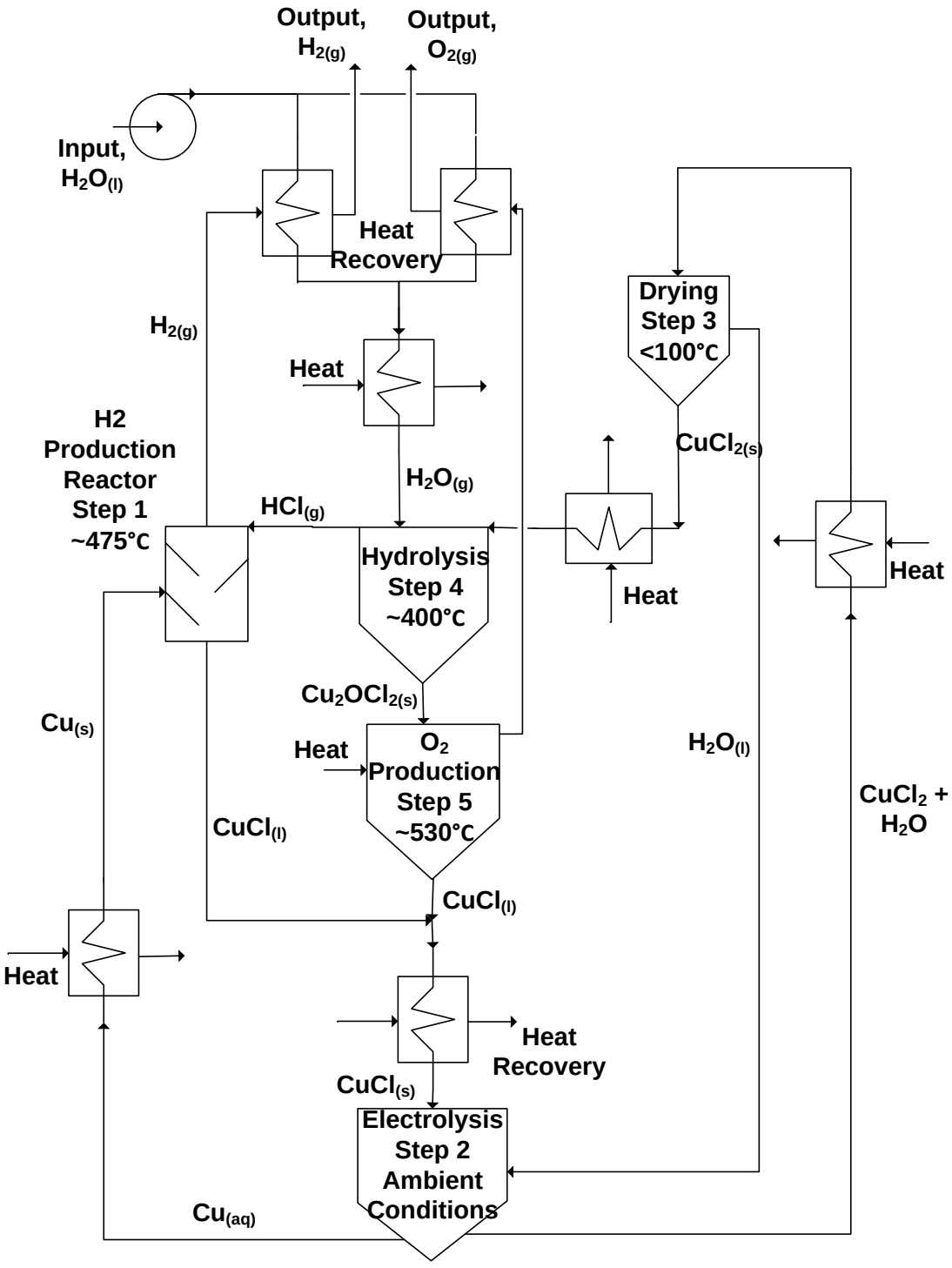

Figure 1. Conceptual Cu–Cl Cycle Layout Based on a 5-Step Process (adapted from Naterer et al., 2008; Lukomski et al., 2010b).

It is desirable to maximize the amount of thermal energy recycled within the Cu–Cl cycle such that it may be transferred between reactions in the cycle and external heat source requirements are reduced. A fraction of the heat produced within the cycle is considered to be low grade, such as low-temperature water or solid powders from which thermal energy may not be used effectively; such barriers may limit the full scale development of Cu–Cl cycle facilities (Wang et al., 2008). Wang et al. (2010a) assessed that approximately 50% of the heat generated within the cycle is recoverable for useful purposes. Wang et al. (2010b) further showed that the SI and Cu–Cl cycles have similar hydrogen production costs and if effective internal heat recycling is achieved they will have an efficiency advantage over conventional electrolysis methods.

Measures to reduce external heat demand have been explored by Wang et al. (2009) in the form of a proposed modified Cu–Cl cycle requiring lower excess steam for the hydrolysis reaction. An excess of steam is required to progress the hydrolysis reaction to completion such that a high yield of product can be obtained and formation of impurities such as CuCl and Cl_2 can be minimized (Lewis et al., 2009). Wang et al. (2009) showed that increasing the steam to $CuCl_2$ ratio in the hydrolysis reaction does not significantly reduce the heat required by the reaction.

The shift in focus toward a 4-Step Cu–Cl process has eliminated a large source of exothermic heat from the cycle normally generated in the thermochemical hydrogen production step (Step 1 of the 5-Step cycle) shown in Table 1. Considering the thermochemical reactions in the 4-Step cycle (Step 3, 4 and 5), the net heat input required by the cycle is 247 kJ/g of hydrogen with a recoverable fraction of 46 kJ/g (Wang et al., 2010b). Accounting for the 50% of recyclable thermal energy, the net external thermal energy, *Q*, required by the 4-Step cycle is 224 kJ for each gram of hydrogen produced. This value is used as an input into the thermalhydraulic calculations performed for the HXs considered in this analysis. It is important to note that heat losses have not be considered in this work, however, the requirements of step 2 (drying stage) have been accounted for even though they are considered low temperature steps and could be met by sources of waste heat.

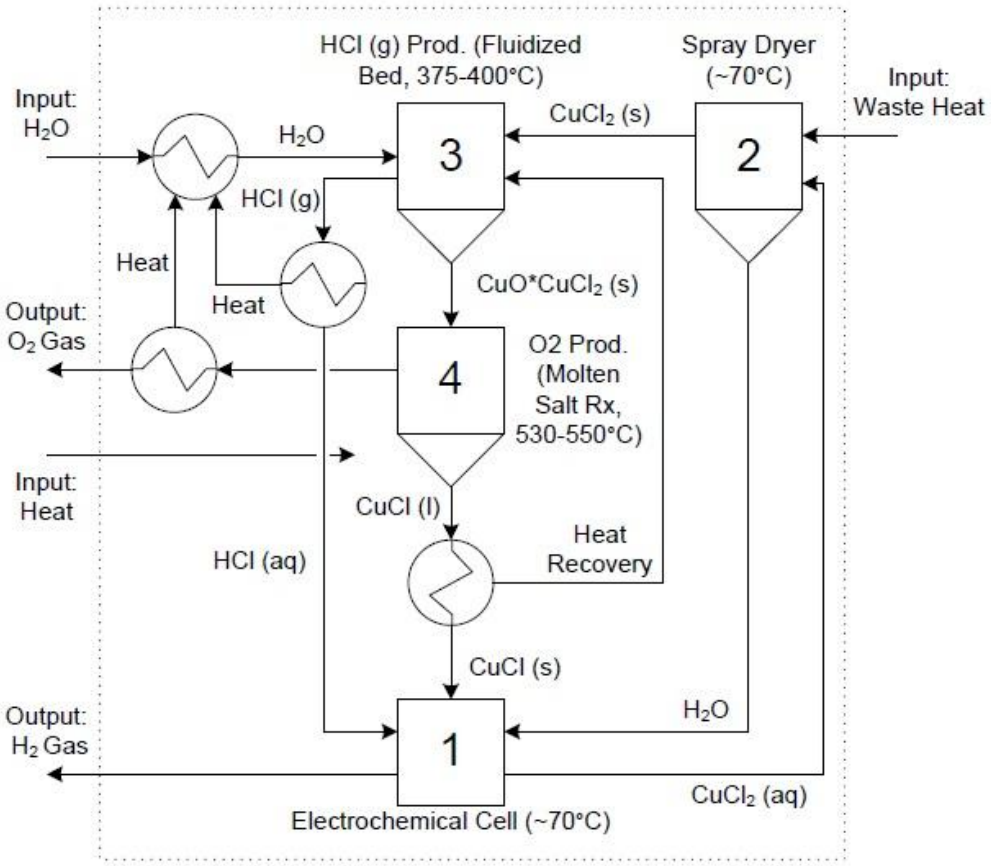

Figure 2. Conceptual Layout for the 4-Step Cu–Cl Cycle (adapted from Naterer et al., 2010).

CHAPTER 2 – GENERATION IV NUCLEAR REACTOR DESIGNS

The energy needs of the future will be met by a diverse mix of technologies based on traditional fossil fuel sources, nuclear fuels and emerging renewable sources such as wind and solar power. The role played by nuclear power will grow worldwide as nations embark on new nuclear programs while others re-consider nuclear power as a viable, safe and efficient alternative for electrical generation. Concurrent to a renewed worldwide interest in the industry, the development of the next generation of nuclear reactor is underway.

The majority of the 443 nuclear reactors currently operating around the world are part of the second generation of reactor design and include the Pressurized Water Reactor (PWR), Boiling Water Reactor (BWR) and Pressurized Heavy Water Reactor (PHWR) as shown in Table 2. Designed predominantly in the 1960s and 1970s with 40-year planned life cycles, many of the early constructions will approach their end of life in the next two decades. Figure 3 shows a distribution of world-wide operating reactor status with a large portion, over 80% above 20 years old. In the absence of renewed growth, the global nuclear industry will experience a significant decline in the next two decades.

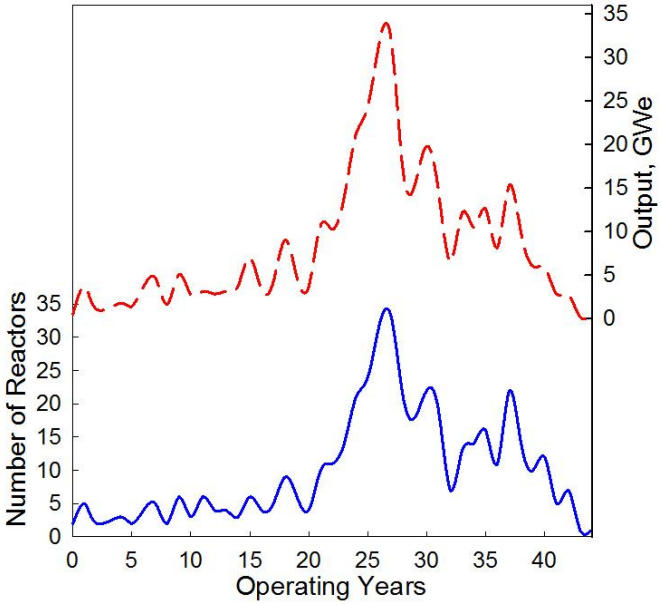

Figure 3. World-wide Status of Currently Operating Nuclear Reactors (PRIS, 2011).

Table 2. World Operating Nuclear Reactor Types (as of April 2011) (PRIS, 2011).

Reactor Type	No. of Reactors	Electrical Output, MW
Boiling Water Reactors	92	83,881
Fast Breeder Reactors	1	560
Gas Cooled Reactor	18	8,949
Light Water Graphite Moderated Reactors	15	10,219
Pressurized Heavy Water Reactors	47	23,042
Pressurized Water Reactors	270	248,723
Global Total	443	375,374

The Generation III and III+ reactors currently emerging in the nuclear markets are characterized by longer operating life, more standardized designs, lower core damage frequencies compared to earlier reactor types and improved fuel burn-up to reduce fuel waste (WNA, 2011).

A 10-member partnership called the Generation IV International Forum (GIF) was formed in 2001 to lead international efforts in developing the next generation of nuclear reactor designs to meet future global energy needs. This next group of reactors will improve upon the achievements of the Generation III and III+ design types through increased thermal efficiency, lower capital and operating costs and more passive safety systems. There are four areas that the GIF is targeting: 1) Creation of more sustainable designs by optimizing fuel usage and minimizing waste products; 2) Improving the safety and reliability of designs to reduce the probability of severe core damage; 3) Providing life cycle cost advantages over other generation technologies while maintaining an acceptable financial risk for investment; 4) Reducing the threat of nuclear proliferation through safer design and improved security (GIF, 2008). Additionally, two other areas have become increasingly important: 5) A need for governments to be actively involved in research and development to support future nuclear infrastructure; 6) Designs which

will enable cogeneration producing energy sources other than electricity (GIF, 2009). Members are focusing on six reactor design concepts that are intended to form the foundation of the future nuclear industry. Commercial integration of Generation IV systems is expected to occur by 2030, as shown in Figure 4.

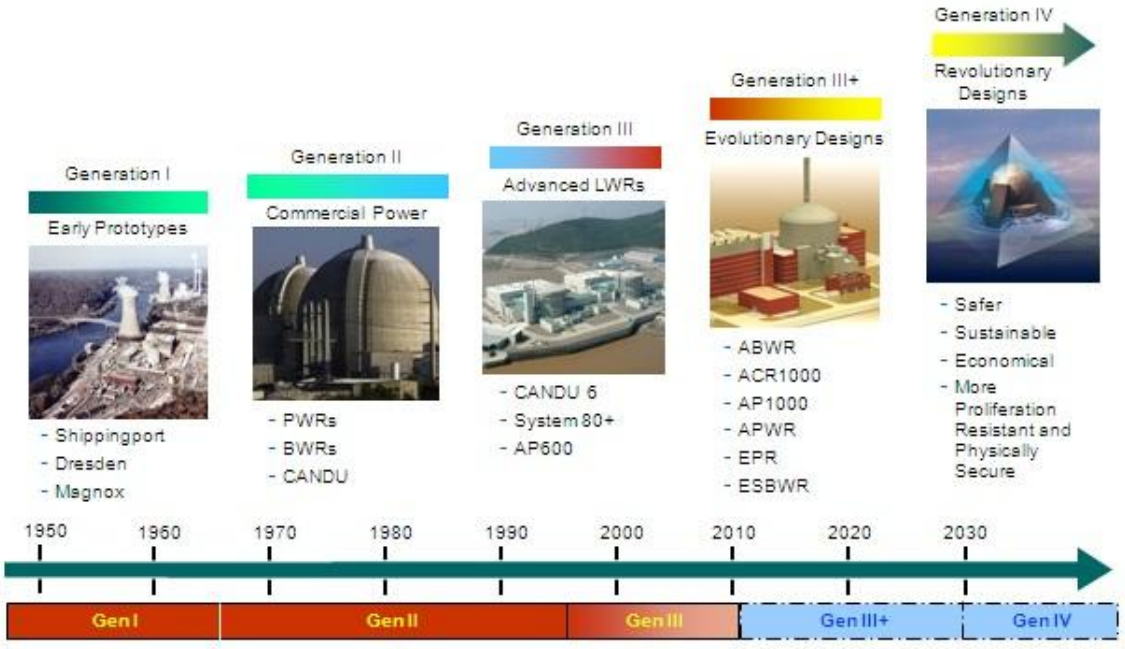

Figure 4. Evolution of Nuclear Reactor Designs (Generation IV Forum, 2008).

A general background of the six design concepts based on details from the GIF is presented with a more detailed review of the SCWR and associated potential NPP design layouts which could be selected for cogeneration applications.

The Sodium-cooled Fast Reactor (SFR) design concept would operate in the fast neutron spectrum using liquid sodium as the primary coolant with reactor outlet conditions of 550°C. A closed fuel cycle would be employed with either metal alloy or Mixed OXide (MOX) fuel allowing for high level waste recycling. In terms of development, this design holds an advantage over other Generation IV designs as SFRs have already been constructed in a number of European countries and Japan (Lineberry and Allen, n.d). As a result, the deployment of SFR technology could occur as early as 2020.

Due to the relatively low reactor outlet temperature, hydrogen cogeneration via thermochemical cycles has not been considered for SFR technology.

As with the SFR, the Lead-cooled Fast Reactor (LFR) would operate in the fast neutron spectrum with a closed nuclear fuel cycle. The low pressure LFR coolant would be either lead or a lead-bismuth eutectic with a metal or nitride nuclear fuel. Increased operating temperatures ranging between 550°C and 800°C could enable thermochemical hydrogen production, however, the proposed SSTAR and ELSY designs would operate at the lower end of this range. Long term development of the LFR could see the rise of materials with reduced lead corrosion rates at higher temperatures allowing for the development of a more advanced reactor design by 2035. Lower temperature designs are anticipated to emerge around 2025.

The Molten Salt Reactor (MSR) would operate at pressures below 500 kPa with a coolant mixture of uranium and plutonium fuel dissolved in a molten fluoride salt mixture. There are various evolutions of the MSR design; however, current focus is on the fast-spectrum MSR (MSFR) and Fluoride-cooled High temperature Reactor (FHR). Advantages of this design include a low fuel inventory and continuous recycling of actinides. The operating temperatures of such reactors could range between 700 – 800°C which would be suitable for thermochemical hydrogen production via the Cu–Cl cycle.

Operating with helium coolant, the Gas-cooled Fast Reactor (GFR) concept would operate in the fast neutron spectrum with outlet temperatures of 850°C achieving high thermal efficiencies. The reactor would operate on a closed fuel cycle with nitride or carbide based fuels embedded with uranium or plutonium. It would be capable of supplying thermal energy for hydrogen production via the Cu–Cl cycle or the SI cycle. The technology used in the GFR is similar in nature to the Very-High Temperature Reactor (VHTR) which would also be cooled by helium.

The VHTR would operate in the thermal neutron spectrum with the helium coolant passing through a graphite moderated core at temperatures of up to 1,000°C. The fuel

would be comprised of a uranium oxide pebble or prism. Due to the very high coolant outlet temperature, this reactor design would be suitable in process heating applications, specifically hydrogen production through the SI and Cu–Cl cycles.

The SCWR is a design concept using SCW as a coolant with reactor inlet and outlet temperatures of 350°C and 625°C, respectively. The reactor would operate above the thermodynamic *critical point* of water (approx. 22.1 MPa, 374°C) where water exists in a single phase state with characteristics of a low density liquid. Two reactor options would be possible for such a reactor: a Pressure Vessel (PV) similar to conventional PWR or BWR reactors or a Pressure Tube (PT) design as an evolution of the CANDU-type PHWR. Due to the increased temperature and pressure of the coolant, such a reactor would operate at efficiencies of approximately 50%, much higher than current nuclear facilities which typically achieve efficiencies of 29 - 34%. The typical operating conditions for several reactor design types are shown in Figure 5. An SCWR design would also enable the direct use of the coolant for expansion in turbines for electricity production, cogeneration of hydrogen via thermochemical cycles, production of industrial isotopes and desalination applications. Figure 6 and 7 depict a PT type and PV type concept, respectively, with the various economic benefits that would stem from such systems.

Although there are two main SCWR design options under consideration there are several potential NPP cycle layouts that can be integrated with the reactor and will be further discussed in Chapter 4.

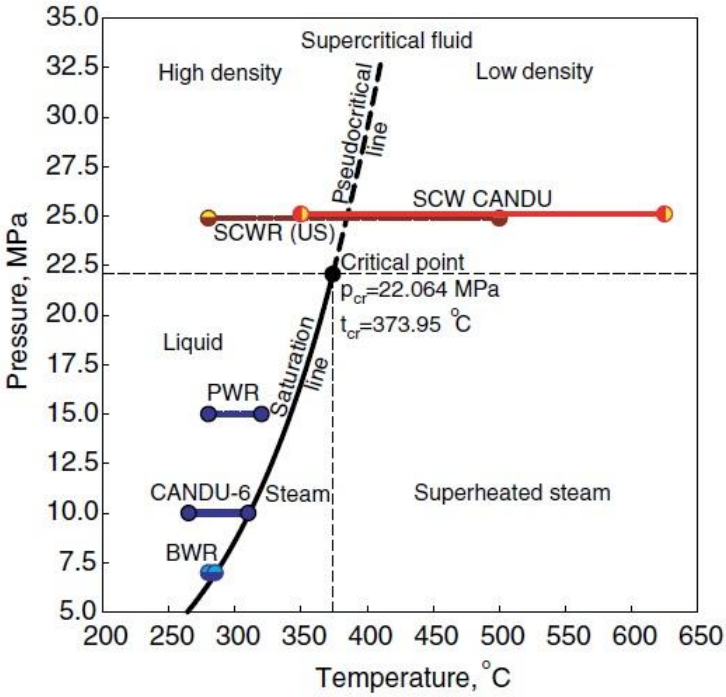

Figure 5. Pressure-Temperature Diagram of Water with Typical Operating Conditions of SCWRs, PWR, CANDU–6 and BWR (Pioro and Duffey, 2007).

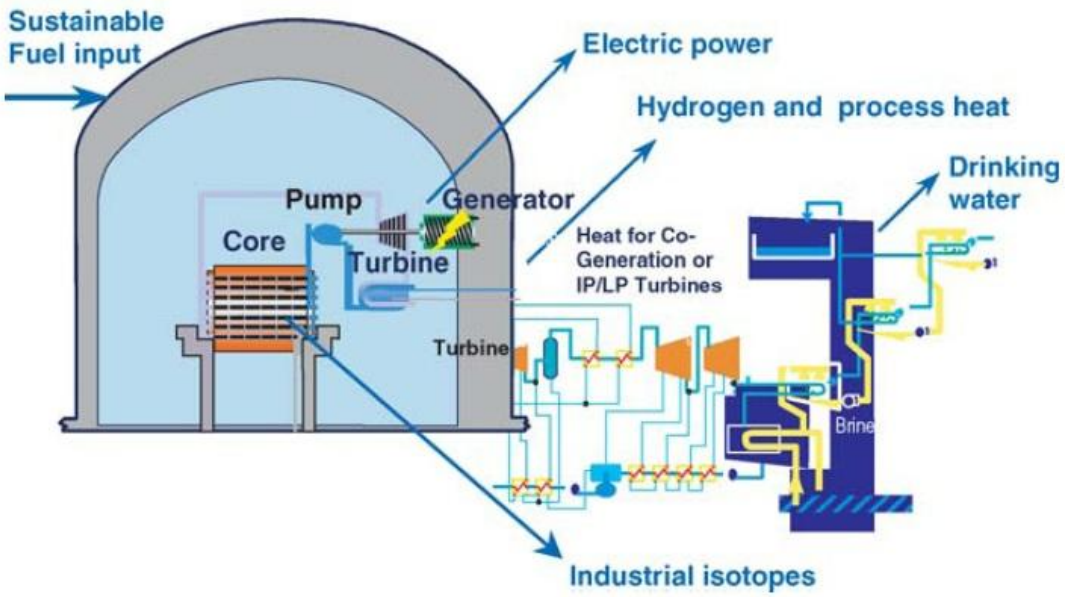

Figure 6. General Concept of Pressure-Tube SCW CANDU Reactor: IP-Intermediate-Pressure Turbine, and LP-Low-Pressure Turbine (Pioro and Duffey, 2007).

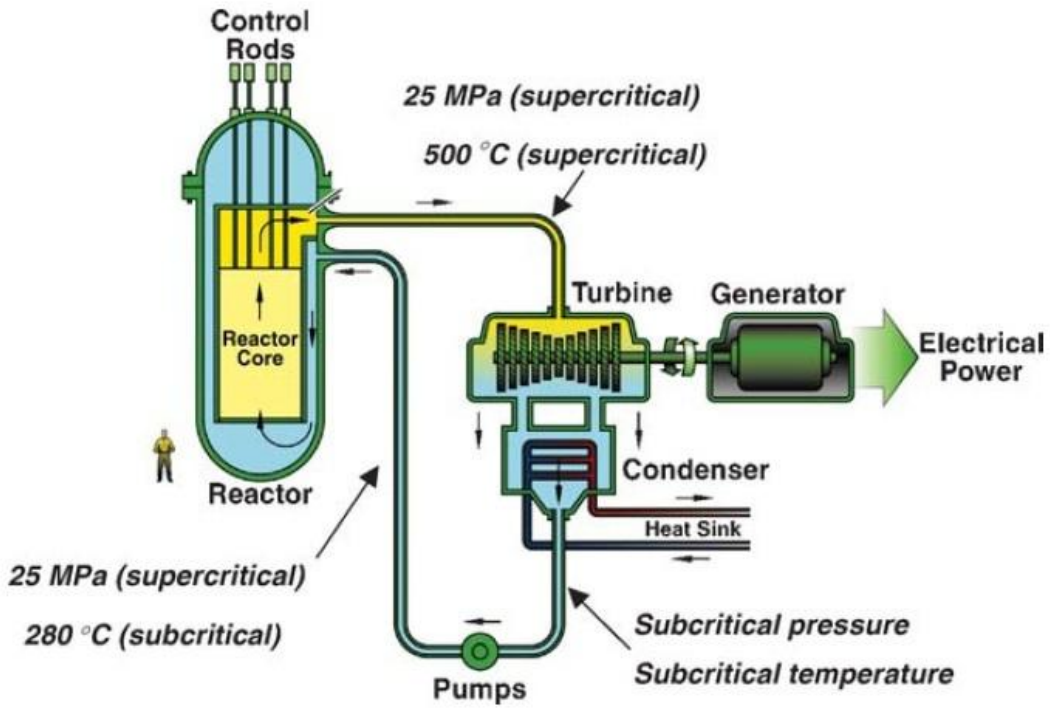

Figure 7. Schematic of US Pressurized-vessel SCW Nuclear Reactor (Pioro and Duffey, 2007).

CHAPTER 3 – SUPERCRITICAL WATER AND HEAT TRANSFER CORRELATIONS

Water is in a *supercritical* state when its pressure is above 22.064 MPa and its temperature exceeds 374°C. This boundary state is termed the *critical point*. Above this point, there is no visible phase distinction and the fluid is characteristic of a low density liquid. Another phenomenon that occurs as water passes through the *critical point* is a rapid variation in thermophysical properties (Pioro and Duffey, 2007). Most notably, the specific heat of water exhibits a peak at the *critical point*.

Variations in properties are also exhibited at pressure and temperature combinations above the *critical point;* however, they are not as significant and become less profound with increasing pressure. These regions are termed *pseudocritical* and the *pseudocritical point* is defined as the fluid state above the *critical point* (temperature and pressure) having a maximum specific heat. The *pseudocritical region* ranges between ±25°C of the *pseudocritical point* and is characterized by significant variation in thermophysical properties. A sample of *pseudocritical* points is depicted in Figure 8 and 9 showing the diminishing peaks in specific heat with increasing pressures. Data was obtained using NIST REFPROP Version 9.0 software (2010) using temperature increments of 1 K. At pressures approximately greater than 40 MPa the effects of the *pseudocritical region* are almost negligible. Pioro and Duffey (2007) have compiled an extensive amount of information related to heat transfer between fluids at *supercritical* pressures.

The response to changes in thermophysical properties is particularly important at the proposed 25 MPa operating pressure of the SCWR. The light-water coolant will pass through the *pseudocritical point* near the entrance of the reactor as it is heated from an inlet temperature of 350°C to 625°C at the outlet. Moreover, knowledge of properties within the *pseudocritical region* is important in the design of a cogeneration HX using SCW as an operating fluid since rapid property changes could affect design parameters.

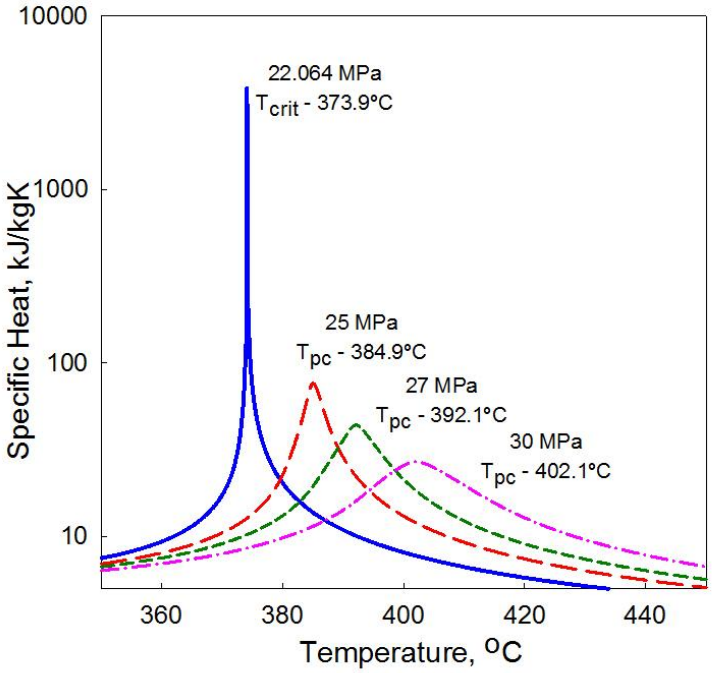

Figure 8. Dependency of the Specific Heat of Water on Temperature and Pressure (NIST, 2010).

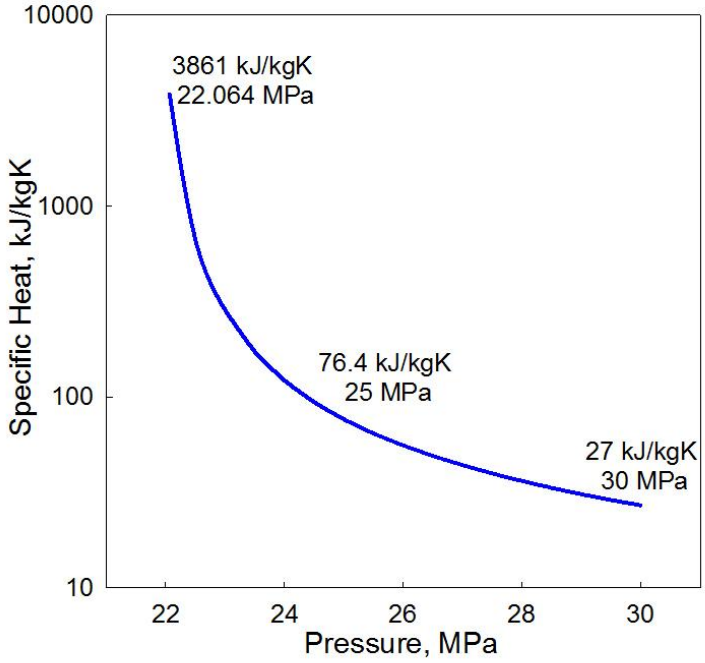

Figure 9. Peak Specific Heat Values of Water at Pseudocritical Points (NIST, 2010).

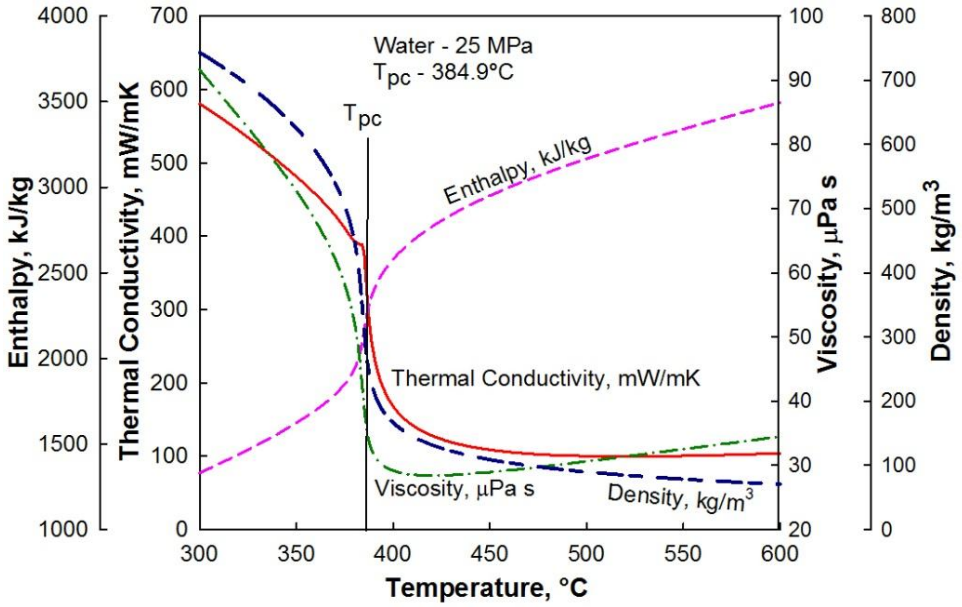

Figure 10. Select Thermophysical Properties of Water in the Pseudocritical Region at 25 MPa (NIST, 2010).

The variation of a select number of thermophysical properties in the *pseudocritical region* at 25 MPa is shown in Figure 10. As fluid temperature increases in the *pseudocritical region*, the fluid density, dynamic viscosity and thermal conductivity all experience near vertical drops in magnitude. The viscosity mildly recovers, however, there is a general downward trend for these properties. The enthalpy of the fluid exhibits a sharp increase across the *pseudocritical point* which is expected as the water holds a greater energy content above that state. These particular properties are necessary to consider as they serve as inputs into several heat transfer correlations which have been used to predict HTCs for SCW fluid flows as described in Section 3.1.

3.1 Heat Transfer Correlations

Performing thermalhydraulic calculations for a cogeneration related HX requires calculation of HTCs for both SCW and SHS operating fluids which can be obtained through various heat transfer correlations. Empirical correlations based on experimental data have been used to predict HTCs at *supercritical* pressures as widespread thermophysical property variations have made it difficult to develop reliable analytical methods (Pioro and Duffey, 2007). Pioro and Duffey (2007) have compiled various heat transfer correlations to support calculations of HTCs for forced convection water flows at *supercritical* pressures. It has been noted that many SCW correlations provide varying results regardless of being developed under similar operating ranges (Mokry et al., 2009). Several leading correlations are briefly described along with rationale in support of the correlation selected for this analysis.

3.1.1 Heat Transfer Correlations for SHS

For many subcritical applications the Dittus and Boelter equation (1930) is a reliable method for calculating HTC values. Based on research of Winterton (1998) and McAdams (1942), Incropera (2007) proposed the use of the Dittus and Boelter equation in the following form for forced convective heat transfer for turbulent flows in circular tubes:

$$\mathbf{Nu}_b = 0.023\, \mathbf{Re}_b^{4/5}\, \mathbf{Pr}_b^{n} \tag{1}$$

Where $n = 0.4$ for heating ($T_w > T_b$) and 0.3 for cooling ($T_b > T_w$) and has been confirmed experimentally in the region of $0.6 \leq \mathbf{Pr}_b \leq 160$, $\mathbf{Re}_b \geq 10{,}000$ and $L/D \geq 10$. This equation is based solely on bulk-fluid properties and is applicable when bulk-fluid temperature and near-wall temperatures are similar.

Another correlation for fully developed flow is the Gnielinski correlation (1976) as documented by Incropera (2007) and includes a friction factor term, *f*, to account for frictional influence on heat transfer which may be obtained from a Moody diagram or

other applicable equations outlined by Incropera (2007). This correlation was obtained at conditions of $0.5 \leq \mathbf{Pr}_b \leq 2000$ and $3000 \leq \mathbf{Re}_b \leq 5 \times 10^6$.

$$\mathbf{Nu}_b = \frac{(f/8)(\mathbf{Re}_b - 1000)\mathbf{Pr}_b}{1+12.7(f/8)^{1/2}\left(\mathbf{Pr}_b^{2/3}-\mathbf{1}\right)} \tag{2}$$

3.1.2 Heat Transfer Correlations for SCW

The Bishop et al. (1964) correlation (shown as Equation 3) was obtained using experimental data for upward SCW flow inside tubes and annuli. The test limits used to derive the correlation are as follows: pressure, P = 22.8 – 27.6 MPa, bulk-fluid temperature, T_b = 282 – 527°C, mass flux, G = 651 – 3662 kg/m^{2}s and heat fluxes, q'', between 0.31 – 3.46 MW/m^2. This correlation requires knowledge of both bulk-fluid and wall-fluid thermophysical properties and a cross section averaged Prandtl number is utilized. Piping entrance effects are accounted for through the last term of the correlation requiring knowledge of pipe diameter and length, however, entrance effects are not considered in this investigation. Results from heat transfer analysis show a data fit of ±15% (Pioro and Duffey, 2007).

$$\mathbf{Nu}_b = 0.0069\, \mathbf{Re}_b^{0.9}\, \overline{\mathbf{Pr}}_b^{0.66} \left(\frac{\rho_w}{\rho_b}\right)^{0.43} \left(1 + 2.4\frac{D}{x}\right) \tag{3}$$

The Swenson et al. correlation (1965), shown as Equation 4, evaluates thermophysical properties mainly at wall conditions. It was developed for the following range of parameters: P = 22.8 – 41.4 MPa; G = 542 – 2150 kg/m^{2}s; T_w = 93 – 649°C; T_b = 75 – 576°C. The correlation replicated experimental data to within $\pm$15% (Pioro et al., 2004). This correlation has been selected in previous studies related to HX applications in with SCW operating fluids (Thind et al., 2009). It has also been used as a basis for the development of other correlations, most recently the Gupta et al. correlation (Mokry et al., 2010b).

$$\mathbf{Nu}_w = 0.00459\, \mathbf{Re}_w^{0.923}\, \overline{\mathbf{Pr}}_w^{0.613} \left(\frac{\rho_w}{\rho_b}\right)^{0.231} \tag{4}$$

The Mokry et al. (2009) correlation, shown in Equation 5, is a recently developed correlation for SCW applications from current experimental data and updated databases for thermophysical properties of water. The data was obtained from a Russian facility with an apparatus consisting of upward SCW flow in a 4 m long bare vertical stainless steel tube with an inner diameter of 10 mm, wall thickness of 2 mm and a surface roughness of 0.63 – 0.8 μm (Mokry et al., 2011).

$$\mathbf{Nu}_b = 0.0061\mathbf{Re}_b^{0.904}\overline{\mathbf{Pr}}_b^{0.684}\left(\frac{\rho_w}{\rho_b}\right)^{0.564} \quad (5)$$

Test conditions for the experimental dataset were P = 24 MPa; q'' = 70 – 1250 kW/m^2; G = 200 – 1500 kg/m^{2}s; and D = 3 – 38 mm. Fluid parameters are evaluated primarily at bulk-fluid conditions. The derived correlation provided results with uncertainties of $\pm$25% for HTC values and approximately $\pm$15% for tube wall temperatures (Mokry et al., 2011).

Recent research by a group at the University of Ottawa (UofO) involved a literature review of 28 data sets consisting of 6663 trans-critical heat transfer data to assist in the development of a wide-range look-up table for heat transfer correlations. This work evaluated the accuracy of correlations against SCW data available at the UofO. It was determined that the Mokry et al. (2009) correlation (earlier termed Gospodinov et al.) showed the lowest Root Mean Square (RMS) deviations in all *supercritical*, near-*supercritical* regions and in the SHS region (Zahlan et al., 2010). Table 3 and 4 show results from the study in the form of average error and RMS calculations for the investigated correlations.

Based on the UO research team's conclusions, the Mokry et al. (2009) correlation was selected as the heat transfer correlation for all operating fluid flows in the topic HXs.

Table 3. Overall Average and RMS Error for Heat Transfer Correlations in the Subcritical Region (Zahlan et al., 2010).

Correlation	Subcritical Liquid		SuperHeated Steam	
	Av.er, %	rms, %	Av.er, %	rms, %
Dittus and Boelter (1930)	10.4	22.5	75.3	127.3
Gnielinski (1976)	–4.3	**18.3**	80.3	130.2
Mokry et al. (2009)	**–1.06**	19.21	**–4.78**	**19.57**
Sieder and Tate (1936)	27.6	37.4	83.8	137.8
Hadaller and Banerjee (1969)	27.3	35.9	19.1	34.4

Table 4. Overall Weighted Average and RMS Error for Heat Transfer Correlations in the Three Supercritical Sub-regions (Zahlan et al., 2010).

Correlation	Liquid-like Region		Gas-like Region		Critical/Pseudo-critical Region	
	Av.er, %	rms, %	Av.er, %	rms, %	Av.er, %	rms, %
Bishop et al. (1965)	6.3	24.2	5.2	18.4	20.9	28.9
Swenson et al. (1965)	1.5	25.2	–15.9	20.4	5.1	23.0
Mokry et al. (2009)	–3.9	**21.3**	–8.5	**16.5**	**–2.3**	**17.0**
Krasnochekov et al. (1967)	15.2	33.7	–33.6	35.8	25.2	61.6
Watts and Chou (1982), Normal	4.0	25.0	–9.7	20.8	5.5	24.0
Watts and Chou (1982), Deteriorated	5.5	23.1	5.7	22.2	16.5	28.4
Griem (1996)	1.7	23.2	4.1	22.8	2.7	31.1
Jackson (2002)	13.5	30.1	11.5	28.7	22.0	40.6
Kuang et al. (2008)	–6.6	23.7	**2.9**	19.2	–9.0	24.1
Cheng et al. (2009)	**1.3**	25.6	**2.9**	28.8	14.9	90.6
Dittus and Boelter (1930)	32.5	46.7	87.7	131.0	-	-
Gnielinski (1976)	42.5	57.6	106.3	153.3	-	-
Sieder and Tate (1936)	20.8	37.3	93.2	133.6	-	-
Hadaller and Banerjee (1969)	7.6	30.5	10.7	20.5	-	-

CHAPTER 4 –SELECT SCW NUCLEAR POWER PLANT LAYOUTS AND COGENERATION HEAT EXCHANGERS

As mentioned in Chapter 2, there are several SCWR design concepts currently under development in addition to NPP cycle layouts available for HX integration. Design details presented below can be applied to either PV or PT type SCWR designs. Discussion is limited to two cycles currently under consideration for the SCWR as they cover the possible SCW NPP designs which would support cogeneration applications. In relation to cogeneration requirements for hydrogen production, reactor outlet conditions of the primary coolant are of prime concern as coolant could be drawn into an HX from this location. Such conditions become inputs into the thermalhydraulic calculations performed in this research. Table 5 outlines the current SCW CANDU design concept parameters. Based on the Cu–Cl cycle's external power requirement of 224 MW per kilogram of hydrogen produced, the fraction of thermal power removed from the NPP is approximately 8.8% of the total thermal output of the SCWR. Theoretically, an SCWR could provide thermal energy for other thermochemical cycles granted that there is compatibility in the maximum temperature requirement of the cycle considered. The total thermal energy removed from the SCWR would also be impacted.

Table 5. Major Parameters of PT SCW CANDU (Mokry et al., 2011).

Parameters	SCW CANDU®
Thermal Power, MW	2540
Coolant Pressure, MPa	25
Mass Flow Rate, kg/s	1320
Length of Bundle String, m	6
Reactor Type	PT
Electric Power, MW	1220
Inlet Temperature, ◦C	350
Number of Fuel Channels	300
Reactor Spectrum	Thermal
Thermal Efficiency, %	48
Outlet Temperature, ◦C	625
Number of Fuel Elements in Bundle	43

Research teams at UOIT, AECL and GE Hitachi have used such inputs to perform NPP cycle calculations to determine optimal NPP arrangements to optimize thermodynamic efficiency (Duffey et al., 2008; Naidin et al., 2009a-e; Pioro et al., 2010).

Three NPP cycle options have been considered for SCW NPP applications: i) direct; ii) indirect; iii) dual cycle (Naidin et al., 2009a).

In a direct cycle SCW NPP layout, the SCW coolant would exit the reactor and be fed into a *supercritical* turbine followed by other subcritical turbines for expansion. This type of cycle would eliminate the need for steam generators thereby reducing the capital and maintenance costs of the NPP. In an indirect cycle, steam generators would be required to transfer thermal energy from a primary coolant circuit to a secondary steam circuit with the steam expanding in a number of turbines. This cycle has a lower thermal efficiency due to the temperature drop experienced across the steam generator and the lower operating pressure of the steam side. An advantage of this arrangement would be a lower probability for radioactive release as the primary coolant is exposed to fewer pathways to the external environment. A dual cycle would combine aspects of both direct and indirect cycles intended to achieve higher efficiency designs.

The above cycles can also be combined with steam reheat technology to further increase thermodynamic efficiency. This concept is based on the primary coolant passing through the reactor core more than once via several types of channels (for PT type), first as a *supercritical* fluid with expansion in an HP turbine and re-entering as SHS to be reheated and expanded in LP turbines. Many fossil-fired power plants operating on SCW cycles utilize *supercritical* turbines and the majority of modern layouts introduced have integrated single-reheat cycle turbines (Pioro et al., 2010). Preliminary analysis for a double reheat design was performed by Naidin et al. (2009c) establishing the highest efficiency of all available cycles; however, the design of a complex reactor steam reheat configuration would significantly increase capital costs of the station and reduce the economic benefit. Therefore, analysis has focused extensively on the single reheat and no-reheat cycles. Both cycles offer locations where a cogeneration HX may be

integrated. For applications specific to hydrogen production via the Cu–Cl cycle the 625°C coolant conditions at the reactor outlet exceed the temperature requirements for the bounding Cu–Cl reaction step (O_2 production, ~500 – 550°C). Figure 11 shows a series piping configuration for the SHS distribution within the Cu–Cl cycle. Given that the endothermic reactions occur over a large temperature difference, a series piping arrangement can provide indirect heating to the required Cu–Cl cycle reactors beginning at the oxygen production step followed by the hydrolysis reactor and finally the drying step. Although Figure 11 depicts drying of $CuCl_2$ as part of the distribution network, the lower temperature requirement of the reaction can be satisfied through alternate heat sources internal or external to the cycle. As the SHS travels between the two facilities it will experience thermal and pressure losses introducing a need for compressor units ensuring that the steam pressure remains above the saturation pressure at all temperatures experienced along the pipe length. Future assessments of predicted thermal losses between the two facilities will also need to be performed to determine the impact on HX designs.

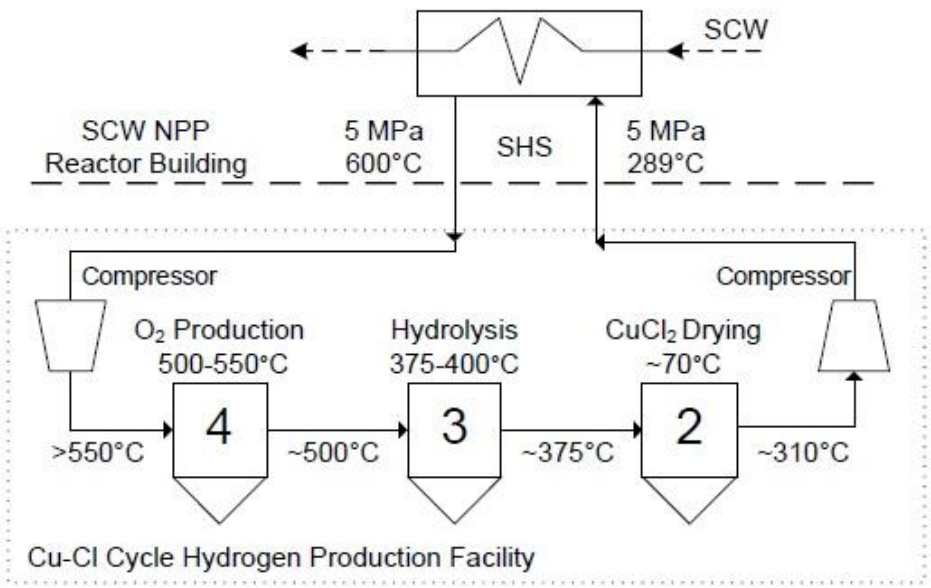

Figure 11. Potential Intermediate SHS Network Inside of a Hydrogen Production Facility.

4.1 No-Reheat Cycle Layout

In the no-reheat cycle layout (Naidin et al., 2009a), shown in Figure 12, subcritical water would enter the feedwater circuit at the exit of the condenser at conditions of 6.77 kPa and 38.4°C. A condensate extraction pump would transport the coolant through five LP heaters where it would be heated through isobaric processes. The water would then enter a deaerator where non-condensable gases would be removed and the liquid would be heated to near-saturated conditions. A reactor feed pump would pressurize the coolant to 25 MPa conditions prior to passing through four additional pre-heaters raising the coolant temperature to 350°C. After being heated by fuel bundles across the reactor core, the coolant outlet temperature would reach 625°C. The coolant pressure drop across the reactor would be negligible relative to the overall pressure of the system. Therefore, it is assumed that for the purposes of this research, the operating pressure of the SCW would remain at 25 MPa at the reactor outlet. The SCW would expand through a double-flow HP turbine with a fraction of coolant extracted to supply the feedwater system preheaters. Dual double-flow Intermediate Pressure (IP)/LP turbines would be required due to coolant volume expansion. A total SCW flowrate of 1190 kg/s was analyzed for a station electrical output of 1200 MW_{el}. Preliminary assessments showed the thermal efficiency for this layout to be approximately 51% (Naidin et al., 2009a).

A location on the coolant loop downstream of the reactor and upstream of the HP turbine (See Figure 13) would be a suitable location for an HX interfaced with a hydrogen production facility. This HX would have SCW as the operating fluid on the HP side and SHS as the LP operating fluid. A location downstream of the HP turbine, as shown in Figure 12, was not selected as a prospective HX location as an SHS temperature of 410°C is not adequate to supply the highest temperature requirement of Cu–Cl cycle. Although this temperature would theoretically meet the requirement of the hydrolysis reaction (~375°C) the loss in temperature across the HX would reduce the steam temperature available for the reaction. A valve upstream of HX A would control the flow diverted to the HX based on a setpoint established between the SCW NPP and the hydrogen production facility considering electrical and hydrogen demand. An increased

hydrogen production rate would require more SCW to be diverted leading to a reduction in electrical output of the station. Similar control valves would be found upstream of the HX designs found on the single reheat cycle layout described in Section 4.2.

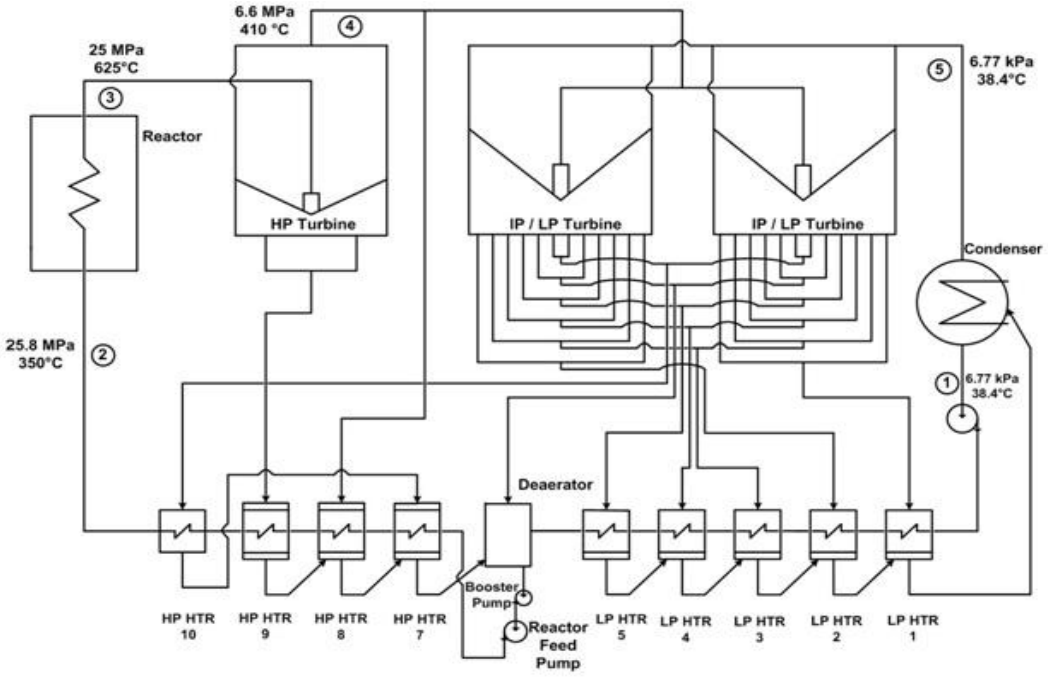

Figure 12. No-Reheat Cycle Layout for a SCW NPP (Naidin et al., 2009a).

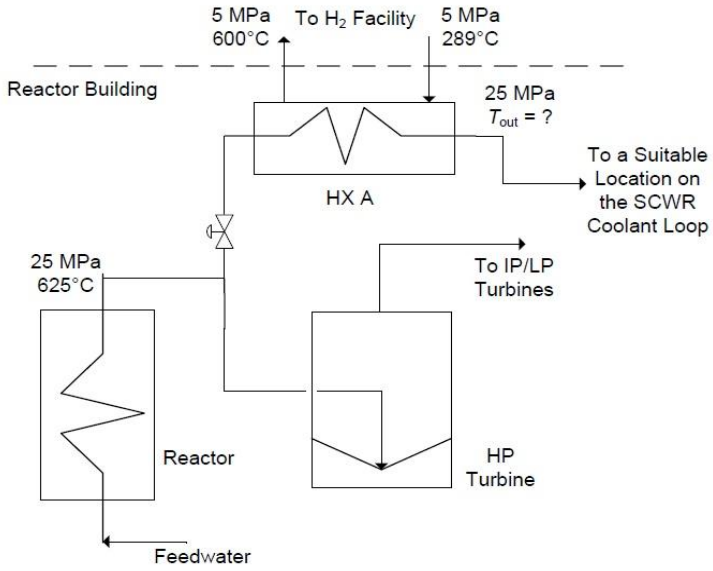

Figure 13. Heat Exchanger Locations in the No-Reheat Cycle SCW NPP Layout (Lukomski et al., 2011c).

4.2 Single-Reheat Layout

The single reheat layout analyzed by Naidin et al. (2009a) involved the introduction of steam reheat channels into a PT reactor core. Figure 14 depicts such a design which would have SCW channels located within the inner reactor region (calandria) and channels operating with SHS flow on the outer periphery. Although this feature would lead to an increased cycle thermal efficiency, the increase in core complexity would require additional research and development and in turn, higher capital costs for the NPP.

The potential single reheat layout NPP is shown in Figure 15. The feedwater system equipment would be the same as for the no-reheat layout with modified coolant flowrates to achieve the required reactor inlet parameters. After passing through the reactor as SCW and expanding through the HP turbine the coolant in an SHS state would re-enter the reactor core at conditions of 6.1 MPa and 395°C. It would be reheated to 625°C, exit the reactor at a pressure of approximately 5.7 MPa and flow to an IP turbine. The flow would then pass to two dual-flow LP turbines and exhaust to the condenser. In this layout, two individual generators would be used with the HP and IP turbines joined to a primary shaft and the LP turbines located on a secondary shaft. Assessments were performed for an SCW NPP plant electrical output of 1200 MW_{el}. The flowrates for the SCW and SHS along the system would be 960 kg/s and 780 kg/s, respectively. The thermal efficiency for this cycle was calculated to be approximately 52%.

For cogeneration of hydrogen, Figure 16 depicts the potential locations of HXs on the NPP coolant loop. The first location would remain downstream of the SCW channels and have the same temperature and pressure conditions as the no-reheat cycle, however, the total flow of SCW would be lower compared to the no-reheat layout. The required mass flowrate of SCW through the cogeneration HX would not change between the two cycles and thus a greater fraction of the single reheat cycle's total flow would be required for the HX. The second available location would be downstream of the steam reheat channels as the reactor outlet temperature of the SHS would suit the Cu–Cl cycle requirements. An HX located between the steam reheat channels and the IP turbine

would remove additional coolant flow from the steam system. This would lead to an imbalance in the work done between the HP and IP turbines as less SHS would be available to expand in the IP turbine. Assessment of these impacts was not within the scope of this work and so the location for the HX is evaluated only for thermalhydraulic properties related to hydrogen production. An HX at this location would operate with SHS on both the HP and LP sides. A control valve upstream of the HX would regulate flow into the HX based on the electrical and hydrogen demand at a given time.

In the single reheat arrangement it is assumed that only one of the two HX designs would be integrated into the NPP cycle, or if both are selected for integration, only one would operate at a given time. As shown in Figure 11, the Cu–Cl cycle reactors could be heated via a single SHS stream leaving the SCW NPP at 600°C. Since both HXs would operate at the same SHS temperatures there is no requirement to have two independent HXs operating simultaneously.

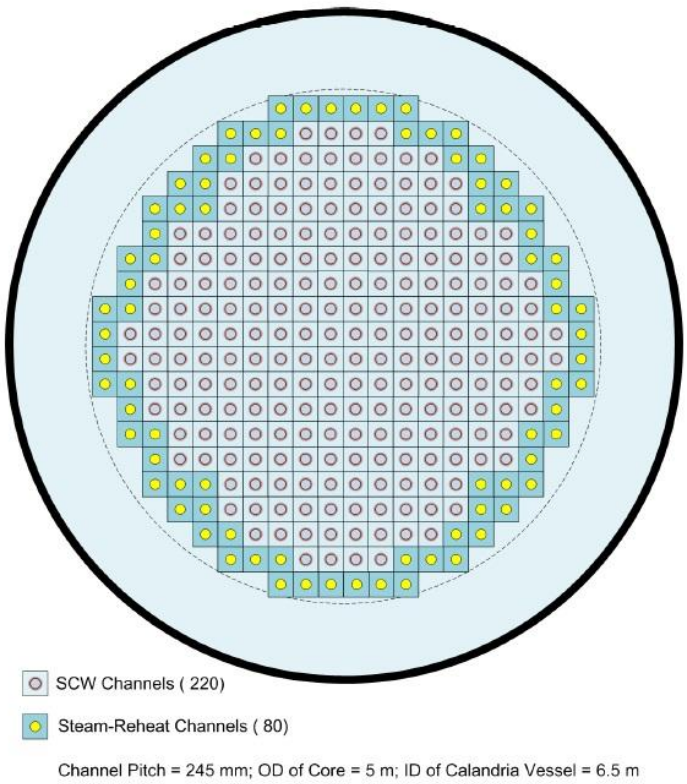

Figure 14. Cross Section of a Single Reheat PT SCWR Core for 1200 MW_{el} NPP (Mokry et al., 2011).

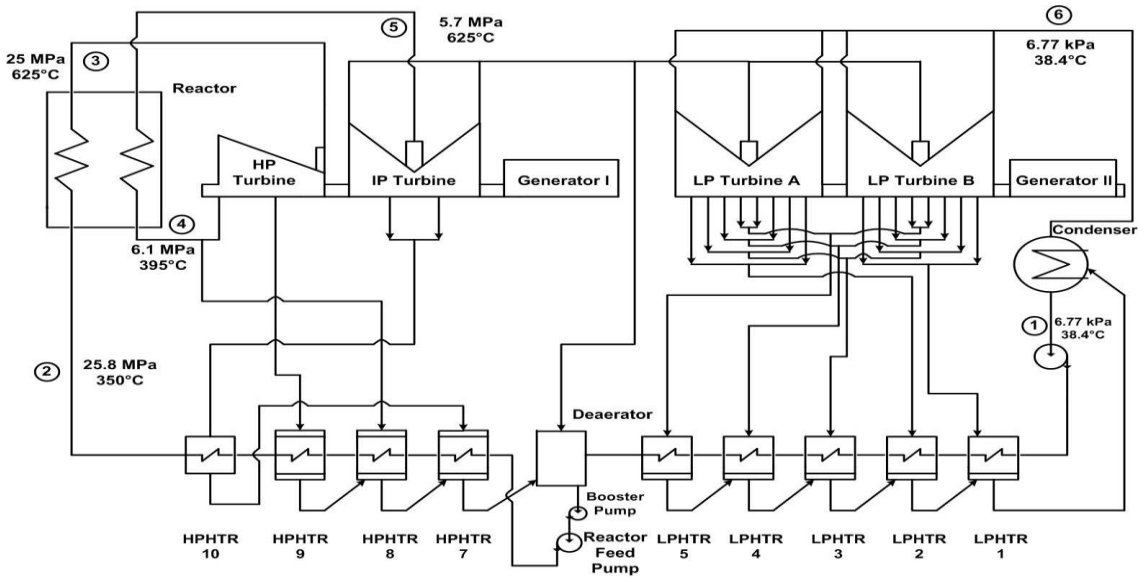

Figure 15. Single Reheat Cycle Layout for a SCW NPP (Naidin et al., 2009a).

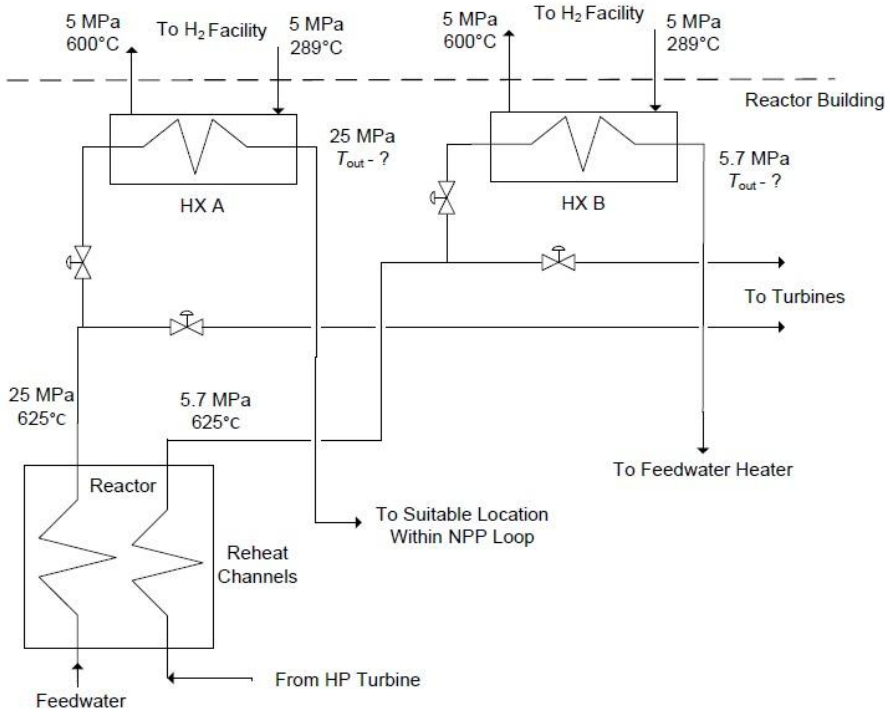

Figure 16. Heat Exchanger Locations in the Single Reheat Cycle NPP Layout (Lukomski et al., 2011b).

4.3 Selection of Heat Exchanger Design and Preliminary Analysis

Two HX design types were initially considered for this analysis: i) counter-flow double-pipe HX; ii) counter-flow shell and tube HX. A counter-flow design was selected over a parallel-flow design to enable a larger temperature difference across the HX to be achieved for both of the operating fluids and permit the SHS temperature on the LP side to reach temperatures of 600°C. Under both design types the SCW would be designated the HP fluid and would operate via the inner pipe (double-pipe design) or tube (shell and tube design). In the case of an HX at the outlet of the reheat channels, the fluid would be HP SHS. The fluid occupying the annulus gap (double-pipe design) or shell side (shell and tube design) would be the LP SHS flowing in the intermediate loop between the SCW NPP and the hydrogen production facility.

The intermediate loop operating fluid for this research was selected as SHS, as proposed by Naidin et al. (2009b). One of the advantages of using SHS would be the chemical compability with SCWR coolant to ensure no potential adverse reactions at the HX interface in the event of pipe leaks. Additionally, the pressure-dependent boiling point of water permits a wide temperature range for heating of reactors in the Cu–Cl cycle. One of the challenges associated with the use of SHS would be the potentially significant pressure loss due to high flow velocities. Use of molten salts (i.e. CuCl) as intermediate heat transfer mediums has been proposed by Naterer et al. (2008) and Le Brun (2007). The advantages of using such materials is the higher specific heat capacities compared to steam or other types of gases which make the salts suitable for heat transfer applications over long distances. A challenge in using molten salts would be managing the phase change of the molten salt into a solid during periods where the SCWR or hydrogen production facility would undergo maintenance and initial heating of the solid to a molten state once operations were to resume. The elevated melting points for certain molten salts (430°C for CuCl) would limit the temperature drop experienced when passing through the Cu–Cl reactors increasing the mass flow rate requirements to ensure sufficient thermal energy transfer. It is worthwhile to analyze the suitability of molten

salts for use as a heat transfer medium, however, this was considered outside the scope of this research.

To distinguish the discussion between the two potential HX locations on the NPP layouts the HX found downstream of the SCW channels on both the no-reheat and single reheat layouts was termed “HX A” while the HX found downstream of the SHS reheat channels on the single reheat layout was termed “HX B”. These distinctions are shown in Figure 13 and 16. At this stage of research, the orientation of the HX piping (vertical or horizontal) was not considered for physical dimensions or choice of the heat transfer correlation. The orientation is assumed to be dependent on the containment structure layout of the SCW NPP and would be developed in parallel as part of future design stages.

As is shown in Figure 13 and 16, all HXs under consideration would need to be located within the containment structure of the SCW NPP. During SCWR operation, low concentrations of radioactive impurities could circulate in the primary coolant on a continuous basis which would increase during accidents involving poential fuel sheath failures. Locating the HX within the reactor/containment building of the SCW NPP would significantly reduce the probability of reactor coolant leakage to the external environment. The HX piping, specifically the inner pipe, would act as the containment boundary between the primary side coolant and the SHS flow. Such concerns support the proposed intermediate coolant loop between the two facilities. Moreover, although delivering the NPP coolant directly to the hydrogen production facility would improve the efficiency of the cycle it would introduce significant regulatory requirements due to the extension of the NPP’s containment boundary. Also, since the SCW NPP and Cu–Cl cycle operate at substantially different pressures (25 MPa versus several atmospheres), the intermediate pressure SHS loop would lower the magnitude of material stress experienced by piping and equipment between the SCW NPP and hydrogen production facility.

Richards et al. (1997) investigated linking a hydrogen facility based on the SI cycle with a modular helium reactor for hydrogen cogeneration. They suggested the distance

between an NPP facilitating hydrogen production and the hydrogen facility should be approximately 100 – 150 m. It is anticipated, however, that this distance would be challenging to implement due to safety considerations incorporated in nuclear reactor operation. A distance of several hundred metres would be a more reasonable assumption. Developing a piping network between the two facilities will be required to determine heat loss characteristics along with mitigating measures to be incorporated into the HX designs.

4.4 Log Mean Temperature Difference Method

Tools developed for HX analysis were considered for their applicability to the current scenario. Analysis tools such as the LMTD method or the Effectiveness-NTU method have a set of underlying assumptions that must be met prior to being applied to HX analysis (Incropera et al., 2007; Shah and Sekulic, 2003). Among these assumptions is that the specific heat of the operating fluid must remain constant across the length of the HX. Moreover, the overall HTC, *U*, of the fluid flow system must also remain unchanged across the HX. In the majority of applications with single phase fluid HXs these methods are appropriate for use and an average temperature along the HX for each fluid can represent overall flow conditions. Using the LMTD method, the average temperature difference between the operating fluids across the HX for a counter flow arrangement is determined from Equation 6:

$$\Delta T_{lm} = \frac{\Delta T_2 - \Delta T_1}{\ln\left(\frac{\Delta T_2}{\Delta T_1}\right)} = \frac{\Delta T_1 - \Delta T_2}{\ln\left(\frac{\Delta T_1}{\Delta T_2}\right)} \tag{6}$$

Where,

$$\Delta T_1 \equiv T_{hot,in} - T_{cold,out} \qquad \Delta T_2 \equiv T_{hot,out} - T_{cold,in}$$

The rate of thermal energy transfer across the HX is the product of the overall HTC, the heat transfer surface area, *A*, and the LMTD value from Equation 6 and shown as follows:

$$\dot{Q} = UA\Delta T_{lm} \tag{7}$$

For SCW operating fluid approaching the *pseudocritical region* the thermophysical properties, as shown in Figure 10, would experience significant fluctuations proving the LMTD method, and other available methods invalid for analysis. Due to this condition, an iterative calculation process was selected for the HX thermalhydraulic analysis and is described further in Chapter 5. Based on the complexity of performing an iterative thermalhydraulic calculation on a shell and tube HX with associated baffles and tubesheets it was decided to limit the scope of analysis to only a double-pipe HX arrangement. Independent investigations for designs such as the shell and tube should be performed in future work.

As HX B operating fluids would be SHS in both cases, the relative change in thermophysical properties along the HX length would be less significant compared to an SCW flow and so an LMTD analysis was performed for one HX B design and compared to the iterative calculations to determine the validity of the method for future research applications.

4.5 Heat Exchanger Piping Material

The HX piping material that is selected must satisfy safety criteria, possess favourable heat transfer characteristics and have good corrosion properties. The two main parameters considered in this analysis were thermal conductivity and pipe burst pressure. Three metals commonly used in nuclear applications were selected for investigation to determine suitability with the desired HX operating conditions: Stainless Steel 304, Inconel–600 and Inconel–718. Table 6 provides a summary of the composition of each material and some characteristics of the metals. The Inconel alloys contain high nickel and chromium contents making them suitable in high-temperature applications. A brief description of each metal follows:

> ***Stainless Steel 304*** – Austenitic nickel-chromium stainless steel with high ductility, drawing and spinning properties; good corrosion and oxidation

properties; commonly used in HX applications and some nuclear applications (Matweb, 2011).

Inconel-600 Alloy – Nickel-chromium alloy with resistance to oxidation at high temperatures, high-purity water corrosion and chloride-ion stress-corrosion cracking; it has high strength qualities combined with good workability and is widely used in the nuclear industry (Special Metals, 2011; Matweb, 2011).

Inconel-718 Alloy – Nickel-chromium alloy, similar to Inconel-600, having good corrosion properties, easy fabrication processes, high tensile, fatigue, creep and rupture strength and good weldability; it is also used extensively in the nuclear industry (Special Metals, 2011; Matweb, 2011).

Table 6. Select Physical Properties and Composition of Materials Considered for Intermediate HX (Matweb, 2011; Special Metals, 2011).

Property	**SS–304**	**Inconel–600**	**Inconel–718**
Density (g/cm^3)	8.00	8.47	8.19
Melting Point (°C)	1,400 – 1,455	1,354 – 1,413	1,260 – 1,336
Composition (%)			
Nickel (+ Cobalt for Inconels)	8.0 – 10.5	> 72.0	51.0 – 56.0
Chromium	18.0 – 20.0	14.0 – 17.0	17.0 – 21.0
Iron	66.3 – 74.0	6.0 – 10.0	17.0
Carbon	<= 0.08	< 0.15	<= 0.08
Manganese	<= 2.0	< 1.0	<= 0.35
Sulfur	<= 0.03	< 0.015	<= 0.015
Silicon	<= 1.0	< 0.5	<= 0.35
Copper	-	< 0.5	<= 0.3
Phosphorus	<= 0.045	-	<= 0.015
Niobium	-	-	4.75 – 5.50
Titanium	-	-	0.65 – 1.15
Molybdenum	-	-	2.8 – 3.3

For the operating conditions of the HX, the inner pipe will need to withstand pressures of 25 MPa and so the burst pressure of each material for anticipated piping dimensions must meet minimum criteria prior to selection for use. In determining burst pressure for a material, it is necessary to know the tensile strength which is further discussed in Chapter 5. Shown in Figure 17, the limiting tensile strength in this grouping was for SS–304. This data presents the general trend in variation of tensile strength for each material influenced by fabrication methods, such as annealing periods and temperatures. Although having a lower tensile strength compared to the Inconel alloys, the limiting design option using an SS–304 inner pipe would still meet the safety burst pressure as shown in the results documented in Chapter 6. Therefore, in terms of the tensile strength parameter, all three materials are considered adequate for this HX.

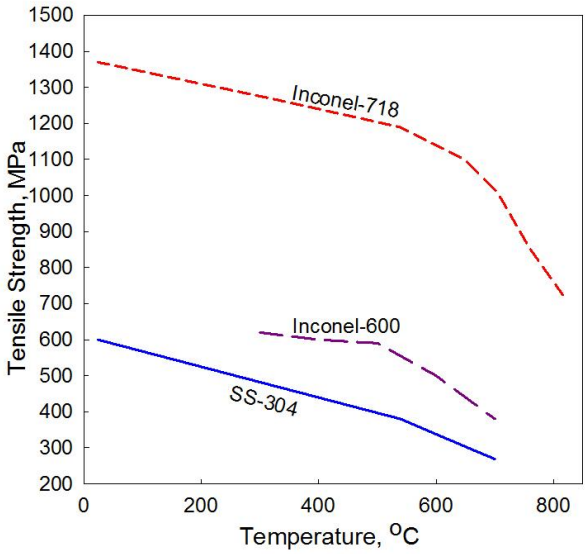

Figure 17. Variation of Tensile Strength for SS–304 (Hendrix Group), Inconel–600 (Annealed, Hot-Rolled Rod) (Special Metals, 2011), Inconel–718 (Hot-Rolled Round, Annealed and Aged 4-in Diameter Rod) (Special Metals, 2011).

The second important parameter relates to a heat transfer property. As shown in Figure 18, the variation in thermal conductivity of the Inconel alloys is linear over the temperature range considered. There is slight non-linear variation in the thermal conductivity of SS–304, but it has a similar behaviour to Inconel–600 and the relative difference is negligible over the temperature range considered. For heat transfer optimization, either the SS–304 or Inconel–600 would be preferred. The Inconel–718 is

approximately 3 W/mK below the other materials, however, if the thermal resistance due to the wall material is much smaller than the fluid interface resistances then this difference in thermal conductivity has a small influence on the overall heat transfer rate. For these preliminary calculations, SS–304 was selected as the HX pipe material based on the bounding burst pressure conditions for the metal. Given that the thermal conductivity profiles of all three materials are nearly identical, the variation did not influence the selection of the piping material. The thermal conductivity of SS–304 is taken from Incropera et al. (2007). Using the available data points a regression model was fit to the data and is shown below:

$$k_w = 2\times10^{-8}\, T_w^{\,3} - 4\times10^{-5}\, T_w^{\,2} - 3.98\times10^{-2}\, T_w + 5.728 \quad \text{(W/m K, } T_w \text{ in K)} \tag{8}$$

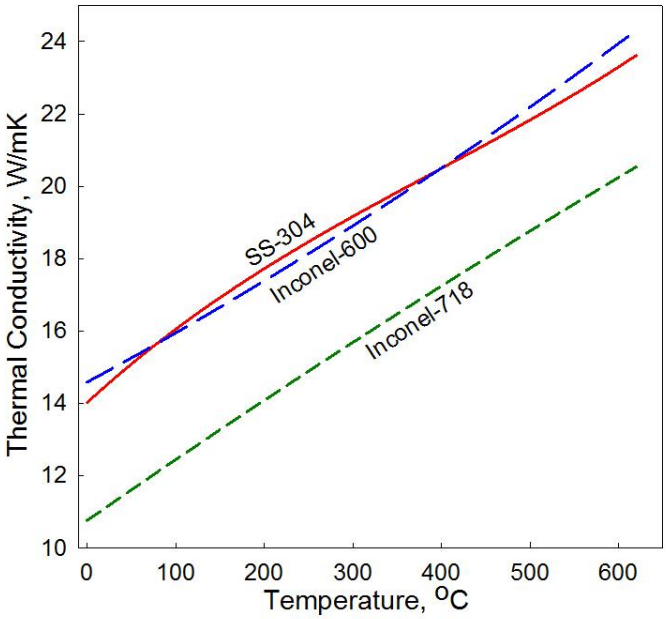

Figure 18. Variation of Material Thermal Conductivities with Temperature (SS–304 - Incropera et al., 2007; Inconels - Special Metals, 2011).

As documented by Pioro and Duffey (2007), SCW thermal power plants have operated as early as 1957, however, integration with NPPs is only now gaining attention. Ornatskiy et al. (1980) recorded tube diameters and thicknesses for several types of tubes used in SCW steam generators in Russia which are shown in Table 7. Using the operational experience from Ornatskiy et al. (1980) attempts were made to select piping sizes for

which the ratio of wall thickness to outer pipe diameter was within the range of ratios determined from their data.

Table 7. Pipe Dimensions in SCW Steam Generator Applications (Ornatskiy et al., 1980).

D_o, mm	Wall Thickness, δ, mm	Ratio (δ/ D_o)
32	6.0	0.188
32	5.0	0.156
25	3.5	0.140
28	6.0	0.214
42	5.0	0.119

4.6 Heat Transfer Enhancement

To optimize the size of the HX design used in this application heat transfer enhancement techniques were considered. Enhancement techniques can be used to increase heat transfer area (finned surfaces), a fluid flow's HTC (surface roughness) or a combination of the preceding factors. It is recommended that any augmentation of the heat transfer surface be applied to the fluid stream that has the dominant thermal resistance in the system (Kuppan, 2000).

Pioro and Duffey (2007) reviewed literature related to heat transfer enhancement of SCW and other fluids in horizontal and vertical circular tubes. Beyond the enhancement of SCW HTCs, pipe augmentation may result in the delay of *deteriorated heat transfer* in higher heat flux and low mass flux scenarios. Experiments have shown that for flow through ribbed tubes temperature peaks were suppressed allowing for higher heat fluxes, in some cases up to 50 – 100% higher compared to smooth tubes, to be applied. The majority of tests with SCW were conducted at pressures of approximately 24 MPa.

In this analysis, focus was given to a passive enhancement technique in the form of helically-corrugated pipes. The use of a helically-corrugated pipe for the inner pipe of a double-pipe HX would introduce a rough surface for both internal and annulus flows resulting in increased heat transfer for both fluids. Additional benefits of helically-corrugated pipes over other types of corrugated pipes include easier fabrication, more

effective heat transfer relative to increased friction factors and low levels of fouling (Sethumadhavan and Rao, 1986). Figure 19 depicts a cross sectional view of an HX pipe with a helically-corrugated inner pipe. This type of arrangement causes secondary flows within the piping resulting in better mixing of the working fluid near the pipe wall and a reduction in the boundary layer also improving heat transfer (Pethkool et al., 2011).

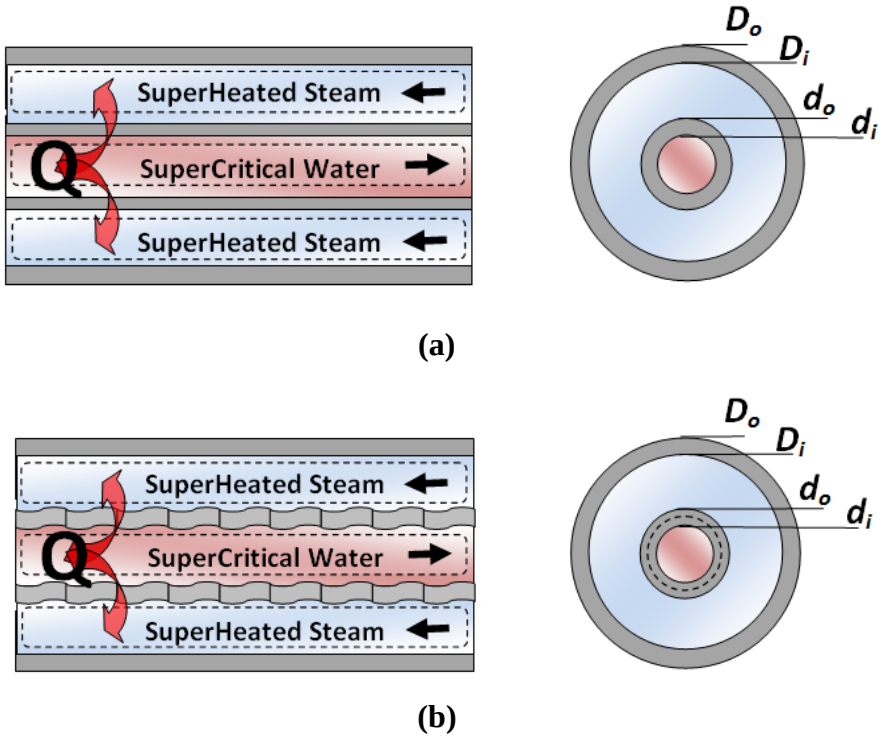

Figure 19. Cross Section of Double-Pipe HX Individual Pipe with (a) Smooth Inner Pipe (b) Helically-Corrugated Inner Pipe.

Helically-corrugated pipes are characterized by three main parameters: pipe diameter, rib height (depth between inner and outer surface) and helical pitch (axial distance between peaks). Studies by Pethkool et al. (2011) investigated various samples of helical pipes in a double-pipe HX and measured enhancement effects on Nusselt number, friction factor and thermal performance factor. The increase in heat transfer across the HX was reported up to 232% while Vicente et al. (2004) reported Nusselt numbers up to 250% greater for helically-corrugated tubes than those for smooth tubes in their experimental analysis.

As discussed in Chapter 6, the thermal resistance of the SCW flow was found to be dominant when the operating conditions were not near the *pseudocritical region*. Within the *pseudocritical region*, the increase in the SCW specific heat along with the widening difference between the wall and bulk-fluid properties caused a notable increase in the flow`s HTC also characterized by a lower thermal resistance compared to the SHS flow and pipe wall material. To account for the change in dominant thermal resistance, enhancement was predicted for both flow streams.

CHAPTER 5 – THERMALHYDRAULIC CALCULATIONS

An iterative process was selected for the HX thermalhydraulic calculations. The basis for this decision stemmed from the potential of widely varying thermophysical properties in the SCW and SHS flows that could not be accounted for in traditional analytical methods such as the LMTD method which assumes, among other properties, constant fluid specific heats across the HX. In the event that the SCW operating fluid would approach the *pseudocritical region*, the thermophysical properties of the fluid would rapidly fluctuate as is shown in Figure 10. To account for the influence of thermophysical property changes in the *pseudocritical region*, iterations were performed at 5 cm and 10 cm axial increments. It was discovered that lowering the step size from 10 cm to 5 cm would improve the accuracy of individual pipe length calculations by approximately 5 cm, a negligible difference in pipe lengths typically exceeding 10 m. Therefore, the impact of the *pseudocritical region* on thermophysical properties could be assessed at either step size. Exceptions to this are discussed later in this chapter. Unless specified otherwise, this investigation used axial increments of 5 cm.

For the counter-flow double-pipe HX, the operating fluids would enter at opposite ends of the HX at the conditions specified in Table 8 for HX A (SCW/SHS) and Table 9 for HX B (HP SHS/LP SHS). The inlet temperature, T_{in}, and pressure, P, parameters for HX A SCW and HX B HP SHS are based on research by Naidin et al. (2009a). The outlet temperature, T_{out}, of the inner pipe operating fluid varies and is governed by the lower temperature limit established for the annulus gap flow. This was defined as 25°C above the saturation temperature of the SHS operating pressure to ensure that SHS flow entering the HX is a single phase fluid without any potential for condensation of the steam. The saturation temperature at 4 MPa and 5 MPa is 250.4°C and 263.9°C, respectively, which in turn translates to limits of 275.4°C and 288.9°C, respectively (NIST, 2010).

Table 8. Operating Fluid Parameters for HX A (SCW/SHS).

Operating Parameter	SCW (Inner Pipe)	SHS (Annulus Gap)
Pressure, P, MPa	25	4, 5
Inlet Temperature, T_{in} °C	625	T_{sat} + 25°C
Outlet Temperature, T_{out} °C	Variable	600

Table 9. Operating Fluid Parameters for HX B (HP SHS/LP SHS).

Operating Parameter	HP SHS (Inner Pipe)	LP SHS (Annulus Gap)
Pressure, P, MPa	5.7	5
Inlet Temperature, T_{in}, °C	625	T_{sat} + 25°C
Outlet Temperature, $T_{out,}$ °C	Variable	600

5.1 Assumptions

Several assumptions were made for this analysis and are documented below:

1. A commercial scale hydrogen production rate of 1 kg/s was selected providing a rate of 86,400 kg/day, which would be classified as a large scale hydrogen production operation; calculations were performed at steady state operating conditions and transient analysis was not considered;
2. Heat losses fromt the system were not accounted for as the outer wall of the outer pipe was assumed to be insulated;
3. Heat transfer was assumed to be one dimensional, in the radial direction; this assumption is challenged for calculations where the SCW enters into the *pseudocritical region* generating large heat fluxes and significant temperature changes which would result in axial heat transfer through the pipe;
4. Unless specified, pressure losses were not considered in this research;
5. Fully-developed flow through straight pipes was assumed and no fouling conditions were experienced on pipe walls;
6. Thermophysical properties for the operating fluids were calculated along the HX pipe length at the same axial position, x; properties calculated at this position were assumed to be representative of conditions within an entire Control Volume (cv) of 5 cm length; for HX A, these positions would

correspond to the SCW inlet to a cv and the exit of SHS from a cv. Figure 21 provides a visual description of this.

5.2 Calculation Methodology

The main computational software used for the analysis was MATrix LABoratory (MATLAB) R2009a. A script was developed, shown in Appendix D, to provide both bulk-fluid and wall-fluid thermophysical properties along the entire length of the HX. These properties would then be used to perform energy balance calculations.

Five input parameters were selected for the script from which all subsequent parameters were calculated. The selected parameters are described as follows:

1. ***SHS/LP SHS Pressure***, P_{SHS} / $P_{LP\ SHS}$ – in terms of MPa; operating pressure of the intermediate circuit SHS that is delivered to the Cu–Cl cycle reactors, limited to 5 MPa and 4 MPa (for HX A) to achieve large SHS temperature differences across the HX.
2. ***Inner Pipe Dimensions***, d_i, d_o – in terms of mm; based on ANSI standard dimensions and input as a pipe outer diameter and wall thickness; discussed in Section 5.2.1.
3. ***Outer Pipe Dimensions***, D_i, D_o – in terms of mm; based on ANSI standard dimensions and input as a pipe outer diameter and wall thickness; discussed in Section 5.2.1.
4. ***SCW/HP SHS Mass Flux***, G_{SCW} / $G_{HP\ SHS}$ – in terms of kg/m^{2}s, values for mass flux were restricted to values that were in agreement with the Mokry et al. correlation test range; individual pipe mass flow rate is determined based on pipe flow area; discussed in Section 5.2.2.
5. ***SHS/LP SHS Mass Flow Rate (per pipe)***, $\dot{m}_{pipe,SHS}$/$\dot{m}_{pipe,LP\ SHS}$ – in terms of kg/s; limited to several flowrates which generated favourable results during initial trial and error testing; discussed in Section 5.2.2.

The software used to calculate the relevant thermophysical properties is NIST REFPROP, Version 9.0 software (2010). Prior to installation of Version 9.0, the latest available version of REFPROP (Version 8.0) was used which for certain test combinations produced fluid properties that led to non-converging wall temperatures (See Chapter 6 and Appendix A). Similar non-convergence was experienced with Version 9 but to a lesser extent. It is recommended that any future reproduction of tests be executed using Version 9, however, the same combinations lead to non-converging results. Discussion on this issue is presented in Chapter 6. The MATLAB script also calculates several material properties for the HX piping in relation to structural integrity. Discussion in Section 5.2.1 outlines all mechanical piping considerations involved in this research.

All of the output parameters were saved in unique Microsoft Excel spreadsheets prepared for each combination evaluated. The output parameters recorded for every cv across the HX length are shown below. Unless otherwise noted, thermophysical properties were calculated for bulk-fluid conditions. As discussed in Chapter 6, results shown in Appendix A document the operating and design parameters for the HX test combinations evaluated and are derived from the calculation outputs below:

Generic Parameters

- Number of HX pipes required for the HX, thermal energy transferred per pipe, single pipe length, average overall HTC, inner pipe wall temperature, inner pipe wall thermal resistance, inner pipe wall thermal conductivity, inner/outer pipe tensile strengths, inner/outer pipe burst pressures

SCW/SHS (HX A) - HP SHS/LP SHS (HX B)

- Cv outlet temperature (SCW/HP SHS), cv inlet temperature (SHS/LP SHS), heat transfer rate, total mass flowrate, fluid density (bulk and wall), bulk-fluid thermal conductivity, fluid dynamic visocity (bulk and wall), Reynolds number, fluid enthalpy (bulk and wall), cross-section averaged specific heat, cross-section averaged Prandtl number, local HTC, flow velocity

Certain parameters calculated through the MATLAB code were manipulated in the Excel spreadsheets to calculate parameters not explicitly found in the code (ie. average overall

HTC, total pipe length, heat transfer area, etc.). A summary of the calculation process described in the remaining sections of Chapter 5 can be found in Appendix C.

5.2.1 Piping Dimensions

Although there is no thorough structural assessment performed as part of this research there is a requirement to know a number of material properties for SS–304 to calculate the burst pressure of the HX piping. This is to ensure that at all positions along the HX length the burst pressure of the inner pipe exceeds the SCW operating pressure of 25 MPa. Only the inner pipe is of major concern since the outer pipe is subjected to SHS pressures of 5 MPa or less. Dimensions for the inner pipe are based on values found in literature (Ornatskiy et al., 1980) and acceptable minimum pipe diameters and wall thicknesses based on burst pressures in excess of the operating pressure using a safety factor of 25% (31.25 MPa for an operating pressure of 25 MPa) as used in previous studies (Thind et al., 2010). The burst pressure of a pipe is dependent on the tensile strength, *S,* wall thickness, δ, and the inner diameter of the pipe, d_i, and is calculated based on Equation 9 documented by Spiegel and Limbrunner (1999):

$$P = \frac{2S \cdot \delta}{d_i} \tag{9}$$

The tensile strength of SS-304 is temperature dependent which influences the burst pressure of the HX piping. Figure 20 shows the variation in tensile strength of SS-304 indicating a decrease in tensile strength with increasing temperature. Therefore, the pipe location having the lowest burst pressure is the SCW entrance to the HX. Effects of thermal cycling were not considered in this work, however, the variability of the SCW outlet temperature would impact the structural properties of the piping on that particular side of the HX, whereas the fixed properties at the SCW entrance/SHS exit would experience constant temperatures, thus less affected by changes in HX operating conditions.

Table 10. SS–304 Tensile Strength with Temperature (Hendrix Group, 2011).

Temperature, °C	24	540	650	700
Tensile Strength, MPa	600	380	303	269

To calculate the inner pipe burst pressure, the inner pipe wall temperature was calculated at each cv increment to obtain the tensile strength. Calculation of wall temperature for the inner pipe is described in the Section 5.2.2. For the outer pipe, the pipe wall temperature was assigned the SHS temperature for each interval since the temperature was assumed to be constant across the wall thickness and the outer surface was insulated. Based on the wall temperature, the tensile strength of SS–304 was calculated using a regression model in Microsoft Excel with an r-squared value of 0.99:

$$S = -0.0004T_w^2 - 0.2034T_w + 605.14 \quad \text{(MPa, } T_w \text{ in °C)} \tag{10}$$

There is a large gap within the data of Table 10 between temperatures of 24°C and 540°C; however, there are several data points within the region where the tensile strength is lowest and of greatest concern for this research. Therefore, the regression equation for tensile strength was considered adequate for use in calculations of burst pressure.

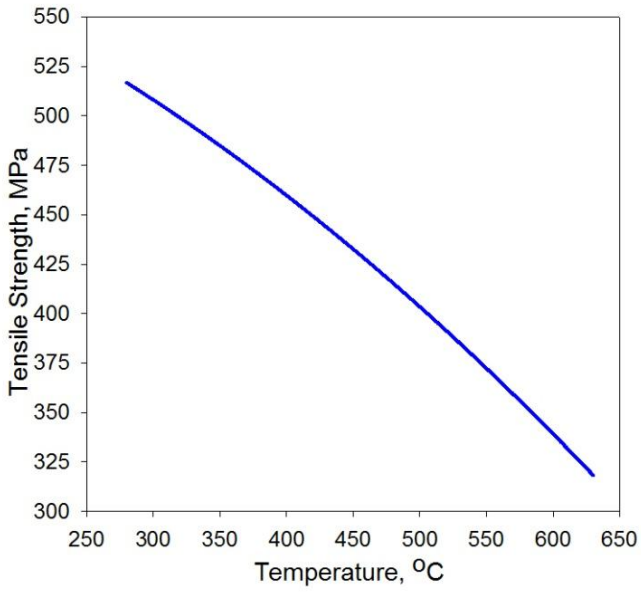

Figure 20. Variation of SS–304 Tensile Strength with Temperature Using a Regression Fit Formula.

Pipe sizes selected for analysis were restricted to those listed within ANSI Standards to produce a more standardized design. Furthermore, dimension selections were maintained within similar ratios of wall thickness to outer pipe diameter from the Ornatskiy et al. (1980) data shown in Table 7. Table 11 shows the ratios of inner piping used in this analysis. Only the inner pipe ratios are presented as the high pressure SCW will interact only with this piping. With the exception of combination 2, all of the ratios are within the bounds of the Ornatskiy et al. (1980) steam generator data. The combinations of piping dimensions used for the inner and outer pipes in this analysis are shown in Table 12. The inside diameter of the piping is calculated according to Equation 11 and Equation 12 where d_i and d_o represent the inner and outer diameters of the inner pipe, respectively, δ_d represents the wall thickness of the inner pipe, D_i and D_o represent the inner and outer diameters of the outer pipe, respectively, and δ_D represents the wall thickness of the outer pipe.

$$d_i = d_o - 2\delta_d \tag{11}$$

$$D_i = D_o - 2\delta_D \tag{12}$$

Table 11. Inner Pipe Dimensions with Wall Thickness to Outer Diameter Ratio.

Combination	d_o, mm	δ_d, mm	Ratio (δ_d/d_o)
1	21.3	3.73	0.175
2	26.7	2.87	0.107
3	26.7	3.91	0.146
4	26.7	5.56	0.208

Table 12. Inner and Outer Pipe Dimension Combinations – ANSI Standards.

Combination	Inner Pipe (d_o/δ_d), mm	Combination	Outer Pipe (D_o/δ_D), mm
1	21.3/3.73	1	26.7/1.65
2	26.7/2.87	2	33.4/1.65
3	26.7/3.91		
4	26.7/5.56	3	33.4/2.77

5.2.2 Temperature Calculations

As defined earlier in this chapter, operating fluid temperatures were calculated iteratively to account for thermophysical property variations experienced in the SCW *pseudocritical region* for a number of test combinations. The fluid temperature of each stream was assumed to be constant inside subsequent cvs and thermophysical properties of each fluid were evaluated at the same axial position, *x*, of HX piping. For example, in a given cv the SCW fluid properties were calculated at the entrance of SCW into a cv while SHS fluid properties were evaluated where the SHS exits from a cv. Figure 21 shows a cross section of an individual HX pipe arrangement showing the thermal energy transfer, *Q*, between the counter-flowing fluids and the reference positions where properties are calculated. All properties for this cv would be calculated at positions *x-1* and *x,* and be valid in that cv.

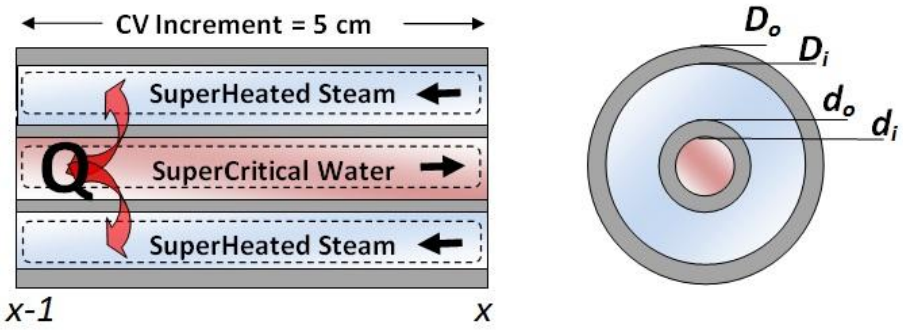

Figure 21. Cross Section of the Double-Pipe HX.

As discussed in earlier sections, the Mokry et al. (2009) correlation was used as the heat transfer correlation for all SCW and SHS flows. As this correlation relies on both bulk-fluid and wall-fluid thermophysical properties the MATLAB script was sectioned into two calculation groups based on local thermophysical properties each calculated at the location specific temperature using NIST REFPROP:

- ***SCW/SHS Bulk-Fluid properties***: Fluid Density, $\rho_{b,SCW}/\rho_{b,SHS}$; Fluid Thermal Conductivity, $k_{b,SCW}/k_{b,SHS}$; Dynamic Viscosity, $\mu_{b,SCW}/\mu_{b,SHS}$; Specific Enthalpy, $H_{b,SCW}/H_{b,SHS}$

- ***SCW/SHS Wall-Fluid properties***: Fluid Density, $\rho_{w,SCW}/\rho_{w,SHS}$; Dynamic Viscosity, $\mu_{w,SCW}/\mu_{w,SHS}$; Specific Enthalpy, $H_{w,SCW}/H_{w,SHS}$

The first parameter required for the Mokry et al. (2009) correlation is the fluid Reynolds number. The SCW mass flow per pipe is first calculated using Equation 13 where $A_{c,i}$ is the cross sectional area of the inner pipe in m^2, and G_{SCW} has been defined as the SCW mass flux in kg/m^2s. This calculation is not required for the SHS flow since the mass flow rate per pipe is a user input parameter for the MATLAB script. The Reynolds number is calculated using Equation 14 and Equation 15 for the inner pipe and annulus gap fluid flows, respectively.

$$\dot{m}_{pipe,SCW} = G_{SCW} A_{c,i} \tag{13}$$

$$\mathbf{Re}_{b,SCW,x} = \frac{G_{SCW} d_i}{\mu_{b,SCW,x}} = \frac{4\dot{m}_{pipe,SCW}}{\pi d_i \mu_{b,SCW,x}} \tag{14}$$

$$\mathbf{Re}_{b,SHS,x} = \frac{G_{SHS} D_{hy}}{\mu_{b,SHS,x}} = \frac{4\dot{m}_{pipe,SHS}}{\pi(d_o + D_i)\mu_{b,SHS,x}} \tag{15}$$

Following the calculation of the bulk-fluid properties, wall-fluid properties were obtained in parallel by first determining the wall temperature to be used in a given cv. The wall temperature was calculated iteratively and considered constant within each cv. For each new cv an initial wall temperature was assumed, arbitrarily selected as 0.08 K below the SCW temperature at the entrance of the cv, to permit the start of an interative calculation for the cv. Using this temperature, the wall-fluid parameters for both streams were calculated. The cross-section averaged specific heat, calculated using Equation 16 was obtained, followed by the cross-section averaged Prandtl number using Equation 17. The Mokry et al. (2009) correlation was then used to calculate the Nusselt number (Equation 18) followed by the local SCW and SHS HTCs in Equation 19 and 20, respectively.

$$\overline{c_{p,x}} = \left(\frac{H_{w,x} - H_{b,x}}{T_{w,x} - T_{b,x}}\right) \tag{16}$$

$$\overline{\mathbf{Pr}_{b,x}} = \left(\frac{\mu_{b,x}\overline{c_{p,x}}}{k_{b,x}}\right) \tag{17}$$

$$\mathbf{Nu}_{b,x} = 0.0061\mathbf{Re}_{b,x}^{0.904}\overline{\mathbf{Pr}}_{b,x}^{0.684}\left(\frac{\rho_{w,x}}{\rho_{b,x}}\right)^{0.564} \tag{18}$$

$$h_{SCW,x} = \frac{\mathbf{Nu}_{b,SCW,x}k_{b,SCW,x}}{d_i} \tag{19}$$

$$h_{SHS,x} = \frac{\mathbf{Nu}_{b,SHS,x}k_{b,SHS,x}}{D_{hy}} \quad \text{where } D_{hy} = \frac{4A_c}{p_{wet}} = D_i - d_o \tag{20}$$

Knowing the local HTCs, the thermal resistances on the SCW and SHS side were calculated according to Equations 21 and 22.

$$R_{SCW,x} = \frac{d_o}{d_i h_{SCW,x}} \tag{21}$$

$$R_{SHS,x} = \frac{1}{h_{SHS,x}} \tag{22}$$

The wall temperature, T_w, was then calculated according to Equation 23 as suggested by Shah and Sekulic (2003). This equation assumes the thermal resistance of the wall to be negligible. As a result, wall thermophysical properties for both operating fluids were calculated using the same wall temperature. To support this assumption, test cases completed showed the thermal resistance of the wall to be between 10-20% of the total resistance network for the majority of the cases evaluated which is reasonably small compared to the contribution of the other resistances. For test cases where the SCW flow entered the *pseudocritical* range near the exit of the HX, the SCW thermal resistance dropped significantly, consequently increasing the thermal resistance contribution of the SHS and pipe wall. This assumption would create errors in the *pseudocritical region* and since wall resistance was neglected in this work, it should be considered in future analysis. An example of the variation in thermal resistance for the operating fluids and pipe wall can be seen in the results shown in Chapter 6.

$$T_{w,x} = \frac{\left(T_{b,SCW,x-1}/R_{SCW,x}\right)+\left(T_{b,SHS,x-1}/R_{SHS,x}\right)}{\left(1/R_{SCW,x}\right)+\left(1/R_{SHS,x}\right)} \quad (23)$$

Two end results were possible for each wall temperature iteration. If the difference between the assumed wall temperature and calculated wall temperature was equal to or exceeded 0.001 K, one half of the difference between calculated and assumed wall temperature was subtracted from the calculated value becoming the new "assumed" value. If the difference between the two parameters was below –0.001 K, the wall temperature was increased by half of the difference. These iterations were performed until the difference in wall temperature between calculations was less than 0.001 K or the number of iterations exceeded 1000. In the majority of cases tested, convergence was reached within 80 iteration steps or less.

Using the wall temperature, the thermal conductivity of the pipe wall was calculated using the regression model for SS–304 referenced in Chapter 4. This supported the calculation of the pipe wall resistance using Equation 24. Note that Equation 24 accounts for the thermal resistance of the wall unlike Equation 23.

$$R_{w,x} = \frac{d_o \ln\left(d_o/d_i\right)}{2k_{w,x}} \quad (24)$$

Having solved for the $R_{SCW,x}$, $R_{SHS,x}$ and $R_{w,x}$ the overall HTC, U_x, was calculated using Equation 25. The overall HTC was defined in terms of the outer wall of the inner pipe.

$$\frac{1}{U_x} = R_{SCW,x} + R_{w,x} + R_{SHS,x} \quad (25)$$

Following the calculation of the overall HTC, energy balances were performed between the two operating fluid streams in successive cvs across the length of the HX.

A second set of iterations were required to solve for operating fluid temperatures in each cv. Thermal energy balance equations were developed for this analysis closely following the process outlined by Ribando et al. (1997) who developed a computer-based tool to perform HX numerical analysis. Equations 26 and 27 define the energy balance for each operating fluid. The difference between the thermal energy content change (increase or decrease) in one of the fluids must equal the thermal energy transferred from or to that fluid. The same conditions must be satisfied for the opposite fluid. In the heat transfer terms in the equations below the temperatures used are the average values of the operating fluid temperature in the cv since the temperature change for both fluids is approximately linear. The heat transfer area for the cv is defined by the outer wall of the inner pipe and shown as A_{inc} in the following equations. It is again important to note that the fluids flow in opposite directions and the SCW outlet temperature, $T_{SCW,x}$, and SHS inlet temperature, $T_{SHS,x}$, are the unknown parameters for each cv. A cv's inlet SCW temperature is shown as $T_{SCW,x\text{-}1}$ while the exit temperature of SHS is shown as $T_{SHS,x\text{-}1}$.

$$\dot{m}_{SCW} c_{p,SCW,x}\left(T_{SCW,x-1} - T_{SCW,x}\right) - U_x A_{inc}\left[\frac{T_{SCW,x-1}+T_{SCW,x}}{2} - \frac{T_{SHS,x}+T_{SHS,x-1}}{2}\right] = 0 \quad (26)$$

$$\dot{m}_{SHS} c_{p,SHS,x}\left(T_{SHS,x} - T_{SHS,x-1}\right) - U_x A_{inc}\left[\frac{T_{SHS,x}+T_{SHS,x-1}}{2} - \frac{T_{SCW,x-1}+T_{SCW,x}}{2}\right] = 0 \quad (27)$$

Similar to the wall temperature calculations, a value for the inlet SHS temperature, $T_{SHS,x}$, was arbitrarily assumed to be 0.08 K less than the outlet SHS temperature in the cv. This assumed value was then used in Equation 28 to calculate an SCW outlet temperature which then allowed the calculation of a new SHS inlet temperature through, Equations 29.

$$T_{SCW,x} = \frac{\left(\dot{m}_{SCW} c_{p,SCW,x} - 0.5 U_x A_{inc}\right) T_{SCW,x-1} + 0.5 U_x A_{inc}\left(T_{SHS,x-1}+T_{SHS,x}\right)}{\dot{m}_{SCW} c_{p,SCW,x} - 0.5 U_x A_{inc}} \quad (28)$$

$$T_{SHS,x} = \frac{\left(\dot{m}_{SHS} c_{p,SHS,x} - 0.5 U_x A_{inc}\right) T_{SHS,x-1} + 0.5 U_x A_{inc}\left(T_{SCW,x-1}+T_{SCW,x}\right)}{\dot{m}_{SHS} c_{p,SHS,x} - 0.5 U_x A_{inc}} \quad (29)$$

From these temperatures, the change in thermal energy of both operating fluids was calculated using Equations 30 and 31 and the difference between the totals was recorded. The difference between the assumed and calculated SHS inlet temperatures was also recorded.

$$Q_{SCW} = \dot{m}_{SCW} c_{p,SCW,x} \left(T_{SCW,x-1} - T_{SCW,x} \right) \tag{30}$$

$$Q_{SHS} = \dot{m}_{SHS} c_{p,SHS,x} \left(T_{SHS,x} - T_{SHS,x-1} \right) \tag{31}$$

Using the same approach as for the pipe wall temperatures, two scenarios were developed for the iterative steps. If the difference between the energy was equal to or exceeded 0.001 J, one half of the difference between the assumed SHS temperature and the calculated SHS inlet temperature was subtracted from the calculated SHS temperature. Oppositely, if the difference between the energies was less than –0.001 J, the SHS temperature was increased by half of the difference. Iterations were performed until the difference between the thermal energies was less than 0.001 J. Convergence was typically achieved within 20 iteration steps.

The iteration process was repeated for each cv until the calculated SHS inlet temperature entering a cv reached the established temperature boundary condition of 25°C above the SHS saturation temperature at the operating pressure. In the case of a 5 MPa operating pressure, iterations were ended once the SHS temperature reached approximately 289°C.

Early testing through a trial and error approach was used to identify design and operating parameters combinations that produced favourable results. Based on the results of the early trials, a matrix of test conditions was developed and used to perform formal trials to identify combinations of parameters suitable for further analysis. Future recommended optimization of the suitable test combinations will assist in determining the optimal design and operating conditions of the HX. The 5 input parameters described earlier in this section and the specific values under each category are shown in Table 13 and 14 for HX A and HX B, respectively. These parameters were treated as user inputs to the MATLAB script. For example, an HX A design with an SHS operating pressure of 5 MPa, an SCW mass flux of 200 kg/m^{2}s, an SHS pipe mass flow rate of 0.10 kg/s, inner

pipe dimensions of 26.7 mm (d_o)/2.87 mm (δ_d) and outer pipe dimensions of 33.4 mm (D_o)/1.6 mm (δ_D) would be coded as 11222. Table 15 shows codes for HX A and HX B that are discussed in greater detail in Chapter 6 and in Appendix B.

Table 13. HX A Test Codes Developed for MATLAB Script.

#	SHS Pressure, MPa	#	SCW Mass Flux, kg/m^{2}s	#	SHS Mass Flowrate, kg/s	#	Inner Pipe Dimensions (d_o / δ_d), mm	#	Outer Pipe Dimensions (D_o / δ_D), mm
1	5	**1**	200	**1**	0.07	**1**	21.3/3.73	**1**	26.7/1.65
		2	250	**2**	0.10	**2**	26.7/2.87	**2**	33.4/1.65
2	4					**3**	26.7/3.91		
		3	300	**3**	0.13	**4**	26.7/5.56	**3**	33.4/2.77

Table 14. HX B Test Codes Developed for MATLAB Script.

#	LP SHS Pressure, MPa	#	HP SHS Mass Flux, kg/m^{2}s	#	LP SHS Mass Flowrate, kg/s	#	Inner Pipe Dimensions (d_o / δ_d), mm	#	Outer Pipe Dimensions (D_o / δ_D), mm
1	5	**1**	400	**1**	0.07	**1**	21.3/3.73	**1**	26.7/1.65
		2	600	**2**	0.10	**2**	26.7/2.87	**2**	33.4/1.65
						3	26.7/3.91	**3**	33.4/2.77

Table 15. HX A and HX B Test Codes Analyzed in Chapter 6/Appendix B.

Type	Code	SHS/LP SHS Pressure, MPa	SCW/HP SHS Mass Flux, kg/m^{2}s	SHS/LP SHS Mass Flowrate, kg/s	Inner Pipe Dimensions (d_o / δ_d), mm	Outer Pipe Dimensions (D_o / δ_D), mm
HX A	**11111**	5	200	0.07	21.3/3.73	26.7/1.65
	11222	5	200	0.10	26.7/2.87	33.4/1.65
	13122	5	300	0.07	26.7/2.87	33.4/1.65
	13232	5	300	0.10	26.7/3.91	33.4/1.65
	13132	5	300	0.07	26.7/3.91	33.4/1.65
	21222	4	200	0.07	21.3/3.73	26.7/1.65
HX B	**11232**	5	400	0.10	26.7/3.91	33.4/2.77
	12111	5	600	0.07	21.3/3.73	26.7/1.65

Two operating pressures for the SHS flow were chosen: 5 and 4 MPa. The saturation temperature at these pressures was reasonably low allowing for significant temperature differences to be achieved by the SHS across an HX pipe. Second, the density of SHS at these pressures supported reasonable flow velocities. Further increasing the pressure of

the SHS would reduce the flow velocity resulting in lower pressure losses; however, this would also decrease the Reynolds number of the SHS flow likely reducing the heat transfer rate. Also, it is anticipated that intermediate loop pressures of 4 or 5 MPa would not create significant technical challenges for integrating the intermediate loop piping into the Cu–Cl reactors which operate at pressures of several atmospheres.

The SCW mass flux and SHS mass flow rates were key parameters in selecting design combinations that would produce favourable HX temperature profiles and fluid flow velocities. A restriction for the SCW flow was that it had to meet the criteria set out by the Mokry et al. (2009) correlation test conditions. Therefore, the lower bounding value for the SCW mass flux was 200 kg/m^{2}s. During preliminary testing, small incremental variations in the SHS flow rate were tested producing significantly different results. Larger SHS flow rates resulted in unreasonable flow velocities. Moreover, larger SHS flow rates generated high heat transfer rates in the early stages of iterations, quickly diminishing the temperature difference between the two operating fluids effectively ceasing further heat transfer for the remainder of the calculations. This was also a consequence, and limitation, of performing calculations in an axial direction from one side of the HX. This is further discussed in Chapter 6.

For HX A, there were 81 separate tests performed using SHS pressures of 5 MPa. Suitable combinations were those that permitted the HX SHS inlet (T_{sat} + 25°C) and outlet (600°C) conditions to be met, in addition to having a maximum SHS flow velocity of less than 75 m/s, assumed for this analysis. Limitations for SHS velocities are derived mainly from pressure drop considerations and sources show that maximum flows should be restricted to between 50 – 70 m/s (Spirax-Sarco, 2011). For this analysis, it was assumed that values up to 75 m/s would be feasible. Using the successful 5 MPa test cases, a total of 15 additional test cases were run for the 4 MPa pressures to compare the effects of varying SHS pressure. From these tests, 11 were determined to be suitable based on the established maximum velocity. In total, 26 suitable combinations for HX A are proposed for future work.

For HX B, 28 combinations were tested. This number is much lower compared to the HX A trials since only one LP SHS operating pressure was tested and both the HP SHS flux and LP SHS mass flow rates were limited to two inputs, as shown in Table 14. Higher flowrates would require a larger volume of HP SHS to be diverted from the NPP loop. Since the HP SHS mass flowrate exiting the reheat channels is only 780 kg/s the allowable steam demand for the HX was limited to just over half of the remaining flow (400 kg/s). Since this selection was made without a firm basis of the NPP's reheat flowrate needs it would be inappropriate to limit some combinations from future consideration. Therefore, combinations with total HP SHS flowrates in excess of 400 kg/s but having maximum LP SHS velocities of less than 75 m/s are distinguished separately as is discussed in Chapter 6. In this research, only 5 HX B combinations were deemed suitable to be progressed for future analysis.

5.2.3 MATLAB Code Verification

A verification process was performed on the primary code developed in MATLAB using Microsoft Excel iterative based calculations. Using the same equations defined in this investigation, calculations were performed independently in Excel to solve for the operating temperatures of the HX using the Mokry et al. (2009) correlation. Calculations regarding the material properties of piping material were not replicated as they were not iterative based and so MATLAB values were assumed to be correct.

Two comparisons were performed against the MATLAB code, one for each of the HX designs under consideration. Results of the two test trials are shown in Appendix B along with percentage difference relative to the MATLAB values for the SCW/HP SHS outlet temperature, SHS inlet temperatures and wall temperatures. From the sample set, ten data points were selected across the length of the HX at equal intervals, including the entrance and exit states of the fluids. In addition, the data points with the maximum differences were identified and listed. Additional points were selected for flow within the *pseudocritical region*. Results showed a negligible difference between the MATLAB and Excel values raising confidence in the calculation procedure used.

5.2.4 Pressure Drop Calculation

Although pressure losses were neglected in the majority of this investigation, this section provides limited discussion as well as pressure drop formulae which were used for a single calculation. The pressure drop across the HX may become a limiting factor in future design calculations due to excessive compressor requirements for the intermediate SHS flow loop.

Due to the large volume of SHS passing through individual pipes, the velocity of the SHS is significantly greater than that of the SCW, as shown in the results listed in Table A3, A5 and A6, which translates into larger pressure losses for the SHS flow. The pressure drop across a section of piping depends on the fluid flow characteristics, density, flow velocity, piping material and pipe diameter. Experimental results have produced friction factors which attempt to quantify the impact of Reynolds number variation and pipe surface conditions on pressure losses. Equations 32 and 33 show a friction factor, *f*, correlation, applied to the SCW and SHS flows, documented in Incropera et al. (2007) and is valid for $3000 \leq \mathbf{Re} \leq 5\times10^6$.

$$f_{SCW,x} = \frac{1}{(1.82\log(\mathbf{Re}_{SCW,x})-1.64)^2} \tag{32}$$

$$f_{SHS,x} = \frac{1}{(1.82\log(\mathbf{Re}_{SHS,x})-1.64)^2} \tag{33}$$

The pressure drop across a section of piping was determined using a modified equation documented by Incropera et al. (2007). Equations 34 and 35 calculate the pressure drop, Δp, in kPa, across a single cv.

$$\Delta p_{SCW,x} = \frac{0.001 x f_{SCW,x}}{2 d_i \rho_{b,SCW,x}} \left(\frac{\dot{m}_{SCW}}{A_c}\right)^2 \tag{34}$$

$$\Delta p_{SHS,x} = \frac{0.001 x f_{SHS,x}}{2 D_{hy} \rho_{b,SHS,x}} \left(\frac{\dot{m}_{SHS}}{A_c}\right)^2 \tag{35}$$

The drop in pressure in both flows influenced the thermophysical properties extracted from the NIST REFPROP program. Pressure losses were evaluated for a single HX A code, 13122, which generated a small HX pipe length. This is further discussed Chapter 6. Due to the short pipe length, the expected pressure losses on both the SCW and SHS flow streams would be limited. Combinations requiring longer pipe lengths would not be advantageous due to the high flow velocities typically associated with such combinations and the large pipe surface area contributing to frictional losses.

In relation to the calculation procedure, pressure drop values increased along the pipe length in the direction of flow which introduces complexity for a counter-flow design. Thus, for the SCW flow, the initial pressure was reduced along the pipe length based on the pressure drop calculated across each subsequent cv, per Equation 36. Oppositely, for the SHS flow, a total pressure drop across the HX pipe length had to be assumed and pressure drops were calculated in the reverse direction to reach the known inlet pressure. The pressure drop profile was calculated according to Equation 37. This required manual iterations to identify a total pressure drop that would result in the correct pressure at the SHS inlet.

$$p_{SCW,x} = p_{SCW,x-1} - \Delta p_{SCW,x} \tag{36}$$

$$p_{SHS,x} = p_{SHS,x-1} + \Delta p_{SHS,x} \tag{37}$$

The MATLAB code found in Appendix D outlines pressure drop calculations for HX A code 13122 and is only applicable for this combination. Trials for other codes require manual manipulation of the SHS pressure drop across the HX.

CHAPTER 6 – RESULTS AND DISCUSSION

Results from this research are divided into HX A and HX B discussions. As discussed in Chapter 5, the methodology involved testing combinations of design and operating parameters (defined in Table 13 and 14) to identify those most suitable for future consideration. Complete data sets for the individual tests can be found in Appendix A, while the discussion here is based on a summary of the main results from these tests. As described in Chapter 5, the test cases satisfy a hydrogen production rate of 1 kg/s and the total thermal energy transferred across the HX is approximately 224 MW which meets the thermal energy requirement of the Cu–Cl cycle. It is important to note that this analysis does not consider thermal losses between the two facilities.

6.1 Results for HX A (SCW/SHS) Design

Tables A3 and A4 contain summary information for 81 HX A combinations. Of these combinations tested at 5 MPa SHS pressure, 15 sets (shown with a green "P") were deemed to be suitable for further investigation as they meet bounding SHS temperatures (T_{sat} + 25°C and 600°C) and the maximum flow velocity of the SHS was below 75 m/s based on restrictions set in Chapter 5.

From the group of test cases, five test combinations exhibited non-coverging wall temperatures (exceeding 1000 iterations) in the SCW *pseudocritical region* and are shown in Table A3 with a yellow "E". No definitive cause was identified for these discontinuities. Reductions in calculation precision were tested from 0.001 to 0.1 K for wall temperature and 0.001 to 0.1 J for energy balance, however, the same outcomes were experienced. It is possible that the properties in the *pseudocritical region* vary so widely, especially for the cross section averaged specific heat and fluid densities that for these particular codes a converging result for the Nusselt number cannot be obtained. Additionally, the Mokry et al. correlation is applicable for *normal* and *improved heat transfer* regimes, however, for flows in the *deteriorated heat transfer* regime it may not produce converging results for all cases. Mokry et al. (2011) proposed an empirical correlation to calculate the minimum applied heat flux prior to the onset of deteriorated

heat transfer; this was shown to be dependent on the mass flux of the operating fluid. Using the correlation, it was determined that SCW flow heat flux values for each of the non-converging combinations exceeded this minimum near the outlet from the HX. Although other combinations also exceeded the minimum heat flux values, the specific operating conditions may have still produced converging results. Since a formal disposition cannot be provided, these combinations should be considered in future work in parallel with work on *deteriorated heat transfer* regimes to determine the overall impact on HX design.

Table A3 lists 15 combinations with maximum SHS velocities exceeding 75 m/s which could limit future viability when considering pressure losses and pipe erosion. Taking this into account, test codes with velocities exceeding 75 m/s are recommended to be excluded from future work. Next, Table A4 documents test combinations which were shown to be thermodynamically incompatible, or alternatively, the operating and physical design parameter combinations would produce an improperly sized HX for the required thermal load. Using Figure 35 as an example, the temperature difference between operating fluids quickly diminishes due to the high heat transfer rate which is the result of the large SHS mass flux and the small pipe dimensions considered for this combination. Other unsuitable combinations would produce similar results and due to this they should not be investigated in future research.

Design parameters and operating conditions for one successful test combination, HX A code 11222, are outlined in Figure 22 to 28. Under these design parameters, the inner pipe burst pressure would be approximately 90 MPa; nearly 3.6 times larger than the 25 MPa operating pressure of the SCW contained within. Since the tensile strength increases as temperature decreases, the burst pressure of both inner and outer piping would increase with increasing distance away from the SCW inlet.

Code 11222 would enable sufficient heat transfer to bring the SCW flow into the *pseudocritical region* near the SCW exit of the HX. As shown in Figure 23, the SCW exits at a temperature slightly above the *pseudocritical* temperature of 384.9°C. This

corresponds to a sharp increase in the local HTC at the inner pipe wall and a near doubling of the overall HTC. Figure 24 shows the thermal resistances of the SCW and SHS flows and the inner pipe wall across the length of the HX. The temperature of the SHS increases drastically as it enters the HX due to the SCW that reaches the *pseudocritical region* at the exit of the HX. The temperature gradient of the SHS increases as the SCW progresses into the *pseudocritical region* limiting the possibility of achieving a desired SCW outlet temperature of 350°C. The heat flux near the exit would be approximately 11 times larger in magnitude compared to the entrance into the HX (230 kW/m^2 versus 21 kW/m^2). The significant SHS temperature variation when the SCW is in the *pseudocritical region* restricts the development of an HX that would have an SCW outlet temperature below the *pseudocritical* temperature. Therefore, an HX with an SCW outlet temperature well above, or very near to this point should be considered in future research.

Thermophysical properties of the SCW flow for HX A code 11222 are shown in Figure 25 and 26. Properties in Figure 26 are used directly in the Mokry et al. (2009) correlation. The SCW wall-fluid enters the *pseudocritical region* prior to the bulk fluid ($T_{b,SCW} > T_{w,SCW}$) which is reflected by the larger fluid enthalpy, viscosity and density variations of the wall fluid. The cross section averaged specific heat and averaged Prandtl numbers (Figure 25 and 26) both exhibit a maximum at approximately 398°C, prior to the *pseudocritical* temperature. Since the Mokry et al. correlation (Equations 5/18) relies on pipe cross-section averaged parameters, the effects of the *pseudocritical point* are experienced differently by the bulk and wall fluids. As the wall fluid is several degrees below the bulk fluid, it reaches the *pseudocritical* temperature which results in rapid property changes and contributes to a peak in the parameters prior to the actual peak that would be experienced if only bulk-fluid parameters were considered. Doubling of the bulk-fluid thermal conductivity (Figure 25) within the *pseudocritical region* does not overcome the six-fold increase in the SCW Nusselt number (Figure 26) which creates a peak in the local SCW HTC (Figure 23) and an associated minimum in the SCW thermal resistance (Figure 24) which is typically the dominant resistance of the fluid flows. This maximum diminishes quickly as the increase

in fluid viscosity reduces the SCW Reynolds number and lowers the Nusselt number (Figure 26). The drop in average specific heat further reduces the Nusselt number.

The thermophysical properties of the SHS flow for HX A code 11222 are shown in Figure 27 and 28. Recall, the SHS flows opposite to the SCW in the HX or right to left on the graphs in the proceeding pages. Variation in the SHS properties is shown to be not as significant given the absence of a *pseudocritical region.* Compared to the SCW flow, the SHS bulk-fluid properties experience more change relative to the wall-fluid properties. This is due to the SHS bulk temperature rising considerably upon entering the HX while the wall temperature is already at a higher temperature resulting in a higher fluid wall temperature (Figure 24). Heating of the SHS is accompanied by a drop in the average specific heat of the fluid and rise in the thermal conductivity (Figure 27). An increase in the fluid viscosity produces a drop in the Reynolds number whereas the average Prandtl number does not change significantly over the HX length (Figure 28). The variations in these parameters are not drastic enough to heavily influence the local HTC which remains essentially constant across the length of the HX. The largest impact on the flow is the decrease in fluid density (Figure 28), which in turn increases flow velocity and consequently pressure losses and pipe erosion.

Although detailed pressure losses were not considered in the majority of this work, maximum flow velocities were recorded to provide insight into potentially limiting arrangements. For code 11222, the maximum SHS flow velocity was estimated to be 52 m/s at the SHS outlet, whereas the maximum SCW flow velocity would be only 3 m/s, occurring at the SCW inlet as shown in Table 16. If the SHS operating pressure reduced to 4 MPa, the maximum velocity would increase to 65 m/s. One of the advantages of a reduced operating pressure would be the larger temperature difference the SHS passes through from the lower boundary condition up to 600°C and the improved heat transfer due to increased turbulence. For code 11222, reducing the pressure to 4 MPa would reduce the overall pipe length required for the HX by approximately 7% (Table 16). Codes such as 11222 exhibit longer HX pipe lengths and maintain a small temperature difference between the two operating fluids over the HX length.

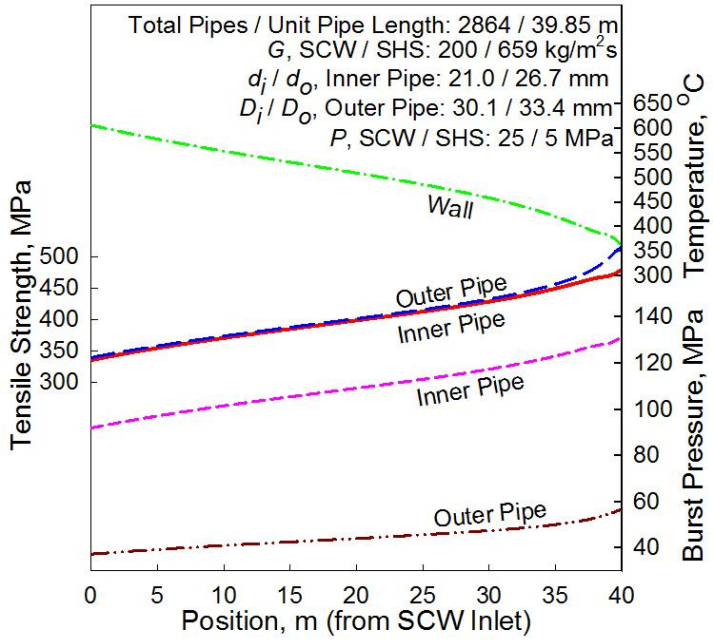

Figure 22. HX A Pipe Burst Pressure and Tensile Strength for SS–304 Pipes, Code 11222, 5–cm Interval.

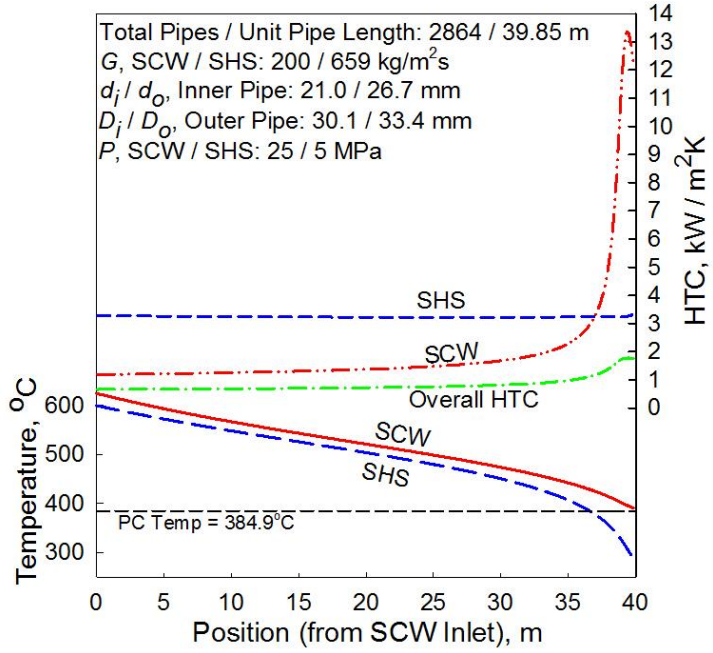

Figure 23. HX A SCW and SHS Fluid Temperature and Local and Overall HTCs Along an HX Pipe Operating Downstream of the SCWR Outlet, Code 11222, 5–cm Interval.

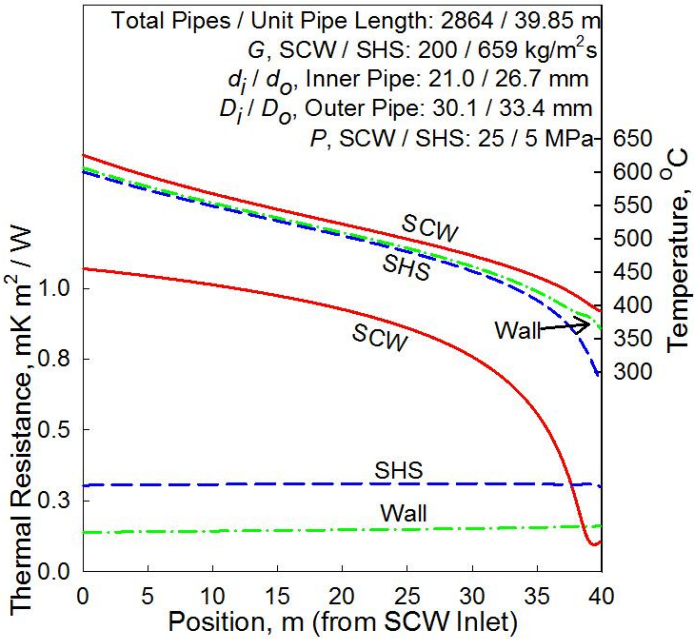

Figure 24. HX A SCW and SHS Fluid Temperature and Thermal Resistances Along an HX Pipe Operating Downstream of the SCWR Outlet, Code 11222, 5–cm Interval.

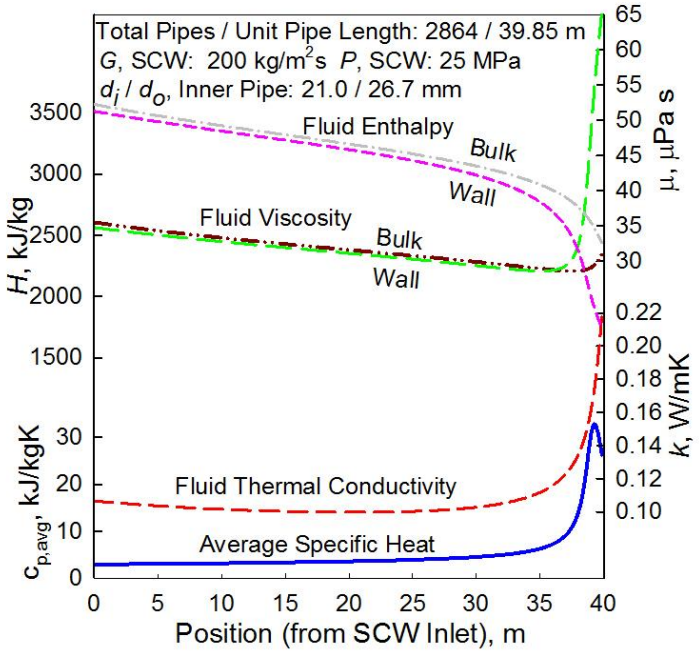

Figure 25. HX A SCW Thermophysical Properties Along an HX Pipe Operating Downstream of the SCWR Outlet Supporting the Mokry et al. Correlation, Code 11222, 5–cm Interval.

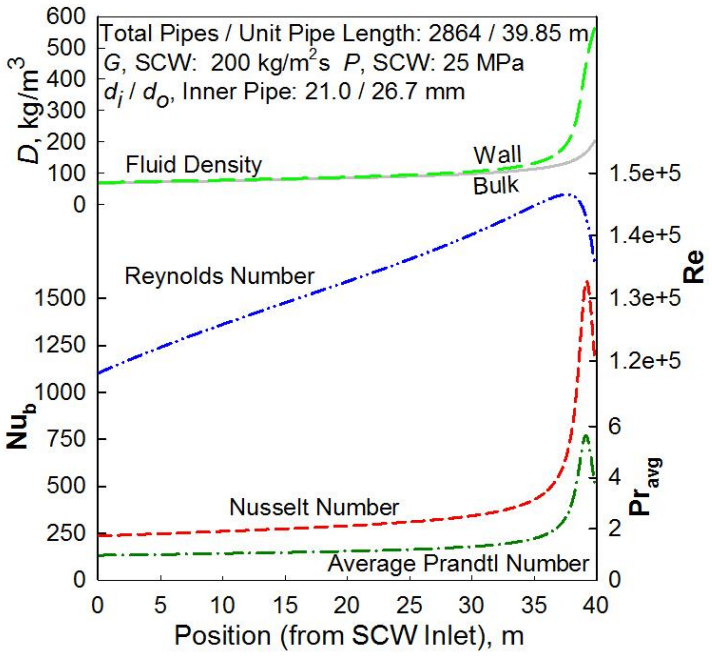

Figure 26. HX A SCW Thermophysical Properties Along an HX Pipe Operating Downstream of the SCWR Outlet Used in the Mokry et al. Correlation, Code 11222, 5–cm Interval.

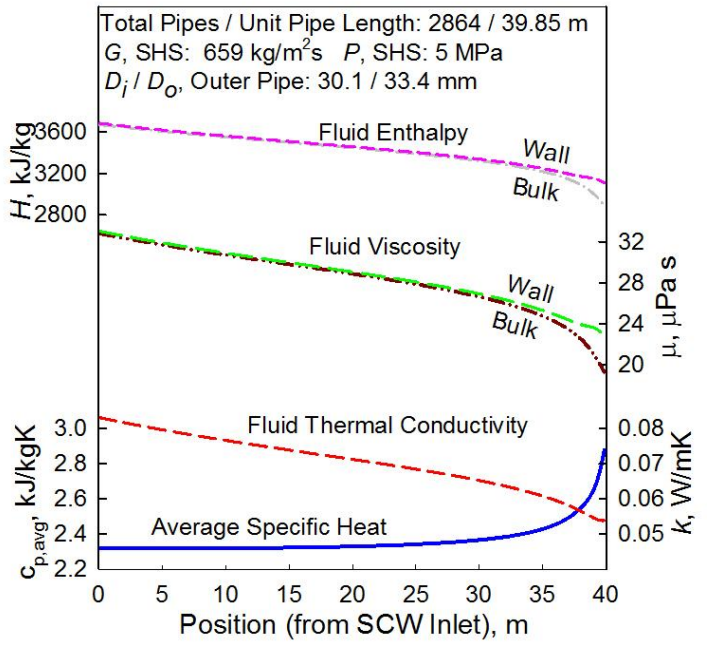

Figure 27. HX A SHS Thermophysical Properties Along an HX Pipe Operating Downstream of the SCWR Outlet Used in the Mokry et al. Correlation, Code 11222, 5–cm Interval.

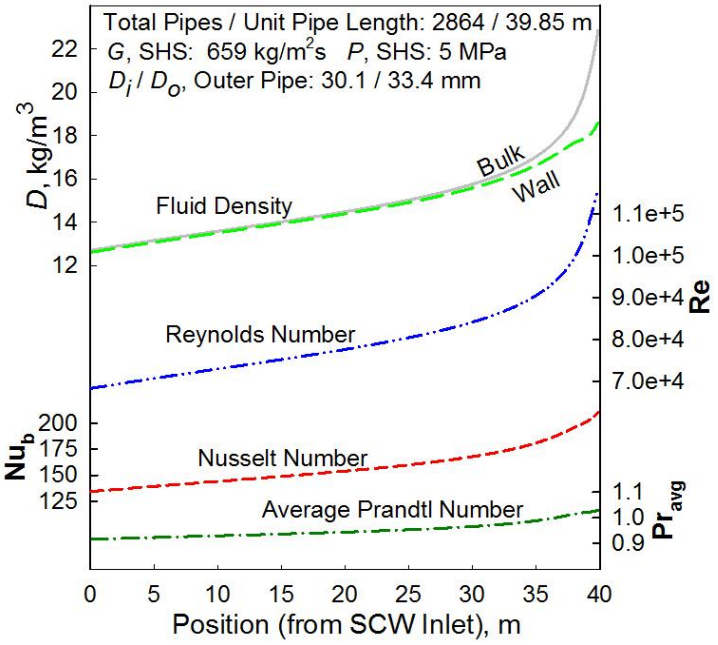

Figure 28. HX A SHS Thermophysical Properties Along an HX Pipe Operating Downstream of the SCWR Outlet Used in the Mokry et al. Correlation, Code 11222, 5–cm Interval.

Pipe dimensions also influence flow characteristics which can lead to improved HTCs. Additionally, higher SHS flows (> 0.1 kg/s per pipe) enable more thermal energy to be transferred between the fluids resulting in lower SCW outlet temperatures for a fixed SHS temperature difference. Alternative HX A code combinations are shown in Figure 29 to Figure 31. For HX A codes 13122 (Figure 29) and 13132 (Figure 30), the SCW would exit the HX at 468°C and 443°C, respectively. As the SCW temperature is well above the *pseudocritical point* the local SCW HTC peaks at lower values compared to combinations such as 11222. This is due in part to the higher SCW mass flux passing through the HX reducing the temperature difference. For higher mass fluxes a larger volume of SCW must be diverted to the HX reducing the amount of SCW expansion in the HP turbine and consequently electrical power output of the SCW NPP. The SCW at the HX exit still contains a high energy content and can be re-introduced into the SCW loop prior to expansion in the HP turbine. If the flow is returned to preheater HXs on the feedwater circuit a substantial amount of useful energy may not be optimally used.

Table 16. HX A Design and Operating Parameter Variation for Code 11222 (5 MPa SHS Pressure) and Code 21222 (4 MPa SHS Pressure).

	HX A Code	11222 (5 MPa)	21222 (4 MPa)
HX General Parameters	Heat Transfer Rate per Pipe, $\dot{Q}$,kW	**78.34**	**79.29**
	Number of HX Pipes, N	**2864**	**2830**
	Average Overall HTC, U_{avg}, W/m^{2}K	**809.2**	**804.5**
	Heat Transfer Area per Pipe, A, m^2	**3.34**	**3.14**
	Length per Pipe, L, m	**39.85**	**37.45**
	Total Pipe Length, L_{Total}, km	**114.13**	**105.98**
SCW – Inner Pipe Flow	Total Mass Flow Rate, $\dot{m}_{SCW}$, kg/s	**198**	**195**
	Inlet/Outlet Temperature, °C	**625/392**	**625/391**
	Inner Diameter, d_i, mm	21	21
	Outer Diameter, d_o, mm	26.7	26.7
	Average Burst Pressure, MPa	86	86
	Pipe Mass Flux, G_{SCW}, kg/m^{2}s	200	200
	Maximum Flow Velocity, u_{SCW}, m/s	3	3
SHS – Annulus Gap Flow	Total Mass Flow Rate, $\dot{m}_{SHS}$, kg/s	**286**	**283**
	Inlet/Outlet Temperature, °C	**287/600**	**274/600**
	Inner Diameter, D_i, mm	30.1	30.1
	Outer Diameter, D_o, mm	33.4	33.4
	Average Burst Pressure, MPa	40	40
	Annulus Mass Flux, G_{SHS}, kg/m^{2}s	659	659
	Maximum Flow Velocity, u_{SHS}, m/s	**52**	**65**

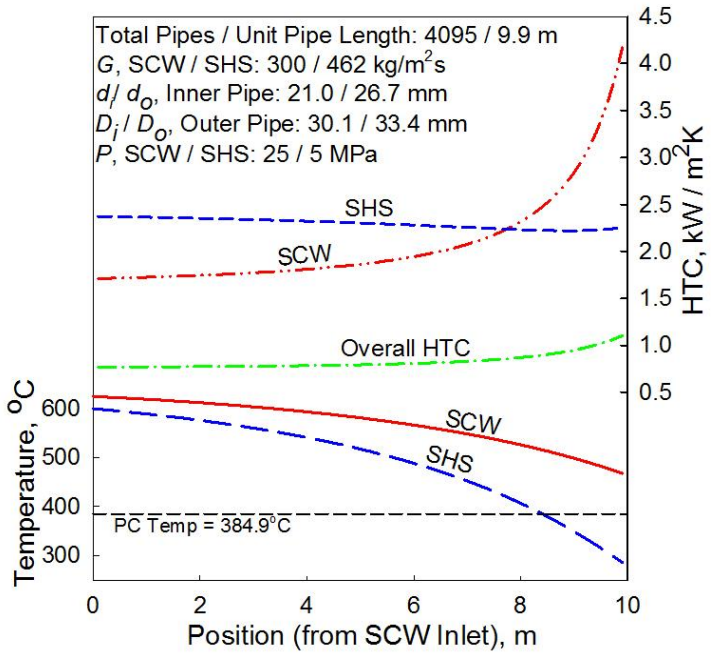

Figure 29. HX A SCW and SHS Fluid Temperature and Local and Overall HTCs Along an HX Pipe, Code 13122, 10–cm Interval.

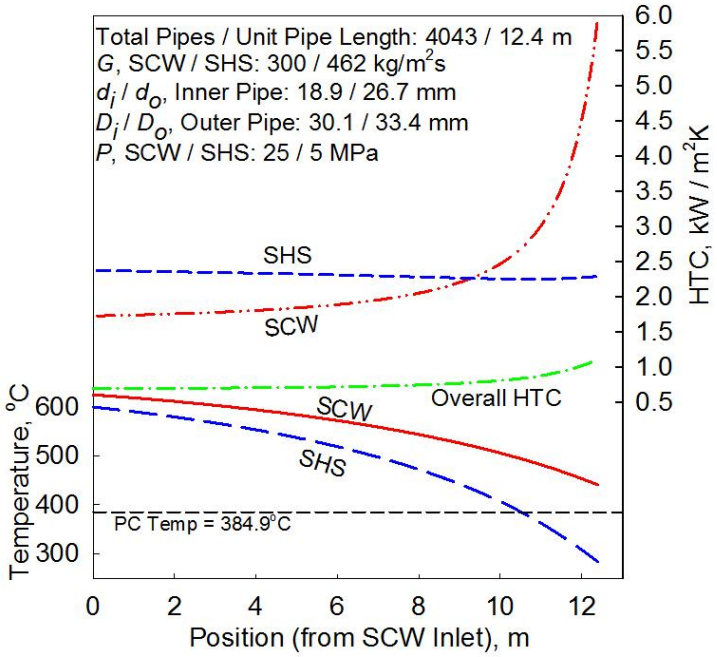

Figure 30. HX A SCW and SHS Fluid Temperature and Local and Overall HTCs Along an HX Pipe for Test Code 13132, 10–cm Interval.

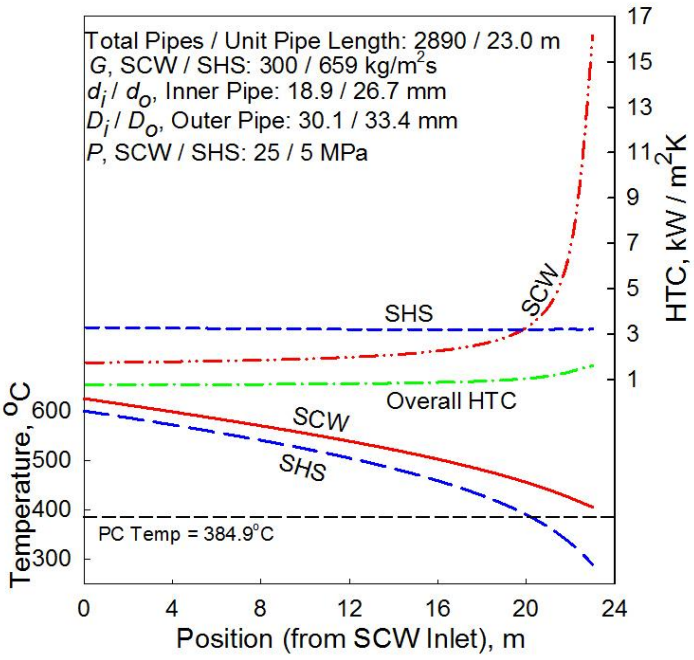

Figure 31. HX A SCW and SHS Fluid Temperature and Local and Overall HTCs Along an HX Pipe for Test Code 13232, 10–cm Intervals.

The effects of augmented heat transfer are shown in Figure 32 and 33. For HX A code 13232, enhancing the local HTCs (both SCW and SHS) by 50% would reduce the total pipe length of the HX from 23.0 m (Figure 31) to 16.8 m (Figure 32), approximately 27%. Trial runs with theoretical enhancement resulting from helically-corrugated pipes are summarized in Figure 33. The impact of increased overall HTCs, shown in Figure 33 as percentages above the base HTC have a diminishing effect as the enhancement level increases. Heat transfer enhancement may significantly reduce the physical size of the HX, an advantage when considering the limited space available in a reactor containment structure. Based on results from previous studies discussed in Chapter 4, the theoretical enhancement assumed here may be conservative. However, it is clear that augmentation methods should be considered in future work.

A frictional pressure loss calculation was performed for HX A code 13122 with results shown in Figure 34. The pressure drop of the SHS is significantly greater compared to the SCW which is heavily influenced by the much larger flow velocity of the SHS. Furthermore, the reduced pressure of the SHS causes a decrease in density and

consequently an increase in the SHS flow velocity. For code 13122, the thermophysical properties of both the SCW and SHS did not vary widely and the temperature profiles for both flows are nearly identical. Compared to Figure 29 which depicts results for the no pressure loss case, the HX with pressure losses accounted for would have a slightly lower total pipe length requirement.

Significant pressure losses on the SHS side would require high powered compressors downstream of the HX to raise the pressure to the original operating value. This could prove to be an economically challenging prospect. Considering an HX design with a high SCW outlet temperature (>~430°C) and short individual pipe lengths may be a suitable alternative for an HX. Such a design would meet the thermal energy requirements of the Cu–Cl cycle, return the SCW to the primary coolant loop at conditions where thermal energy can still be extracted and minimize the pressure losses of the SHS flow.

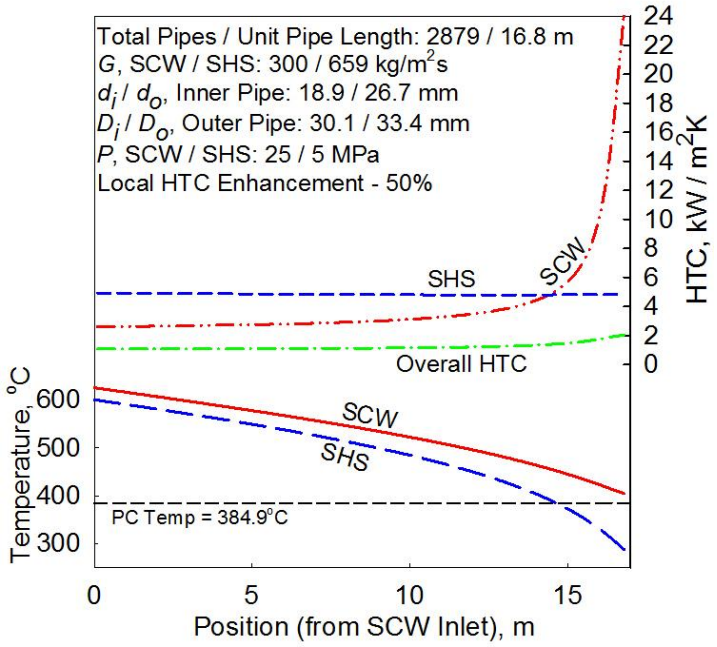

Figure 32. HX A SCW and SHS Fluid Temperature and Local and Overall HTC Along an HX Pipe for Test Code 13232 with 50% Enhanced Local HTCs, 10–cm Interval (Lukomski et al., 2011a).

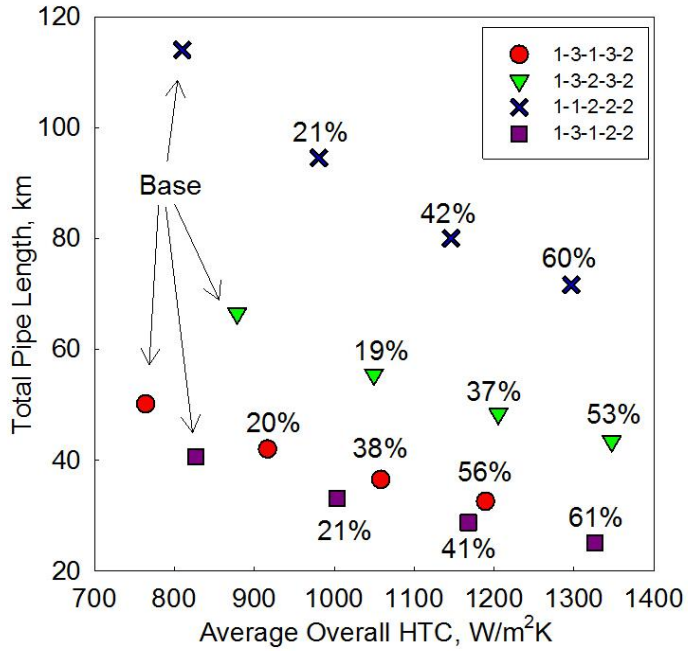

Figure 33. HX A Impact of Theoretical Heat Transfer Enhancement of Local HTCs (25%, 50% and 75%) on Overall HTC and HX Piping Requirements, 10–cm Intervals. (Lukomski et al., 2011a).

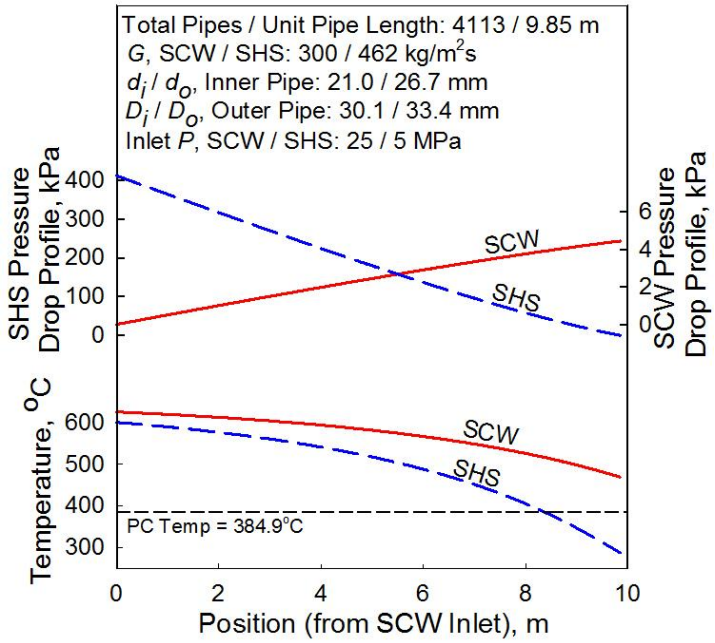

Figure 34. HX A SCW and SHS Fluid Temperature and Pressure Loss Profiles Along an HX Pipe for Code 13122, 5–cm Interval.

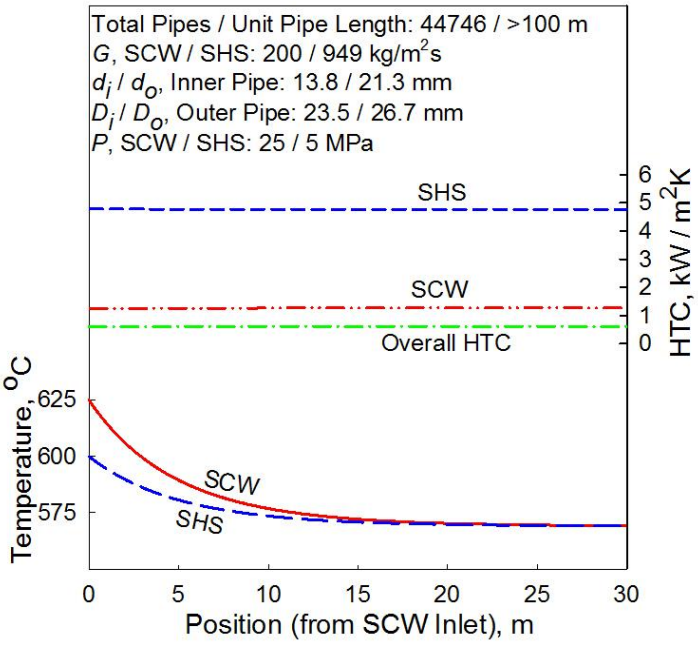

Figure 35. Example of Poor HX A Test Code 11111 Where Operating Fluid Temperature Difference Approaches Zero.

For the combinations tests listed in Table A3, total piping requirements for HX A ranged between 40.5 km (code 13122) to 247.65 km (code 13113) and a maximum SCW mass flow rate requirement of 423 kg/s (code 13122).

HX A can be integrated into both a no-reheat and single reheat NPP cycle for an SCW NPP. Calculation results support 26 combinations of HX operating conditions and design parameters which can be further pursued. Combinations within this grouping can further be divided into those which have SCW outlet temperatures far from the *pseudocritical point* (~420–460°C) and those that are near (<410°C). Since the thermal load for the Cu–Cl cycle will be met in either case, the focus of the HX A design can be on *where* the SCW is to be re-introduced into the SCW NPP loop. It has been established that the temperature of the SCW will not fall below the *pseudocritical point* due to the high energy content of the flow and so re-entry to the SCW NPP cycle at reactor inlet conditions (25 MPa/350°C) cannot be achieved.

To optimize the size of the HX, the operating pressure of the SHS flow may be lowered or augmentation methods such as helically-corrugated piping may be incorporated to increase the overall HTC. The advantage of lowering the pressure is that the lower saturation pressure allows for a larger temperature difference to be achieved across the HX reducing the total SHS flow rate requirement for the HX. A disadvantage is the resulting increase in flow velocity has a direct square relationship impact on the pressure drop of the flow, potentially limiting future consideration of the operating arrangement. Those combinations with high SHS mass fluxes will have large flow velocities contributing to greater pressure drops across the HX. As a result, it may be prudent to consider arrangements having short individual pipe lengths that will limit pressure losses and lead to higher SCW outlet temperatures returned to the NPP coolant loop.

Lastly, integrating HX A into the containment structure of the SCW NPP would be less challenging for test combinations having shorter pipe lengths. From all the test combinations investigated, the smallest volume for an HX unit would be approximately 53 m^3 (cube of 3.8 m side length), required for code 13122. This value is based on the total volume of piping for the HX in addition to a conservative 50% gap/auxiliaries factor applied to account for pipe spacing, inlet/outlet tie-ins to the HX and other support structures. The maximum size of HX would be 387 m^3 (cube of 7.3 m side length) required for code 13112. Minimizing the HX's impact on the containment design would be a preference, further supporting the use of smaller pipe length, high SCW outlet temperature combinations.

6.2 Results for HX B (HP SHS/LP SHS) Design

Table A6 contains summary information for 19 combinations used for HX B. Of the 19 trials only 5 combinations were suitable for further consideration (shown with a green "P"). The 5 combinations having LP SHS mass flow rate requirements beyond 400 kg/s but acceptable flow velocities are shown with a blue "R" indicating that they may be reviewed in future analysis if the flowrates diverted from the SCW NPP can exceed 50% of the total flow. The remaining combinations were characterized by excessive LP SHS flows (>75 m/s), or were not thermodynamically stable, again meaning that the

arrangement would produce an improperly sized HX either due to physical dimensions or operating conditions (Table A7).

Operating conditions for HX B are much less severe compared to HX A given the system would reach maximum pressures of only 5.7 MPa on the HP SHS side. The concern over burst pressure in this application is significantly reduced. However, Figure 36 shows that for HX B code 11232, the inner pipe burst pressure exceeds the operating pressure by approximately 19 times. The temperature profiles for this HX design, as shown in Figure 37, remain more uniform since neither fluid experiences phase changes or *critical/pseudocritical* effects. Unlike the HX A cases, the HTCs under the HX B design remain nearly constant across the HX which is also reflected in the minimal variation of thermal resistances depicted in Figure 38. Thermophysical properties of the HP SHS and LP SHS flows are depicted in Figure 39 through Figure 42. The counterflow design of the HX results in the operating fluids experiencing opposite effects: high temperature SHS moving to a low temperature SHS and vice versa.

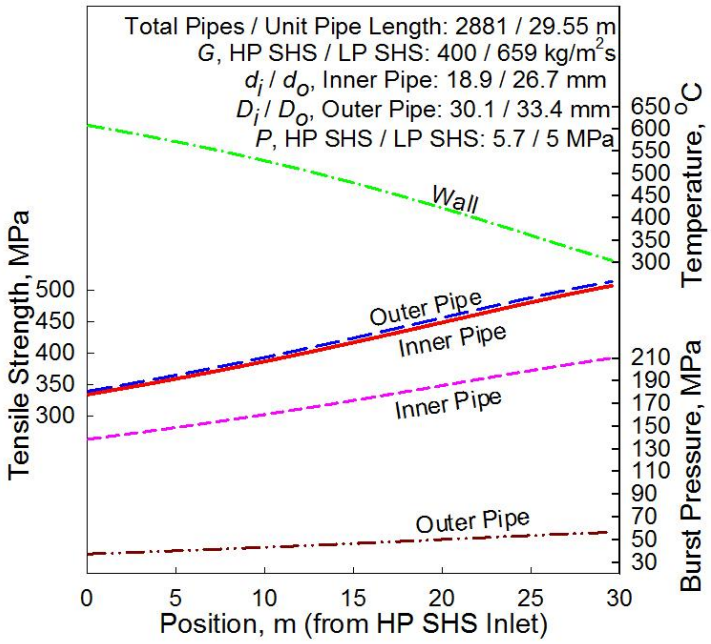

Figure 36. HX B Pipe Burst Pressure and Tensile Strength for SS–304 Pipes, Code 11232, 5–cm Interval.

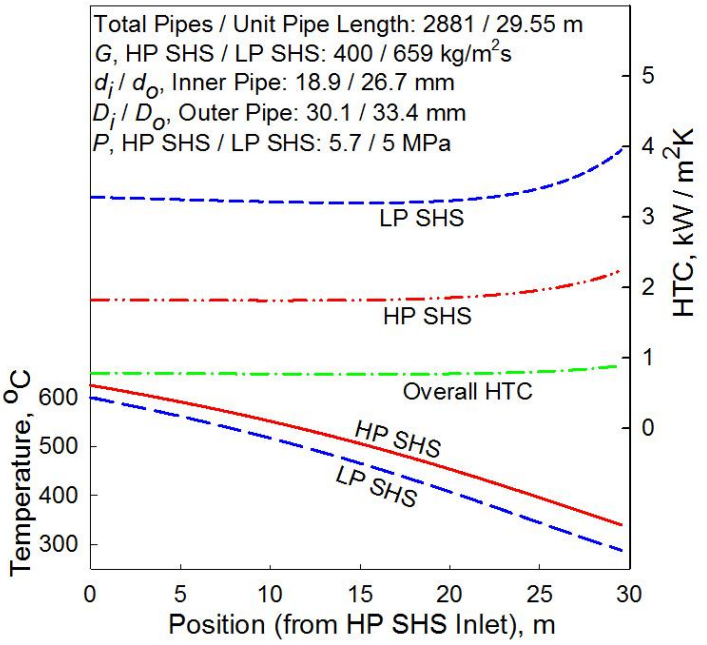

Figure 37. HX B HP SHS and LP SHS Fluid Temperature and Local and Overall HTCs Along an HX Pipe Operating Downstream of the SCWR Outlet, Code 11232, 5–cm Interval.

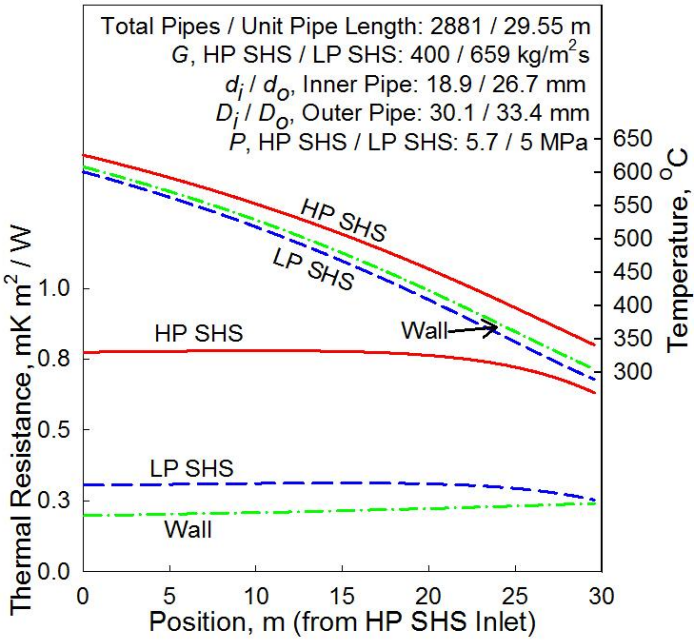

Figure 38. HX B HP SHS and LP SHS Fluid Temperature and Thermal Resistances Along an HX Pipe Operating Downstream of the SCWR Outlet, Code 11232, 5–cm Interval.

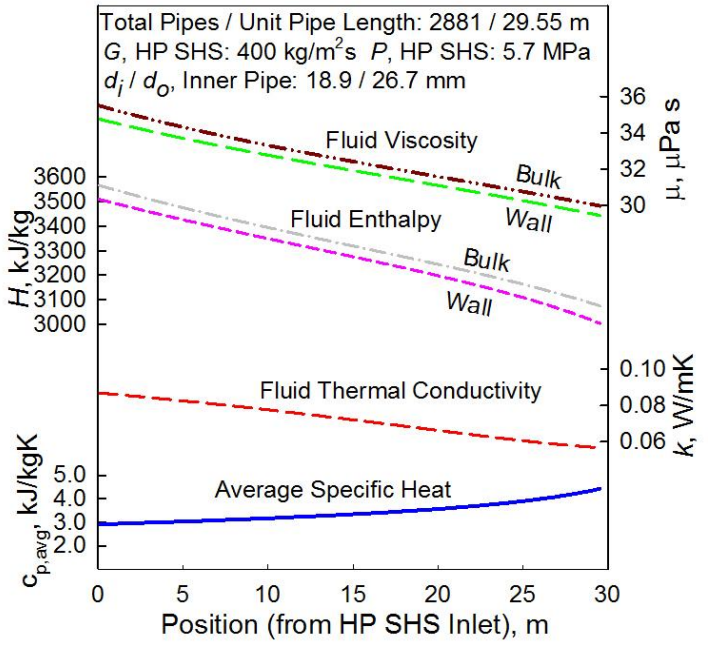

Figure 39. HX B HP SHS Thermophysical Properties Along an HX Pipe Operating Downstream of the SCWR Outlet Supporting the Mokry et al. Correlation, Code 11232, 5–cm Interval.

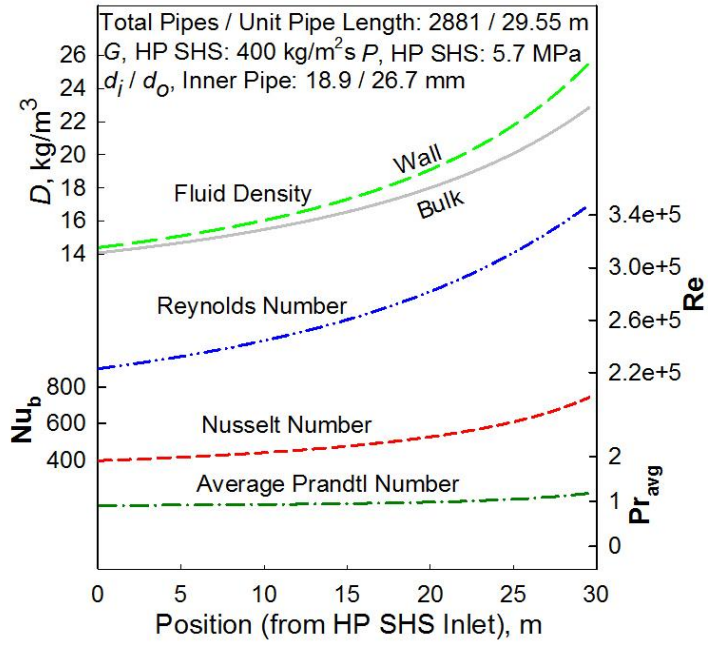

Figure 40. HX B HP SHS Thermophysical Properties Along an HX Pipe Operating Downstream of the SCWR Outlet Used in the Mokry et al. Correlation, Code 11232, 5–cm Interval.

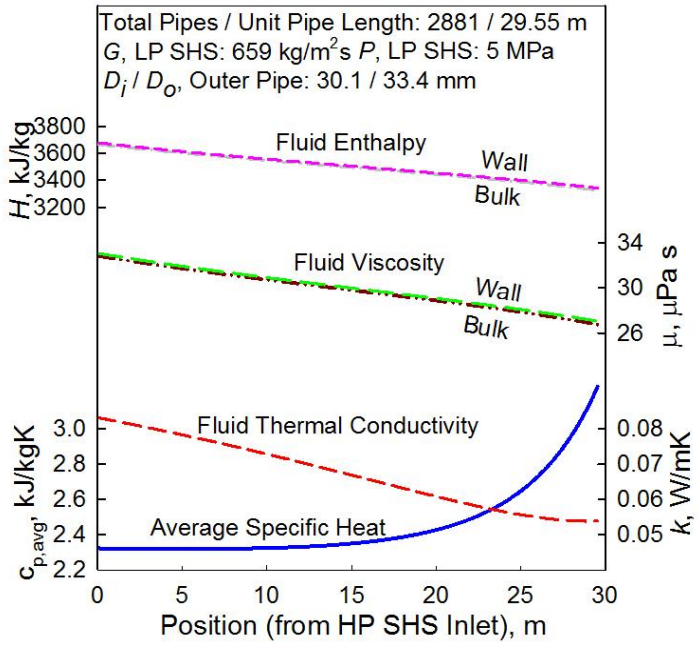

Figure 41. HX B LP SHS Thermophysical Properties Along an HX Pipe Operating Downstream of the SCWR Outlet Supporting the Mokry et al. Correlation, Code 11232, 5–cm Interval.

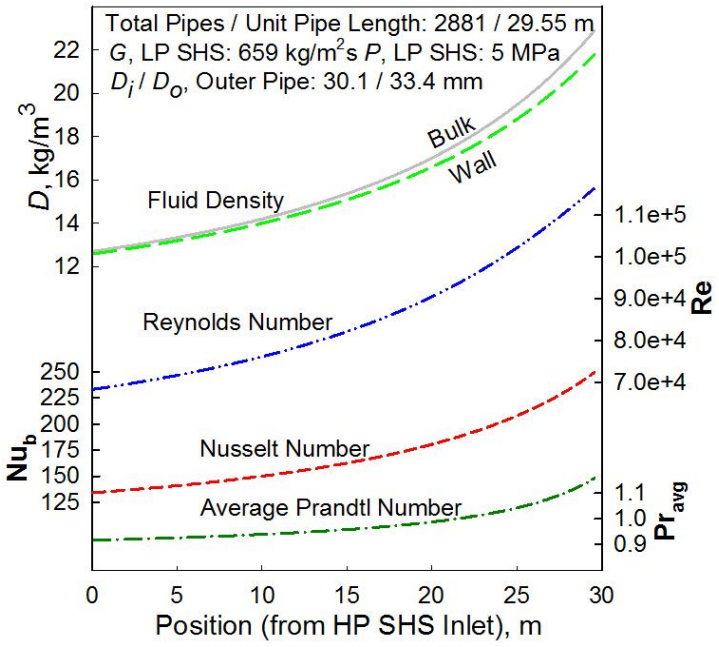

Figure 42. HX B LP SHS Thermophysical Properties Along an HX Pipe Operating Downstream of the SCWR Outlet Used in the Mokry et al. Correlation, Code 11232, 5–cm Interval.

As discussed in Chapter 4, the LMTD method was tested for the HX B design since the fluid specific heats would vary less across the HX compared to HX A. The cross-section averaged specific heats are shown in Figure 39 and 40, however, a similar trend would be expected for the bulk-fluid values.

Table 17. Comparison of HX B MATLAB Iterative Calculations and LMTD Method Calculations for Code 11232.

User Input Design/Operating Parameters			
HP SHS Pressure, $P_{HP\ SHS}$, MPa	5.7	LP SHS Pressure, $P_{LP\ SHS}$, MPa	5
HP SHS Inlet/Outlet Temperature, T_{in}/T_{out},°C	625/340	LP SHS Inlet/Outlet Temperature, T_{in}/T_{out},°C	289/600
Inner Pipe Inner Diameter, d_i, mm	18.9	Outer Pipe Inner Diameter, D_i, mm	30.1
Inner Pipe Outer Diameter, d_o, mm	26.7	Outer Pipe Outer Diameter, D_o, mm	33.4
Inner Pipe Mass Flux, $G_{HP\ SHS}$, kg/m^{2}s	400	Annulus Mass Flux, $G_{LP\ SHS}$, kg/m^{2}s	659

	Iterative Calculation	**LMTD Method Calculation**
Heat Transfer Rate per Pipe, $\dot{Q}$, kW	77.88	77.95
Average Overall HTC, $U_{avg,}$ W/m^{2}K	**784**	**766**
No. of HX Pipes, N	2881	2878
Heat Transfer Surface Area per Pipe, A, m^2	**2.48**	**2.79**
Length per Pipe, L, m	**29.55**	**33.25**
Total Pipe Length, L_{Total}, km	**85.13**	**95.69**
HP SHS Total Mass Flow Rate, $\dot{m}_{HP\ SHS}$, kg/s	323	322
HP SHS Maximum Flow Speed, $u_{HP\ SHS}$, m/s	28	29
LP SHS Total Mass Flow Rate, $\dot{m}_{LP\ SHS}$, kg/s	288	289
LP SHS Maximum Flow Speed, $u_{LP\ SHS}$, m/s	52	52

To confirm the functionality of the method for future HX B design applications, a test calculation using the LMTD method was carried out for HX B code 11232 with results shown in Table 17. The LMTD method overpredicted the individual pipe length requirement of the HX at 33.25 m compared to 29.55 m for the iterative based calculations. The average overall HTC for the LMTD method was slightly below that for the iterative case. One explanation for this is that the large temperature differences cause the specific heats of the SHS flows to vary across the HX length, enough to create an error in the heat transfer area requirements. Based on these results, it is recommended that the LMTD method not be considered in future studies for an HX B design.

For the HX B test combinations investigated, the overall volume required for the HX would be less compared to the HX A combinations. The smallest HX size was obtained for code 23122 with a volume requirement of approximately 52 m^3 (cube of 3.7 m side length) accounting for the same factors specified for HX A. The largest HX would be for combination 23112, having a volume of approximately 349 m^3 (cube of 7 m side length).

The design of HX B may be considered more standardized given that both operating fluids are at a relatively low pressure compared to HX A. For this design, the flow rate drawn from the SCW NPP will be larger compared to HX A and will make up a larger fraction of the remaining primary coolant flow. Given that the HP SHS exits the HX between approximately 340 – 390°C a suitable re-entry point back into the NPP loop will need to be considered. Due to the substantial steam flowrate, this may be a significant consideration in the future HX B design. To address concerns of diversion from the SCW NPP coolant loop and pressure losses in future research, the focus of HX B studies should be on combinations having low total HP SHS flow requirements with low LP SHS flow velocities.

CHAPTER 7 – CONCLUSIONS

The intent of this work was to evaluate the feasibility of linking an SCWR to a hydrogen production facility operating on a thermochemical 4-step Cu–Cl cycle through an HX located at specific locations on an SCW NPP coolant loop. This cogeneration application would enable an environmentally sustainable hydrogen production process to help meet the world's future energy needs.

A literature survey was performed to discover recent progress related to the Cu–Cl cycle and the development of the SCWR and other Generation IV nuclear reactors. For the Cu–Cl cycle, current focus lies with the 4-step cycle based on research at institutions such as UOIT. The net external thermal energy requirements for the cycle were determined to be 224 MW per kilogram of hydrogen produced. Using effective recycling of heat amongst the reactions is a key aspect of the cycle which could reduce external energy requirements. The SCWR is one of 6 next generation reactors being researched. For this reactor, two NPP cycle layouts are under consideration: no-reheat and single reheat; both of which could operate with an HX linked to a hydrogen production facility. While the no-reheat cycle can incorporate one HX design, the single reheat layout can incorporate two distinct designs. Following review of a select number of heat transfer correlations, the Mokry et al. (2009) correlation was chosen based on favourable reviews in recent studies.

One HX design, HX A would operate with SCW in the inner pipe and SHS in the annulus gap and be located at the reactor outlet for the no-reheat or single reheat NPP layouts. A second design, HX B, specifically designed for the single reheat NPP layout, would have HP SHS in the inner pipe and LP SHS in the annulus gap. To determine suitable operating and design parameters for an HX, a matrix of test conditions based on a number of user inputs was created: SHS (HX A) / LP SHS (HX B) operating pressure, SHS (HX A) / LP SHS (HX B) pipe mass flow rate, SCW (HX A) / HP SHS (HX B) mass flux and inner and outer pipe dimensions. These parameters were then tested with a MATLAB script which performed iterative energy balance calculations for the two types

of HXs in a counter-flow double-pipe arrangement using NIST REFPROP as the thermophysical property database. The script was verified using Microsoft Excel iterative calculations. Comparison of the results from the two sources showed minimal differences in predicted SCW/SHS/pipe wall temperatures providing assurance that formulas were properly recorded. Stainless Steel 304 was assessed to be a suitable HX piping material based on minimum adequate burst pressure and thermal conductivity characteristics. Both Inconel–600 and Inconel–718 may also be used in future studies due to superior material properties.

For both the HX A and HX B designs, operating and design parameter combinations were identified which met the total Cu–Cl cycle thermal energy demand with the intermediate SHS fluid returning to the hydrogen production facility at temperatures of up to 600°C. In total, there were 124 HX combinations tested (96 HX A, 28 HX B) of which 31 were deemed suitable for investigation in subsequent analysis. Suitability criteria included the requirement to raise the SHS flow from the inlet temperature to 600°C, limit the maximum SHS flow velocity to 75 m/s and for HX B, consider combinations with total HP SHS flowrates of less than 400 kg/s.

An HX A design would require a significant level of research and development due to the severe conditions of the operating fluids. Due to the significant heat transfer occurring within the SCW *pseudocritical region*, the SHS flow experiences an extreme temperature rise immediately upon entering the HX and quickly approaches the operating temperature of the SCW. This limits the temperature at which the SCW leaves the HX to be above the *pseudocritical* temperature. Several combinations reached an SCW outlet temperature of 389°C, slightly above the *pseudocritical* temperature of 384.9°C for 25 MPa. The majority of combinations produced SCW outlet temperatures significantly above the *pseudocritical* temperature (~440 – 460°C) or within the *pseudocritical region* (<410°C). Focusing on these combinations would help to identify the optimal re-entry points into the NPP coolant loop. In terms of physical size requirements, it is estimated that approximately 53 m^3, or a cube of side length 3.8 m, would be required for the smallest size HX designs. Heat transfer enhancement methods were considered for HX A

in the form of helically-corrugated pipes showing that significant reductions in pipe length requirements can be achieved.

Although pressure losses were not thoroughly evaluated as part of this work, brief discussion was provide and testing of one combination. Pressure losses may limit the development of combinations having long piping requirements and high SHS flow velocities. For future work on HX A, it is recommended that focus be directed on combinations characterized by short pipe lengths, reasonably higher SCW outlet temperatures (>~430°C) and lower SHS flow velocities as these will combine adequate heat transfer qualities and limit pressure losses across the HX.

For the HX B design, the operational characteristics are much less stringent compared to those for HX A as the operating fluids are both SHS at significantly lower pressures. The challenge associated with this design is the required HP SHS mass flow rate for a number of combinations exceeds half of the available coolant flow on the main NPP coolant loop. It was assumed that just over 50% of the available SHS in the NPP coolant loop could be diverted to the HX while maintaining a reduced level of electrical output. Limitations on SHS flow diversion should be considered as part of detailed calculation processes. For the suitable test combinations, the HP SHS outlet temperatures from the HX range from approximately 340 to 390°C which would also require re-entry points to be developed for the steam flow. For the HX B side requirements, the estimated volume required for the smallest HX design would be approximately 52 m^3, or a cube of side length 3.7 m. The focus of HX B studies should be on combinations having low total HP SHS flow requirements with low flow velocities.

A thermal approximation was performed for an HX B combination using the LMTD method; however, it was shown that this method would not be appropriate under the operating scenarios investigated in this work. This is due to the significant variation in thermophysical properties due to the extremely large temperature differences experienced by the operating fluids resulting in LMTD assumptions being invalid.

From a heat transfer perspective, thermalhydraulic calculations have shown that the counter-flow double-pipe HX is a viable choice in linking an SCW NPP with a hydrogen production facility based on the Cu–Cl cycle. The information from this research may act as a basis for future research with the MATLAB script being modified to suit the requirements of the research path.

CHAPTER 8 – FUTURE WORK

Research in this field will undergo continuous evolution since developments in the SCWR design concept parameters or Cu–Cl cycle processes may significantly influence the design parameters for the HX. It is recommended that, in addition to more detailed investigations on the suitable combinations identified in this work, future analysis should consider the following topics:

- Potential SCW and HP SHS re-entry locations along the NPP coolant loop for HX A and HX B arrangements, respectively, should be considered – such points will be governed by the selected NPP layout;
- Optimization of the recommended test combinations should be performed to identify suitable ranges of design and operating conditions;
- Validation of the MATLAB script to determine code limitations; resolution of non-converging test combinations encountered during this research by considering the effects of deteriorated heat transfer regime along HX piping;
- Pressure loss calculations should be refined, accounting for sources beyond friction losses briefly discussed in this analysis;
- The impact of HX geometry should be considered (influence of vertical/horizontal flow) along with the applicability of the Mokry et al. correlation as a heat transfer correlation for horizontal flows;
- Modification of the inner pipe wall temperature calculation in the MATLAB script to account for the pipe wall thermal resistance in response to scenarios where the resistance cannot be neglected (i.e. SCW flow experiences *pseudocritical* effects lowering the relative thermal resistance); thermal resistance of the pipe wall was neglected for wall temperature calculation in this analysis;
- Consideration of alternative intermediate loop operating fluids (i.e. molten salts) to assess feasibility for use in cogeneration HXs.

REFERENCES

Bishop, A., Sandberg, R., and Tong, L., 1964. Forced Convection Heat Transfer to Water at Near-critical Temperatures and Supercritical Pressures, Atomic Power Division, Pittsburgh, PA., USA: Westinghouse Electric Corporation.

Dittus, F.W. and Boelter, L.M.K., 1930. Heat Transfer in Automobile Radiators of the Tubular Type, University of California, Berkeley, Publications on Engineering, Vol. 2, Issue 13. pp. 443-461.

Dokiya, D. and Kotera, Y., 1976. Hybrid Cycle with Electrolysis Using a Cu-Cl System, International Journal of Hydrogen Production and Applications. Vol. 1, Issue 6, pp. 144-153.

Duffey, R.B., Pioro, I., Zhou, X. et al., 2008. Supercritical Water-Cooled Nuclear Reactors: Current and Future Concepts – Steam Cycle Options. Proceedings of the 16th International Conference on Nuclear Engineering, Orlando, Florida, USA, Paper No. 48869. 9 Pages.

Forsberg, C. W., 2007. Future Hydrogen Markets for Large-Scale Hydrogen Production Systems, Internationa Journal of Hydrogen Energy, Vol. 32, pp. 431-439.

Generation IV International Forum, 2009. GIF R&D Outlook for Generation IV Nuclear Energy System., 38 slides.

Generation IV International Forum, 2008. Introduction to Generation IV Nuclear Energy Systems and the International Forum, 23 slides.

Hendrix Group. (n.d.). Stainless Steel Data – High Temperature Properties. Accessed June 2, 2011 from
http://www.hghouston.com/Resources/MaterialPropertyData/StainlessSteelData/HighTemperatureProperties.aspx

Incropera, F. P., Dewitt, D. P., Bergman, T. L., Lavine, A. S., 2007. Fundamentals of Heat and Mass Transfer – 6th Edition. New Jersey: John Wiley & Sons, Inc.

Jones, R. H., and Thomas, G. J., 2008. Materials for the Hydrogen Economy, CRC Press. Taylor & Francis Group: Boca Raton, Florida.

Kuppan, T., Heat Exchange Design Handbook, Marcel Dekker: New York, NY. 2000. 1119 Pages.

Lewis, M., Ferrandon, M., and Tatterson, D. 2009. R&D Status for the Cu-Cl Thermochemical Cycle, DOE Hydrogen Program.

Lewis, M.A. and Masin, J.G., 2009. The Evaluation of Alternative Thermochemical Cycles-Part II: The Down-Selection Process, International Journal of Hydrogen Energy, Vol. 34, Issue 9, pp. 4125-4135.

Le Brun, 2007. Moten Salts and Nuclear Energy Production, Journal of Nuclear Materials, Vol. 360(1) pp. 1-5.

Lineberry, M.J., and Allen, T.R., n.d. The Sodium-cooled Fast Reactor, Argonne National Laboratory. 8 Pages.

Lukomski, A., Gabriel, K., and Pioro, I., 2011a. Use of a Supercritical Water-Cooled Reactor for Process Heat to Support Thermochemical Hydrogen Production. Proceedings of the 14th International Topical Meeting on Nuclear Reactor Thermalhydraulics, NURETH-14, Toronto, Ontario, 12 Pages.

Lukomski, A., Gabriel, K., Pioro, I. and Naterer, G., 2011b. Intermediate Double-Pipe Heat Exchanger for Thermochemical Hydrogen Co-Generation with SCW NPP, Proceedings of the 19th International Conference on Nuclear Engineering, Makuhari, Chiba, Japan. Paper No. 43640. 9 Pages.

Lukomski, A., Pioro, I. and Gabriel, K., 2011c. Hydrogen Production Using Process Heat from a Supercritical Water-cooled Nuclear Power Plant via a Double-pipe Heat Exchanger, Proceedings of the 5th International Symposium on SCWRs, Vancouver, British Columbia, Canada, March 13-16, 2011. Paper #71. 12 Pages.

Lukomski, A., Pioro, I. and Gabriel, K. 2010a. Characteristics of Cu-Cl Cycle Based Hydrogen Production Via Linkage With a SuperCritical Water Reactor (SCWR) to Provide Process Heating, Proceedings of the 34th CNS-CNA Student Conference, Montreal, Quebec, Canada, May 24-27 2010. 10 Pages.

Lukomski, A. J., Pioro, I., Gabriel, K. 2010b. Preliminary Discussion on the Linking of a Supercritical Water Reactor (SCWR) and Cu-Cl Cycle Based Hydrogen Production Facility, Proceedings of the 2nd Canada-China Joint Workshop on Supercritical Water-Cooled Reactors, Toronto, Ontario, Canada, 2010 April 23-28, 2010. 12 Pages.

Matweb. (n.d.). Material Property Data. Accessed June 2, 2011, from http://www.matweb.com/index.aspx.

Mokry, S., Lukomski, A., Gabriel, K., Pioro, I., Naterer, G., 2011a. Thermalhydraulic and Heat Transfer Correlation for an Intermediate Heat Exchanger Linking a Supercritical Water-Cooled Reactor and a Copper-Chlorine Cycle for Hydrogen Production, Proceedings of the International Conference on Hydrogen Production (ICH2P), Thessaloniki, Greece. 17 Pages.

Mokry, S., Pioro, I., Farah, A. et al. 2011b. Development of Supercritical Water Heat-Transfer Correlation for Vertical Bare Tubes, Nuclear Engineering and Design, Vol. 241, Issue 4, pp. 1126-1136.

Mokry, S., Pioro, I., Kirillov, P., Gospodinov, Y., 2010a. Supercritical-water Heat Transfer in a Vertical Bare Tube, Nuclear Engineering and Design, Vol. 240, Issue 3, pp. 568-576.

Mokry, S., Farah, A., King, K., Gupta, S., Pioro, I., 2010b. Updated Heat-Transfer Correlations for Supercritical Water in Vertical Bare Tubes, Proceedings of the 7th International Conference on Heat Transfer, Fluid Mechanics and Thermodynamics, Antalya, Turkey, July 19-21, 2010. pp 1121-1131.

Mokry, S., Farah A., King, K., et al., 2009. Development of Supercritical Water Heat-Transfer Correlation for Vertical Bare Tubes, Proceedings of the International Conference Nuclear Energy for New Europe 2009, Bled, Slovenia, September 14-17, 2009. Paper #210. 14 Pages.

Naidin, M., Mokry, S. and Pioro, I., 2009a. SCW NPPs: Layouts and Thermodynamic Cycles, Proceedings of the International Conference Nuclear Energy for New Europe 2009, Bled, Slovenia, September 14-17, Paper #704, 12 Pages.

Naidin, M., Mokry, S., Monichan, R., et al., 2009b. Thermodynamic Analysis of SCW NPP Cycles with Thermo-chemical Co-generation of Hydrogen, Proceedings of the International Conference on Hydrogen Production, Oshawa, Ontario, Canada, May 3-6, pp. 178-192.

Naidin, M., Mokry, S, Baig, F., et al., 2009c. Thermal Design Options for Pressure-channel SCWRs with Co-Generation of Hydrogen, Journal of Engineering for Gas Turbines and Power, Vol. 131. pp. 012901-1-8.

Naidin, M.C., Monichan, R, Zirn, U. et al., 2009d. Thermodynamic Considerations for a Single-Reheat Cycle SCWR, Proceedings of the 17th International Conference on Nuclear Engineering, Brussels, Belgium. Paper No. 75984. 8 Pages.

Naidin, M.C., Pioro, I., Zirn, U., Chophla, K. et al., 2009e. Supercritical Water Reactor NPP Concept: No-Reheat Cycle Option, Proceedings of the 17th International Conference on Nuclear Engineering, Brussels, Belgium. Paper No. 75989. 9 Pages.

Naterer, G.F., Suppiah, S., Stolberg, L. et al., 2010. Canada's Program on Nuclear Hydrogen Production and the Thermochemical Cu-Cl Cycle, International Journal of Hydrogen Energy, Vol. 35, pp. 10905-10926.

Naterer, G., Suppiah, S., Lewis, M. et al., 2009a. Recent Canadian Advances in Nuclear-Based Hydrogen Production and the Thermochemical Cu-Cl Cycle, International Journal of Hydrogen Energy, Vol. 34, pp. 2901-2917.

Naterer, G., Gabriel, K., Lu, L. et al., 2009b. Recent Advances in Nuclear Based in Hydrogen Production with the Thermochemical Copper-Chlorine Cycle. Journal of Engineering for Gas Turbines and Power, Vol. 131, 032905. 10 Pages.

Naterer, G.F, Gabriel, K., Wang, Z.L, et al., 2008. Thermochemical Hydrogen Production with a Copper-Chlorine Cycle I: Oxygen Release from Copper Oxychloride Decomposition, International Journal of Hydrogen Energy, Vol. 33, pp. 5439-5450.

National Institute of Standards and Technology, 2010. NIST Reference Fluid Thermodynamic and Transport Properties-REFPROP. NIST Standard Reference Database 23, Ver. 9.0. Boulder, CO, U.S.: Department of Commerce.

Ornatskiy, A.P., Dashkiev, Yu.G. and Perkov, V.G., 1980. Supercritical Steam Generators, (In Russian), Vyshcha Shkola Publishing House, Kiev, Ukraine, 287 Pages.

Pethkool, S., Eiamsa-ard, S., Kwankaomeng, S., Promvonge, P., 2011. Turbulent Heat Transfer Enhancement in a Heat Exchanger Using Helically Corrugated Tube, International Communications in Heat and Mass Transfer. Vol. 38, Iss. 3, pp 340-347.

Pioro, I., Mokry, S., Draper, S., 2011. Specifics of Thermophysical Properties and Forced-Convective Heat Transfer at Critical and SuperCritical Pressures. UOIT. 64 pages.

Pioro, I., Mokry, S., Peiman, W., Grande, L., and Saltanov, E., 2010. Supercritical Water-cooled Nuclear Reactors: NPP Layouts and Thermal Design Options of Pressure Channels. Proceedings of the Pacific Basin Nuclear Conference, Cancun, Mexico. 31 Pages.

Pioro, I. and Duffey, R., 2007. Heat Transfer and Hydraulic Resistance at Supercritical Pressures in Power Engineering Applications, ASME Press, New York, NY, USA, 334 Pages.

Power Reactor Information System, 2011. Nuclear Power Plants Information – Operational & Long Term Shutdown Reactors by Type. Last Updated April 20, 2011. http://www.iaea.org/programmes/a2/. Accessed May 7, 2011.

Press, R.J., Santhanam, K.S.V., Miri, M.J., Bailey, A.V., Takacs, G.A., 2009. Introduction to Hydrogen Technology, John Wiley & Sons, Inc.: Hoboken, New Jersey.

Rand, D.A.J and Dell, R.M., 2008. Hydrogen Energy – Challenges and Prospects, The Royal Society of Chemistry: Cambridge, UK.

Ribando, R.J., O'Leary, G.W., and Carlson-Skalak, S., 1997. General Numerical Scheme for Heat Exchanger Thermal Analysis and Design, Computer Applications in Engineering Education. Vol. 5, Issue 4, pp. 231-242.

Richards, M., Shenoy, A., Schultz, K. et al., 2006. H2-MHR Conceptual Designs Based on the Sulphur-Iodine Process and High-Temperature Electrolysis, International Journal of Nuclear Hydrogen Production and Applications, Vol. 1, No. 1, pp. 36-50.

Ryland, D.K., Li, H., Sadhankar, R.R., 2006. Electrolytic Hydrogen Generation using CANDU Nuclear Reactors, Proceedings of the Second Intl Green Energy Conference, Oshawa, Ontario, Canada, 2006 June 25-29.

Sethumadhavan, R. and Rao, R., 1986. Turbulent Flow Friction and Heat Transfer Characteristics of Single and Multistart Spirally Enhanced Tubes, Trans. ASME, Journal of Heat Transfer, 108, pp. 55-61.

Shah, R. and Sekulic, D., 2003. Fundamentals of Heat Exchanger Design. 1st Edition, John Wiley and Sons, Inc.: Hoboken, New Jersey, USA, 750 Pages.

Special Metals, (n.d.). Inconel Alloy 600. Accessed June 2, 2011 from http://www.specialmetals.com/products/inconelalloy600.php

Special Metals, (n.d.). Inconel Alloy 718. Accessed June 2, 2011 from http://www.specialmetals.com/products/inconelalloy718.php

Spiegel, L. and Limbrunner, G.G., 1999. Applied Statics and Strength of Materials, 2nd Edition, Prentice Hall Inc: Upper Saddle River, New Jersey, USA, 644 Pages.

Spirax-Sarco. 2011. Pipes and Pipe Sizing. Accessed August 8, 2011 from http://www.spiraxsarco.com/resources/steam-engineering-tutorials/steam-distribution/pipes-and-pipe-sizing.asp

Swenson, H.S., Carver, J.R., and Kakarala, C.R., 1965. Heat Transfer to Supercritical Water in Smooth-Bare Tubes, Journal of Heat Transfer, Trans. ASME Series C, 87 (4), pp. 477-484.

Thind, H., Pioro, I., and Harvel, G., 2010. Supercritical Water-cooled Nuclear Reactor with Intermediate Heat Exchangers, Proceedings of the 18th International Conference on Nuclear Engineering (ICONE-17), Xi'an, China, May 17-21. Paper #30. 10 Pages.

Vicente, P.G, Garcia, A., Viedma, A., 2004. Experimental Investigation on Heat Transfer and Frictional Characteristics of Spirally Corrugated Tubes in Turbulent Flow at Different Prandtl Numbers, International Journal of Heat and Mass Transfer, Vol. 47, pp. 671-681.

Wang, Z., Naterer, G.F., and Gabriel, K.S., 2010a. Thermal Integration of SCWR Nuclear and Thermochemical Hydrogen Plants, Proceedings of the 2nd Canada-China Joint Workshop on Supercritical Water-Cooled Reactors (CCSC-2010), Toronto, Ontario, Canada, April 25-28, 12 Pages.

Wang., Z.L., Naterer, G.F., Gabriel, K., et al., 2010b. Comparison of Sulfur-Iodine and Copper-Chlorine Thermochemical Hydrogen Production Cycles, Int. J. of Hydrogen Energy, Vol. 35, pp. 4820-4830.

Wang, Z.L., Naterer, G.F, Gabriel, K., et al., 2009. New Cu-Cl Thermochemical Cycle for Hydrogen Production with Reduced Excess Steam Requirements, International Journal of Green Energy, Vol. 6, pp. 616-626.

Wang, Z., Gabriel, K., Naterer, G.F., 2008. Thermochemical Process Heat Requirements of the Copper-Chlorine Cycle for Nuclear-based Hydrogen Production, Proceedings of the 29th Conference of the Canadian Nuclear Society, Toronto, Ontario, Canada, June 1-4. 11 Pages.

World Nuclear Association, 2011. Advanced Nuclear Power Reactors. Last updated March 2011. http://www.world-nuclear.org/info/inf08.html. Accessed May 8, 2011.

Zahlan, H., Groeneveld, D.C., Tavoularis, S., 2010. Look-up for Trans-Critical Heat Transfer, Proc. 2nd Canada-China Joint Workshop on Supercritical Water-Cooled Reactors (CCSC-2010), Toronto, Ontario, Canada, April 25-28, 18 Pages.

APPENDIX A – RESULTS TABLES

The tables on the following pages detail the results of testing combinations for both HX A and HX B designs. The testing matrices for the two types of HXs are shown in Table 13 and 14 and below as Table A1 and A2 for reference.

Table A1. (As shown in Chapter 5) HX A Test Combinations Developed for MATLAB Script.

#	SHS Pressure, MPa	#	SCW Mass Flux, kg/m^2s	#	SHS Mass Flowrate, kg/s	#	Inner Pipe Dimensions (d_o / δ_d), mm	#	Outer Pipe Dimensions (D_o / δ_D), mm
1	5	**1**	200	**1**	0.07	**1**	21.3/3.73	**1**	26.7/1.65
		2	250	**2**	0.10	**2**	26.7/2.87	**2**	33.4/1.65
2	4					**3**	26.7/3.91		
		3	300	**3**	0.13	**4**	26.7/5.56	**3**	33.4/2.77

Table A2. (As shown in Chapter 5) HX B Test Combinations Developed for MATLAB Script.

#	LP SHS Pressure, MPa	#	HP SHS Mass Flux, kg/m^2s	#	LP SHS Mass Flowrate, kg/s	#	Inner Pipe Dimensions (d_o / δ_d), mm	#	Outer Pipe Dimensions (D_o / δ_D), mm
1	5	**1**	400	**1**	0.07	**1**	21.3/3.73	**1**	26.7/1.65
		2	600	**2**	0.10	**2**	26.7/2.87	**2**	33.4/1.65
						3	26.7/3.91	**3**	33.4/2.77

Table A3. HX A (SCW/SHS) MATLAB Results for Test Combinations Using 5 MPa SHS Operating Fluid, 5–cm Intervals.

		HX GENERAL PARAMETERS						SCW – INNER PIPE FLOW							SHS – ANNULUS GAP FLOW						
Code (See Tab. A1/A2)	Pass (P)/Fail (F)/Error (E)	Heat Transfer Rate per Pipe, Q,kW	Number of HX Pipes, N	Average Overall HTC, U_{avg}, W/m^{2}K	Heat Transfer Area per Pipe, A, m^2	Length per Pipe, L, m	Total Pipe Length, L_{Total}, km	Total Mass Flow Rate, $\dot{m}_{SCW}$, kg/s	Inlet/Outlet Temperature, °C	Inner Diameter, d_i, mm	Outer Diameter, d_o, mm	Minimum Burst Pressure, MPa	Pipe Mass Flux, G_{SCW}, kg/m^{2}s	Maximum Flow Velocity, u_{SCW}, m/s	Total Mass Flow Rate, $\dot{m}_{SHS}$, kg/s	Inlet/Outlet Temperature, °C	Inner Diameter, D_i, mm	Outer Diameter, D_o, mm	Minimum Burst Pressure, MPa	Annulus Mass Flux, G_{SHS}, kg/m^{2}s	Maximum Flow Velocity, u_{SHS}, m/s
11132	P	54.51	4116	658.7	1.97	23.45	96.52	230	625/401	18.9	26.7	139	200	3	288	289/600	30.1	33.4	37	462	36
11222	P	78.34	2864	809.2	3.34	39.85	114.13	198	625/392	21	26.7	92	200	3	286	287/600	30.1	33.4	37	659	52
12122	P	54.82	4093	772.1	1.00	11.95	48.91	353	625/446	21	26.7	91	250	4	287	287/600	30.1	33.4	37	462	36
12142	P	54.56	4112	626.3	3.17	37.8	155.43	196	625/391	15.6	26.7	239	250	4	288	289/600	30.1	33.4	37	462	36
12232	P	77.94	2879	816.6	3.15	37.6	108.25	202	625/393	18.9	26.7	139	250	4	288	289/600	30.1	33.4	37	659	52
12322	P	101.12	2219	964.8	4.22	50.3	111.62	191	625/390	21	26.7	92	250	4	288	289/600	30.1	33.4	37	857	67
13111	P	54.84	4091	951.8	2.69	40.15	164.25	185	625/389	13.8	21.3	181	300	4	286	287/600	23.4	26.7	48	949	75
13112	P	54.48	4119	533.6	4.78	71.45	294.3	186	625/389	13.8	21.3	178	300	4	288	289/600	30.1	33.4	37	197	16
13113	P	54.64	4107	632.8	4.04	60.3	247.65	185	625/389	13.8	21.3	179	300	4	287	288/600	27.86	33.4	67	276	22
13122	P	54.89	4088	827	0.83	9.9	40.47	423	625/468	21	26.7	91	300	4	286	287/600	30.1	33.4	37	462	36
13132	P	54.89	4088	763.2	1.04	12.35	50.49	343	625/443	18.9	26.7	138	300	4	286	287/600	30.1	33.4	37	462	36
13142	P	54.52	4116	670.3	1.86	22.15	91.17	235	625/403	15.6	26.7	238	300	4	288	289/600	30.1	33.4	37	462	36

Code (See Tab. A1/A2)	Pass (P)/Fail (F)/Error (E)	Heat Transfer Rate per Pipe, Q,kW	Number of HX Pipes, N	Average Overall HTC, U_{avg}, W/m^{2}K	Heat Transfer Area per Pipe, A, m^2	Length per Pipe, L, m	Total Pipe Length, L_{Totab} km	Total Mass Flow Rate, $\dot{m}_{SCW}$, kg/s	Inlet/Outlet Temperature, °C	Inner Diameter, d_i, mm	Outer Diameter, d_o, mm	Minimum Burst Pressure, MPa	Pipe Mass Flux, G_{SCW}, kg/m^{2}s	Maximum Flow Velocity, u_{SCW}, m/s	Total Mass Flow Rate, $\dot{m}_{SHS}$, kg/s	Inlet/Outlet Temperature, °C	Inner Diameter, D_i, mm	Outer Diameter, D_o, mm	Minimum Burst Pressure, MPa	Annulus Mass Flux, G_{SHS}, kg/m^{2}s	Maximum Flow Velocity, u_{SHS}, m/s
13232	P	77.95	2879	879.3	1.93	23	66.22	242	625/405	18.9	26.7	139	300	4	288	289/600	30.1	33.4	37	659	52
13322	P	101.25	2216	1060	2.29	27.3	60.5	229	625/401	21	26.7	92	300	4	288	289/600	30.1	33.4	37	857	67
13332	P	101.63	2208	950	4.94	58.85	129.94	185	625/389	18.9	26.7	139	300	4	287	288/600	30.1	33.4	37	857	67
11122	E*	54.94	4084	708.9	1.35	16.05	65.55	282	625/420	21	26.7	92	200	3	286	287/600	30.1	33.4	37	462	36
12123	E*	55.52	4041	1048.4	0.74	8.85	35.76	349	625/445	21	26.7	92	250	4	283	284/600	27.86	33.4	68	1408	111
12132	E*	54.44	4122	714.9	1.31	15.6	64.3	288	625/423	18.9	26.7	138	250	4	289	289/600	30.1	33.4	37	462	36
12222	E*	78.41	2862	894.8	1.82	21.7	62.11	247	625/407	21	26.7	92	250	4	286	287/600	30.1	33.4	37	659	52
13222	E*	78.01	2877	957.4	1.35	16.05	46.18	298	625/426	21	26.7	91	300	4	288	288/600	30.1	33.4	37	659	52
11123	F	54.46	4120	929.1	1.02	12.2	50.26	284	625/421	21	26.7	92	200	3	288	289/600	27.86	33.4	67	1408	**111**
11133	F	55.04	4077	838.1	1.55	18.5	75.42	228	625/400	18.9	26.7	140	200	3	285	286/600	27.86	33.4	67	1408	**111**
11223	F	78.66	2853	990.5	2.73	32.6	93.01	197	625/391	21	26.7	92	200	3	285	286/600	27.86	33.4	67	2012	**158**
12133	F	54.94	4084	941	1.00	11.9	48.6	286	625/422	18.9	26.7	140	250	4	286	287/600	27.86	33.4	67	1408	**111**
12143	F	54.75	4098	775.9	2.56	30.55	125.19	195	625/391	15.6	26.7	241	250	4	287	288/600	27.86	33.4	67	1408	**111**
12223	F	77.78	2885	1135.3	1.43	17.05	49.19	249	625/408	21	26.7	92	250	4	289	289/600	27.86	33.4	67	2012	**158**

Code (See Tab. A1/A2)	Pass (P)/Fail (F)/Error (E)	Heat Transfer Rate per Pipe, Q,kW	Number of HX Pipes, N	Average Overall HTC, U_{avg}, W/m^{2}K	Heat Transfer Area per Pipe, A, m^2	Length per Pipe, L, m	Total Pipe Length, L_{Total}, km	Total Mass Flow Rate, $\dot{m}_{SCW}$, kg/s	Inlet/Outlet Temperature, °C	Inner Diameter, d_i, mm	Outer Diameter, d_o, mm	Minimum Burst Pressure, MPa	Pipe Mass Flux, G_{SCW}, kg/m^{2}s	Maximum Flow Velocity, u_{SCW}, m/s	Total Mass Flow Rate, $\dot{m}_{SHS}$, kg/s	Inlet/Outlet Temperature, °C	Inner Diameter, D_i, mm	Outer Diameter, D_o, mm	Minimum Burst Pressure, MPa	Annulus Mass Flux, G_{SHS}, kg/m^{2}s	Maximum Flow Velocity, u_{SHS}, m/s
12233	F	78.37	2863	1001.9	2.58	30.7	87.89	200	625/392	18.9	26.7	140	250	4	286	287/600	27.86	33.4	67	2012	**158**
12323	F	101.67	2207	1172.1	3.50	41.75	92.14	190	625/390	21	26.7	92	250	4	287	288/600	27.86	33.4	67	2615	**206**
13123	F	54.69	4103	1143.2	0.60	7.15	29.34	425	625/469	21	26.7	92	300	4	287	287/600	27.86	33.4	68	1408	**111**
13133	F	55.02	4079	1025.6	0.77	9.2	37.53	343	625/443	18.9	26.7	139	300	4	286	286/600	27.86	33.4	68	1408	**111**
13143	F	54.59	4111	853.9	1.46	17.4	71.53	235	625/403	15.6	26.7	240	300	4	288	288/600	27.86	33.4	67	1408	**111**
13223	F	78.31	2866	1251.6	1.03	12.3	35.25	297	625/426	21	26.7	92	300	4	287	287/600	27.86	33.4	67	2012	**158**
13233	F	78.27	2867	1110.1	1.53	18.25	52.32	241	625/405	18.9	26.7	140	300	4	287	287/600	27.86	33.4	67	2012	**158**
13323	F	101.12	2219	1318	1.84	21.95	48.71	230	625/401	21	26.7	92	300	4	288	289/600	27.86	33.4	67	2615	**206**
13333	F	101.3	2215	1137	4.12	49.15	108.87	186	625/389	18.9	26.7	140	300	4	288	289/600	27.86	33.4	67	2615	**206**

Entries with E* indicate combinations which experienced discontinuities during iterative calculations – they *may* be considered for future analysis.

Table A4. HX A (SCW/SHS) Unsuccessful MATLAB Results for Test Codes Using 5 MPa SHS Operating Fluid, 5–cm Intervals.

Code	P_{SHS}, MPa	G_{SCW}, kg/m^{2}s	$\dot{m}_{SHS,pipe}$, kg/s	d_o / δ_d, mm, Inner Pipe	D_o / δ_D, mm, Outer Pipe	Code	P_{SHS}, MPa	G_{SCW}, kg/m^{2}s	$\dot{m}_{SHS,pipe}$, kg/s	d_o / δ_d, mm, Inner Pipe	D_o / δ_D, mm, Outer Pipe
11111	5	200	0.07	21.3/3.73	26.7/1.65	12113	5	250	0.07	21.3/3.73	33.4/2.77
11112	5	200	0.07	21.3/3.73	33.4/1.65	12211	5	250	0.1	21.3/3.73	26.7/1.65
11113	5	200	0.07	21.3/3.73	33.4/2.77	12212	5	250	0.1	21.3/3.73	33.4/1.65
11142	5	200	0.07	26.7/5.56	33.4/1.65	12213	5	250	0.1	21.3/3.73	33.4/2.77
11143	5	200	0.07	26.7/5.56	33.4/2.77	12242	5	250	0.1	26.7/5.56	33.4/1.65
11211	5	200	0.1	21.3/3.73	26.7/1.65	12243	5	250	0.1	26.7/5.56	33.4/2.77
11212	5	200	0.1	21.3/3.73	33.4/1.65	12311	5	250	0.13	21.3/3.73	26.7/1.65
11213	5	200	0.1	21.3/3.73	33.4/2.77	12312	5	250	0.13	21.3/3.73	33.4/1.65
11232	5	200	0.1	26.7/3.91	33.4/1.65	12313	5	250	0.13	21.3/3.73	33.4/2.77
11233	5	200	0.1	26.7/3.91	33.4/2.77	12332	5	250	0.13	26.7/3.91	33.4/1.65
11242	5	200	0.1	26.7/5.56	33.4/1.65	12333	5	250	0.13	26.7/3.91	33.4/2.77
11243	5	200	0.1	26.7/5.56	33.4/2.77	12342	5	250	0.13	26.7/5.56	33.4/1.65
11311	5	200	0.13	21.3/3.73	26.7/1.65	12343	5	250	0.13	26.7/5.56	33.4/2.77
11312	5	200	0.13	21.3/3.73	33.4/1.65	13211	5	300	0.1	21.3/3.73	26.7/1.65
11313	5	200	0.13	21.3/3.73	33.4/2.77	13212	5	300	0.1	21.3/3.73	33.4/1.65
11322	5	200	0.13	26.7/2.87	33.4/1.65	13213	5	300	0.1	21.3/3.73	33.4/2.77
11323	5	200	0.13	26.7/2.87	33.4/2.77	13242	5	300	0.1	26.7/5.56	33.4/1.65
11332	5	200	0.13	26.7/3.91	33.4/1.65	13243	5	300	0.1	26.7/5.56	33.4/2.77
11333	5	200	0.13	26.7/3.91	33.4/2.77	13311	5	300	0.13	21.3/3.73	26.7/1.65
11342	5	200	0.13	26.7/5.56	33.4/1.65	13312	5	300	0.13	21.3/3.73	33.4/1.65
11343	5	200	0.13	26.7/5.56	33.4/2.77	13313	5	300	0.13	21.3/3.73	33.4/2.77
12111	5	250	0.07	21.3/3.73	26.7/1.65	13342	5	300	0.13	26.7/5.56	33.4/1.65
12112	5	250	0.07	21.3/3.73	33.4/1.65	13343	5	300	0.13	26.7/5.56	33.4/2.77

Table A5. HX A (SCW/SHS) MATLAB Results for Test Combinations Using 4 MPa SHS Operating Fluid, 5–cm Intervals.

		HX GENERAL PARAMETERS						SCW – INNER PIPE FLOW							SHS – ANNULUS GAP FLOW						
Code (See Tab. A1/A2)	Pass (P)/Fail (F)/Error (E)	Heat Transfer Rate per Pipe, $\dot{Q}$,kW	Number of HX Pipes, N	Average Overall HTC, U_{avg}, W/m^{2}K	Heat Transfer Area per Pipe, A, m^2	Length per Pipe, L, m	Total Pipe Length, L_{Total}, km	Total Mass Flow Rate, $\dot{m}_{SCW}$, kg/s	Inlet/Outlet Temperature, °C	Inner Diameter, d_i, mm	Outer Diameter, d_o, mm	Minimum Burst Pressure, MPa	Pipe Mass Flux, G_{SCW}, kg/m^{2}s	Maximum Flow Velocity, u_{SCW}, m/s	Total Mass Flow Rate, $\dot{m}_{SHS}$, kg/s	Inlet/Outlet Temperature, °C	Inner Diameter, D_i, mm	Outer Diameter, D_o, mm	Minimum Burst Pressure, MPa	Annulus Mass Flux, G_{SHS}, kg/m^{2}s	Maximum Flow Velocity, u_{SHS}, m/s
21132	P	55.52	4042	655.5	1.90	22.65	91.55	226	625/400	18.9	26.7	139	200	3	283	273/600	30.1	33.4	37	462	46
21222	P	79.29	2830	804.5	3.14	37.45	105.98	195	625/391	21	26.7	92	200	3	283	274/600	30.1	33.4	37	659	65
22122	P	55.76	4024	768.3	0.99	11.8	47.48	347	625/444	21	26.7	91	250	4	282	272/600	30.1	33.4	37	462	46
22142	P	55.38	4051	622.6	2.97	35.4	143.41	193	625/391	15.6	26.7	239	250	4	284	274/600	30.1	33.4	37	462	46
22232	P	79.2	2833	812.2	2.98	35.5	100.57	198	625/392	18.9	26.7	139	250	4	283	274/600	30.1	33.4	37	659	65
23112	P	55.27	4060	527.1	4.38	65.5	265.93	183	625/389	13.8	21.3	178	300	4	284	275/600	30.1	33.4	37	197	19
23113	P	55.27	4060	626.2	3.69	55.15	223.91	183	625/389	13.8	21.3	179	300	4	284	275/600	27.86	33.4	67	276	27
23122	P	55.5	4043	821.8	0.82	9.8	39.62	419	625/467	21	26.7	91	300	4	283	273/600	30.1	33.4	37	462	46
23132	P	55.22	4063	758.1	1.02	12.15	49.37	341	625/442	18.9	26.7	138	300	4	284	275/600	30.1	33.4	37	462	46
23142	P	55.55	4039	666.9	1.80	21.45	86.64	231	625/401	15.6	26.7	238	300	4	283	273/600	30.1	33.4	37	462	46
23232	P	79.17	2835	874.9	1.87	22.3	63.22	238	625/404	18.9	26.7	139	300	4	284	274/600	30.1	33.4	37	659	65

Code (See Tab. A1/A2)	Pass (P)/Fail (F)/Error (E)	Heat Transfer Rate per Pipe, $\dot{Q}$,kW	Number of HX Pipes, N	Average Overall HTC, U_{avg}, W/m^{2}K	Heat Transfer Area per Pipe, A, m^2	Length per Pipe, L, m	Total Pipe Length, L_{Total}, km	Total Mass Flow Rate, $\dot{m}_{SCW}$, kg/s	Inlet/Outlet Temperature, °C	Inner Diameter, d_i, mm	Outer Diameter, d_o, mm	Minimum Burst Pressure, MPa	Pipe Mass Flux, G_{SCW}, kg/m^{2}s	Maximum Flow Velocity, u_{SCW}, m/s	Total Mass Flow Rate, $\dot{m}_{SHS}$, kg/s	Inlet/Outlet Temperature, °C	Inner Diameter, D_i, mm	Outer Diameter, D_o, mm	Minimum Burst Pressure, MPa	Annulus Mass Flux, G_{SHS}, kg/m^{2}s	Maximum Flow Velocity, u_{SHS}, m/s
22322	F	102.33	2193	966.3	3.90	46.55	102.08	189	625/390	21	26.7	92	250	4	285	275/600	30.1	33.4	37	857	**85**
23111	F	55.03	4077	947.2	2.44	36.45	148.61	184	625/389	13.8	21.3	181	300	4	285	276/600	23.4	26.7	48	949	**94**
23322	F	102.22	2195	1053.8	2.21	26.3	57.73	227	625/400	21	26.7	92	300	4	285	276/600	30.1	33.4	37	857	**85**
23332	F	102.81	2183	945.4	4.50	53.6	117.01	183	625/389	18.9	26.7	139	300	4	284	274/600	30.1	33.4	37	857	**85**

Table A6. HX B (HP/LP SHS) MATLAB Results for Test Combinations Using 5 MPa LP SHS Operating Fluid, 5–cm Intervals.

		HX GENERAL PARAMETERS						HP SHS – INNER PIPE FLOW							LP SHS – ANNULUS GAP FLOW						
Code (See Tab. A1/A2)	Pass (P)/Fail (F)/Review (R)	Heat Transfer Rate per Pipe, $\dot{Q}$,kW	Number of HX Pipes, N	Average Overall HTC, U_{avg}, W/m^{2}K	Heat Transfer Area per Pipe, A, m^2	Length per Pipe, L, m	Total Pipe Length, L_{Total}, km	Total Mass Flow Rate, $\dot{m}_{HP\ SHS}$, kg/s	Inlet/Outlet Temperature, °C	Inner Diameter, d_i, mm	Outer Diameter, d_o, mm	Minimum Burst Pressure, MPa	Pipe Mass Flux, $G_{HP\ SHS}$ kg/m^{2}s	Maximum Flow Velocity, $u_{HP\ SHS}$, m/s	Total Mass Flow Rate, $\dot{m}_{LP\ SHS}$, kg/s	Inlet/Outlet Temperature, °C	Inner Diameter, d_i, mm	Outer Diameter, d_o, mm	Minimum Burst Pressure, MPa	Pipe Mass Flux, $G_{LP\ SHS}$ kg/m^{2}s	Maximum Flow Velocity, $u_{LP\ SHS}$, m/s
11222	P	78.04	2875	873.8	1.51	18.0	51.75	397	625/389	21	26.7	91	400	28	288	288/600	30.1	33.4	37	659	52
11232	P	77.88	2881	784.1	2.48	29.55	85.13	323	625/341	18.9	26.7	138	400	28	288	289/600	30.1	33.4	37	659	52
12111	P	54.4	4125	1025	0.99	14.8	61.05	372	625/375	13.8	21.3	180	600	43	289	289/600	23.4	26.7	48	949	75
12112	P	54.51	4117	555.4	1.83	27.35	112.6	372	625/374	13.8	21.3	177	600	43	288	289/600	30.1	33.4	37	197	16
12113	P	54.55	4114	665.1	1.53	22.85	94	371	625/374	13.8	21.3	178	600	43	288	289/600	27.86	33.4	67	276	22
11122	R	54.48	4118	789	0.86	10.2	42	**568**	625/458	21	26.7	91	400	28	288	289/600	30.1	33.4	37	462	36
11132	R	54.43	4123	715.3	1.10	13.1	54.01	**462**	625/420	18.9	26.7	138	400	28	289	289/600	30.1	33.4	37	462	36
12122	R	54.83	4092	940.4	0.60	7.2	29.46	**847**	625/512	21	26.7	91	600	43	286	287/600	30.1	33.4	37	462	36
12132	R	54.63	4107	853.6	0.72	8.55	35.11	**690**	625/487	18.9	26.7	137	600	43	287	288/600	30.1	33.4	37	462	36
12222	R	78.11	2873	1066.8	0.88	10.5	30.17	**595**	625/465	21	26.7	91	600	43	287	288/600	30.1	33.4	37	659	52
12232	R	77.72	2887	954.6	1.13	13.45	38.83	**485**	625/430	18.9	26.7	138	600	43	289	289/600	30.1	33.4	37	659	52
11123	F	54.65	4106	1039.9	0.65	7.75	31.82	**567**	625/457	21	26.7	92	400	28	287	288/600	27.86	33.4	68	1408	**111**
11133	F	54.75	4098	912.5	0.86	10.3	42.21	**459**	625/419	18.9	26.7	139	400	28	287	288/600	27.86	33.4	68	1408	**111**

Code (See Tab. A1/A2)	Pass (P)/Fail (F)/Review (R)	Heat Transfer Rate per Pipe, $\dot{Q}$,kW	Number of HX Pipes, N	Average Overall HTC, U_{avg}, W/m^{2}K	Heat Transfer Area per Pipe, A, m^2	Length per Pipe, L, m	Total Pipe Length, L_{Total}, km	Total Mass Flow Rate, $\dot{m}_{HP\ SHS}$, kg/s	Inlet/Outlet Temperature, °C	Inner Diameter, d_i, mm	Outer Diameter, d_o, mm	Minimum Burst Pressure, MPa	Pipe Mass Flux, $G_{HP\ SHS}$ kg/m^{2}s	Maximum Flow Velocity, $u_{HP\ SHS}$, m/s	Total Mass Flow Rate, $\dot{m}_{LP\ SHS}$, kg/s	Inlet/Outlet Temperature, °C	Inner Diameter, d_i, mm	Outer Diameter, d_o, mm	Minimum Burst Pressure, MPa	Pipe Mass Flux, $G_{LP\ SHS}$ kg/m^{2}s	Maximum Flow Velocity, $u_{LP\ SHS}$, m/s
11223	F	78.11	2873	1077.8	1.22	14.6	41.95	397	625/389	21	26.7	92	400	28	287	288/600	27.86	33.4	67	2012	**158**
11233	F	77.82	2883	939.4	2.07	24.65	71.07	323	625/341	18.9	26.7	140	400	28	288	289/600	27.86	33.4	67	2012	**158**
12123	F	54.66	4105	1325.6	0.43	5.1	20.94	**850**	625/513	21	26.7	92	600	43	287	288/600	27.86	33.4	68	1408	**111**
12133	F	54.38	4126	1155.9	0.53	6.3	25.99	**693**	625/488	18.9	26.7	139	600	43	289	289/600	27.86	33.4	68	1408	**111**
12223	F	77.65	2890	1396.2	0.67	8.0	23.12	**598**	625/466	21	26.7	92	600	43	289	289/600	27.86	33.4	68	2012	**158**
12233	F	77.84	2883	1206.4	0.89	10.65	30.7	**484**	625/430	18.9	26.7	139	600	43	288	289/600	27.86	33.4	68	2012	**158**

Table A7. HX B (HP/LP SHS) Unsuccessful MATLAB Results for Test Combinations Using 5 MPa LP SHS Operating Fluid, 5–cm Intervals.

Code	$P_{LP\ HS}$, MPa	$G_{HP\ SHS}$, kg/m^{2}s	$\dot{m}_{LP\ SHS,pipe}$, kg/s	d_o / δ_d, mm, Inner Pipe	D_o / δ_D, mm, Outer Pipe
11111	5	400	0.07	21.3/3.73	26.7/1.65
11112	5	400	0.07	21.3/3.73	33.4/1.65
11113	5	400	0.07	21.3/3.73	33.4/2.77
11211	5	400	0.1	21.3/3.73	26.7/1.65
11212	5	400	0.1	21.3/3.73	33.4/1.65
11213	5	400	0.1	21.3/3.73	33.4/2.77
12211	5	600	0.1	21.3/3.73	26.7/1.65
12212	5	600	0.1	21.3/3.73	33.4/1.65
12213	5	600	0.1	21.3/3.73	33.4/2.77

APPENDIX B – CODE VERIFICATION

The tables below show the comparison between independent MATLAB and Excel calculations as described in Chapters 5 and 6. Tables B1 to Tables B3 are for HX A code 11222 and Tables B4 to B6 show results for HX B code 12111.

Table B1. HX A (SCW/SHS) Code 11222 Comparison of CV SCW Outlet Temperatures at Several HX Positions from MATLAB and Microsoft Excel.

	11222 – CV SCW Outlet Temperature, $T_{SCW,out}$, ($T_{SCW,x}$) °C			
POSITION *x*, m	**MATLAB $T_{SCW,out}$**	**EXCEL $T_{SCW,out}$**	**DIFFERENCE×10^3**	**%×10^3**
0	625	625	Initial Condition	-
4	599.32	599.32	0.120	0.020
8	577.16	577.16	0.093	0.016
12	557.38	557.38	–0.280	–0.050
15.95	539.29	539.29	–0.927	–0.172
19.95	521.62	521.62	–1.865	–0.357
23.95	503.80	503.80	–3.186	–0.632
27.9	485.05	485.05	–5.085	–1.048
31.9	463.26	463.26	–7.932	–1.712
35.9	435.08	435.09	–13.407	–3.081
38	414.19	414.21	–20.055	–4.842
38.5	407.92	407.94	–20.368	–4.993
39	401.20	401.22	–19.486	–4.857
39.5	394.84	394.86	–16.828	–4.262
39.85	391.14	391.16	–13.811	–3.531
Maximum % Difference Data Points				
5.65	589.82	589.82	**0.158**	**5.65**
38.35	409.86	409.88	**–20.398**	**38.35**

Table B2. HX A (SCW/SHS) Code 11222 Comparison of SHS Inlet Temperatures at Several HX Positions from MATLAB and Microsoft Excel.

	11222 – CV SHS Inlet Temperature, $T_{SHS,in}$, ($T_{SHS,x}$) °C			
POSITION ***x*, m**	**MATLAB** $T_{SHS,in}$	**EXCEL** $T_{SHS,in}$	**DIFFERENCE×10^3**	**%×10^3**
0	600	600	Initial Condition	-
4	577.68	577.68	–0.087	–0.015
8	557.80	557.81	–0.429	–0.077
12	539.43	539.43	–1.067	–0.198
15.95	521.97	521.97	–1.986	–0.381
19.95	504.18	504.18	–3.280	–0.651
23.95	485.27	485.28	–5.127	–1.057
27.9	464.02	464.03	–7.824	–1.686
31.9	436.89	436.90	–12.551	–2.873
35.9	395.56	395.58	–24.360	–6.158
38	356.29	356.34	–45.908	–12.883
38.5	341.77	341.82	–52.436	–15.340
39	323.72	323.78	–59.622	–18.414
39.5	302.61	302.68	–66.159	–21.858
39.85	286.91	286.97	–68.423	–23.843
Maximum % Difference Data Points				
0.25	598.51	598.51	**0.000**	**0.000**
39.85	286.91	286.97	**–68.423**	**–23.843**

Table B3. HX A (SCW/SHS) Code 11222 Comparison of Wall Temperatures at Several HX Positions from MATLAB and Microsoft Excel.

	11222 – CV Wall Temperature, T_w, °C			
POSITION x, m	**MATLAB T_w**	**EXCEL T_w**	**DIFFERENCE×10^3**	**%×10^3**
0	-	-	-	-
4	582.84	582.84	–0.042	–0.007
8	562.51	562.51	–0.304	–0.054
12	543.90	543.90	–0.869	–0.160
15.95	526.39	526.39	–1.706	–0.324
19.95	508.78	508.78	–2.884	–0.567
23.95	490.37	490.37	–4.541	–0.926
27.9	470.14	470.15	–6.900	–1.468
31.9	445.35	445.36	–10.677	–2.397
35.9	411.35	411.37	–17.538	–4.263
38	389.08	389.10	–15.343	–3.943
38.5	385.53	385.56	–25.494	–6.612
39	382.12	382.14	–24.130	–6.314
39.5	373.80	373.82	–25.630	–6.856
39.85	365.08	365.11	–29.482	–8.075
Maximum % Difference Data Points				
1.2	598.60	598.60	**0.008**	**0.001**
39.85	365.08	365.11	**–29.482**	**–8.075**

Table B4. HX B (HP/LP SHS) Code 12111 Comparison of HP SHS Outlet Temperatures at Several HX Positions from MATLAB and Microsoft Excel.

	12111 – CV HP SHS Outlet Temperature, $T_{HP\ SHS,out}$, ($T_{HP\ SHS,x}$) °C			
POSITION ***x*, m**	**MATLAB** $T_{HP\ SHS,out}$	**EXCEL** $T_{HP\ SHS,out}$	**DIFFERENCE×10^3**	**%×10^3**
0	625	625	Initial Condition	-
1.5	611.87	611.87	0.091	0.015
3	596.72	596.72	0.115	0.019
4.45	579.88	579.88	0.043	0.007
5.95	559.87	559.87	–0.081	–0.014
7.4	537.72	537.72	–0.268	–0.050
8.9	511.55	511.55	–0.540	–0.105
10.4	481.77	481.78	–0.921	–0.191
11.85	449.41	449.41	–1.400	–0.312
13.35	412.40	412.40	–1.918	–0.465
14.8	374.06	374.06	–1.505	–0.402
Maximum % Difference Data Points				
2.6	600.98	600.98	**0.127**	**0.021**
13.35	412.40	412.40	**–1.918**	**–0.465**

Table B5. HX B (HP/LP SHS) Code 12111 Comparison of LP SHS Inlet Temperatures at Several HX Positions from MATLAB and Microsoft Excel.

	12111 – CV LP SHS Inlet Temperature, $T_{LP\ SHS,in}$, ($T_{LP\ SHS,x}$) °C			
POSITION ***x*, m**	**MATLAB** $T_{LP\ SHS,in}$	**EXCEL** $T_{LP\ SHS,in}$	**DIFFERENCE×10^3**	**%×10^3**
0	600	600	Initial Condition	-
1.5	582.92	582.92	–0.033	–0.006
3	563.21	563.21	–0.155	–0.028
4.45	541.30	541.30	–0.348	–0.064
5.95	515.31	515.31	–0.628	–0.122
7.4	486.60	486.60	–0.999	–0.205
8.9	452.87	452.87	–1.494	–0.330
10.4	414.91	414.92	–2.093	–0.504
11.85	374.53	374.54	–2.694	–0.719
13.35	330.38	330.38	–3.183	–0.963
14.8	288.79	288.79	–3.498	–1.211
Maximum % Difference Data Points				
0.1	598.94	598.94	**0.000**	**0.000**
14.8	288.79	288.79	**–3.498**	**–1.211**

Table B6. HX B (HP/LP SHS) Code 12111 Comparison of Wall Temperatures at Several HX Positions from MATLAB and Microsoft Excel.

	12111 – CV Wall Temperature, T_w, °C			
POSITION x, m	**MATLAB T_w**	**EXCEL T_w**	**DIFFERENCE×10^3**	**%×10^3**
0	-	-	-	-
1.5	591.32	591.32	0.002	0.000
3	572.96	572.96	–0.076	–0.013
4.45	552.57	552.57	–0.232	–0.042
5.95	528.39	528.39	–0.464	–0.088
7.4	501.67	501.68	–0.778	–0.155
8.9	470.27	470.27	–1.202	–0.256
10.4	434.83	434.84	–1.732	–0.398
11.85	396.90	396.90	–2.299	–0.579
13.35	354.75	354.75	–2.820	–0.795
14.8	313.56	313.56	–3.000	–0.957
Maximum % Difference Data Points				
0.85	598.50	598.50	**0.009**	**0.001**
14.8	313.56	313.56	**–3.000**	**–0.957**

APPENDIX C – SUMMARY OF CALCULATION STEPS

The following is a summary of the iterative calculation steps as described in Chapter 5 and executed via the MATLAB script documented in Appendix D. The calculations begin with a selection of independent parameters: intermediate loop operating pressure in MPa, mass flux of fluid in the HX inner pipe in kg/m^{2}s, pipe mass flow rate of the fluid in the HX annulus gap in kg/s, inner pipe dimensions (outer diameter and thickness) in mm and outer pipe dimensions (outer diameter and thickness) in mm. All major calculation steps are shown below and performed for both operating fluids in the HX at each cv, unless otherwise noted. For simplicity, variables are shown in terms of HX A operating fluids. Where thermophysical properties were required, the NIST REFPROP (2010) database provided information via MATLAB.

1. Inner diameters of the inner, d_i, and outer, D_i, pipes are calculated (Eqns. 11 – 12)

Determination of Inner Pipe Wall Temperature

2. Calculation of Reynolds number, $\mathbf{Re}_{b,x}$, and extraction of bulk-fluid thermophysical properties for the cv (Eqns. 13 – 15)
3. An initial uniform inner pipe wall temperature is assumed to be 0.08 K below the SCW temperature to enable iterative calculations to proceed
4. Extraction of wall-fluid thermophysical properties for the cv and calculation of the cross-section averaged specific heat, $\overline{c_{p,x}}$, used to calculate cross-section averaged Prandtl number, $\overline{\mathbf{Pr}_{b,x}}$ (Eqns. 16 – 17)
5. Using $\mathbf{Re}_{b,x}$, $\overline{\mathbf{Pr}_{b,x}}$, wall-fluid density, $\rho_{w,x}$ and bulk-fluid density, $\rho_{b,x}$, the Mokry et al. correlation is used to calculate the Nusselt number, $\mathbf{Nu}_{b,x}$, (Eqns. 5, 18); for applicable test combinations, enhancement of the HTC is through increases to the $\mathbf{Nu}_{b,x}$ of 25, 50 and 75% above the base case
6. The local HTCs, $h_{SCW,x}, h_{SHS,x}$, are calculated followed by the thermal resistances of the operating fluids, $R_{SCW,x}, R_{SHS,x}$ and pipe wall $R_{w,x}$ including the thermal conductivity of the pipe wall, $k_{w,x}$ (Eqns. 8, 19 – 22, 24)

7. The cv inner pipe wall temperature, $T_{w,x}$, is calculated and compared to the temperature assumed in Step 3; if the difference between the values is equal to or exceeds 0.001 K, one half of the difference between the calculated and assumed value is subtracted from the calculated value and becomes the new "assumed" value; if the difference between the compared values is less than –0.001 K, the calculated value is increased by half of the difference; if the difference is between –0.001 K and 0.001 K the iteration is terminated (Eqn. 23)
8. After finding an acceptable wall temperature, the overall HTC, U_x, is calculated using the thermal resistances of the fluids (Eqn. 25)

Determination of Operating Fluid Temperatures for CV

9. An initial inner SHS cv inlet temperature is assumed to be 0.08 K below the SHS cv outlet temperature to enable iterative calculations to proceed
10. Using rearranged energy balance equations and U_x from Step 8, an SCW cv outlet temperature, $T_{SCW,x}$, is calculated; subsequently a new SHS inlet temperature, $T_{SHS,x}$ is calculated using a rearranged energy balance (Eqns. 26 – 29)
11. Using the calculated temperatures, the heat transfer rate of both operating fluids is calculated and compared; if the difference between the values is equal to or exceeds 0.001 J, one half of the difference between the assumed and calculated SHS temperature is subtracted from the calculated value becomes the new "assumed" value; if the difference between the compared values is less than –0.001 J, the calculated value is increased by half of the difference; if the difference is between –0.001 J and 0.001 J the iteration is terminated (Eqns. 30 – 31)
12. The MATLAB script moves to the next cv where Steps 2 to 11 are repeated until the calculated SHS cv inlet temperature reaches 25°C above T_{sat} at the operating pressure when the iteration process is terminated

Material Strength Calculation

13. For each cv, the tensile strength, *S*, of the inner pipe is calculated based on $T_{w,x}$ allowing for the calculation of the pipe burst pressure, *P* (Eqns. 9 – 10)

Pressure Loss Calculations

14. For test combinations where pressure losses were evaluated, the friction factor, $f_{,x}$, is calculated based on $\mathbf{Re}_{b,x}$ (Eqns. 32 – 33)
15. The pressure drop across a cv is calculated based on $f_{,x}$ as well as other thermophysical and design parameters (Eqns. 34 – 35); Note: only the HX inlet pressures are known for each operating fluid and given that all calculations progress from one end of the HX to the other, an outlet pressure must be assumed for the SHS flow and pressure drops are added across the HX to achieve the inlet pressure

Once all values are known they are stored in individual Microsoft Excel spreadsheets for analysis and further data manipulation.

Verification of the calculations is completed using iterative calculations in Excel based on the same formulae outlined in Chapter 5.

APPENDIX D – MATLAB SCRIPT

This MATLAB script was developed to perform thermalhydraulic assessments on a number of HX designs. It has been formatted to allow for direct transfer to a MATLAB m-file.

```
%%%%%%%%%%%%%%%%%%%%%%%%%%%%%%%%%%%%%%%%%%%%%%%%%%%%%%%%%%%%%%%%%%%%%%%%%%%%%%%%
%     Thermalhydraulic Calculations for HX Located on SCW NPP SCWR  %
%             No-Reheat and Single Reheat Cycle Layouts             %
%             HX A - Located downstream of reactor outlet           %
%      HX B - Located downstream of steam reheat reactor outlet     %
%           Counterflow HX, SCW Inner Tube, SHS Annulus Gap         %
%                  Andrew Lukomski - 2011 - UOIT                    %
%            Assumption - H2 production rate is 1 kg/s              %
%%%%%%%%%%%%%%%%%%%%%%%%%%%%%%%%%%%%%%%%%%%%%%%%%%%%%%%%%%%%%%%%%%%%%%%%%%%%%%%%

clear all; clc; format long;
fluid = 'WATER.FLD'; % Water is defined as the operating fluid
pi    = 3.14159265358979; % Definition of Pi

%%%%%%%%%%%%%%%%%%%%%%%%%%%%%%%%%%%%%%%%%%%%%%%%%%%%%%%%%%%%%%%%%%%%%%%%%%%%%%%%
% Parameters for iterative calculations are defined as follows:
% system-parameter
% e.g. scwmflowtot -> SCW loop - mass flow rate - total
% Acronyms used: SCW - SuperCriticalWater, SHS - SuperHeatedSteam
%%%%%%%%%%%%%%%%%%%%%%%%%%%%%%%%%%%%%%%%%%%%%%%%%%%%%%%%%%%%%%%%%%%%%%%%%%%%%%%%

% Define operating requirements of the Cu-Cl Cycle (4-Step, electrolytic production)
% Energy requirements found in ISSCWR paper Lukomski et al. (2011) based on conclusions of Wang et
al.(2010)

% Thermal Energy Required by Cu-Cl Cycle
h2maxreq = 247178.22 ; % kJ/kg, Maximum Energy Requirement, No Recycling
disp('The total heat energy requirement in kJ/kg is: ')
disp(h2maxreq)
```

```
% Recyclable Thermal Energy Within Cu-Cl Cycle
h2maxrecyc = 45640 ; % kJ/kg, Maximum Thermal Energy Recoverable
h2fracrecyc = 0.5; % fraction of heat recycled internal to the Cu-Cl Cycle
disp('The maximum amount of heat recyclable (kJ/kg) and actual amount of heat recycled (kJ/kg) from the
CuCl Cycle is: ')
disp(h2maxrecyc), disp(h2fracrecyc*h2maxrecyc)

% Net Thermal Energy Requirement
h2energyreq = h2maxreq - (h2maxrecyc*h2fracrecyc); % kJ/s, Actual Heat Requirement of Cu-Cl Cycle
disp('The actual heat energy requirement in kJ/kg is: ')
disp(h2energyreq)

heatexcalc = input('What HX is to be modeled? HX A SCW/SHS-1, HX B SHS/SHS Iterative-2, HX B SHS/SHS Log
Mean-3: ');
printresults = input('Do you want to print results? Yes-1, No-0: ');

if(heatexcalc == 1 || heatexcalc == 2)
pressurelosses = input('Do you want to account for pressure losses? Yes-1, No-0: ') % Each test case must
be prepared manually, see section on pressure losses
end
%%%%%%%%%%%%%%%%%%%%%%%%%%%%%%%%%%%%%%%%%%%%%%%%%%%%%%%%%%%%%%%%%%%%%%%%%%%%%%%
% Heat Exchanger located at Reactor Outlet SCW Channels (HX A) / Reheater Outlet Channels
% (HX B) Calculations - Iterative based
% Note - Variables are in terms of SCW and SHS based on the interface of
% the HX downstream of the SCWR's SCW channels. Although coolant flow for HX B
% on the SCWR side is no longer supercritical, variable titles are still shown
% as 'scw' to distringuish between the SHS flows on the HX sides.
%%%%%%%%%%%%%%%%%%%%%%%%%%%%%%%%%%%%%%%%%%%%%%%%%%%%%%%%%%%%%%%%%%%%%%%%%%%%%%%

if (heatexcalc == 1 || heatexcalc == 2) % 1 Corresponds to HX A, 2 Corresponds to HX B

        frachx1 = 1; % Input fraction of total thermal energy required that is transferred by this HX
        hx1req = frachx1 * h2energyreq;
        disp('The energy transferred via HX A is: '), disp(hx1req)
```

```
htcenhancement = 1; % Default Fraction of Heat Transfer Enhancement - i.e. 25% increase corresponds to 1.25

% Coded Test Matrix Available to Simplify User Inputs
codedtest = 1;%input('Use Coded Test Parameters? Yes - 1, No - 0: '); % Coded Tests Use Predetermined
Combinations

    if(codedtest == 1)
        if(heatexcalc == 1) % HX A
        entershspressure  = input('Input SHS Pressure (MPa) - 5 MPa=1, 4 MPa=2: ');
            testpressure = [5000 4000];
        enterscwmassflux  = input('Input SCW Mass Flux (kg/m2s) - 200=1, 250=2, 300=3: ');
            testscwmassflux  = [200 250 300];
        entershspipeflow  = input('Input SHS Pipe Mass Flow (kg/s) - 0.07=1, 0.1=2, 0.13=3: ');
            testshspipeflow  = [0.07 0.10 0.13];
        enterinnerpipedim = input('Input Inner Pipe Combo (mm) - 21.3/3.73=1, 26.7/2.87=2, 26.7/3.91=3,
26.7/5.56=4: ');
            testinnerpipedim = [0.0213 0.0267 0.0267 0.0267]; testinnerpipethi = [0.00373 0.00287 0.00391
0.00556];
        enterouterpipedim = input('Input Outer Pipe Combo (mm) - 26.7/1.65=1, 33.4/1.65=2, 33.4/2.77=3: ');
            testouterpipedim = [0.0267 0.0334 0.0334]; testouterpipethi = [0.00165 0.00165 0.00277];
        htcenhancement = input('Input Fraction of Heat Transfer Enhancement - ie. 25% = 1.25: ');
        end

        if(heatexcalc == 2) % HX B
        entershspressure  = input('Input LP SHS Pressure (MPa) - 5 MPa= 1: ');
            testpressure = [5000];
        enterscwmassflux  = input('Input HP SHS Mass Flux (kg/m2s) - 400= 1, 600= 2: ');
            testscwmassflux  = [400 600];
        entershspipeflow  = input('Input LP SHS Pipe Mass Flow (kg/s) - 0.07= 1, 0.10= 2: ');
            testshspipeflow  = [0.07 0.10];
        enterinnerpipedim = input('Input Inner Pipe Combo (mm) - 21.3/3.73= 1, 26.7/2.87= 2, 26.7/3.91= 3:
');
            testinnerpipedim = [0.0213 0.0267 0.0267]; testinnerpipethi = [0.00373 0.00287 0.00391];
        enterouterpipedim = input('Input Outer Pipe Combo (mm) - 26.7/1.65= 1, 33.4/1.65= 2, 33.4/2.77= 3:
');
            testouterpipedim = [0.0267 0.0334 0.0334]; testouterpipethi = [0.00165 0.00165 0.00277];
        htcenhancement = input('Input Fraction of Heat Transfer Enhancement - ie. 25% = 1.25: ');
```

```
        end
    end

%%%%%%%%%%%%%%%%%%%%%%%%%%%%%%%%%%%%%%%%%%%%%%%%%%%%%%%%%%%%%%%%%%%%%%%%%%%%%%%
% HX Operating and Design Parameters on SCW Side
%%%%%%%%%%%%%%%%%%%%%%%%%%%%%%%%%%%%%%%%%%%%%%%%%%%%%%%%%%%%%%%%%%%%%%%%%%%%%%%

    if(heatexcalc == 1) % HX A
    scwpress = 25000; % kPa, SCW pressure; Pressure losses are neglected
    end
    if(heatexcalc == 2) % HX B
    scwpress = 5700; % kPa, SHS pressure; Pressure losses are neglected
    end

    scwtempin = 898.15; % K, SCW HX Inlet temperature

    scwpipediaout = 0.0267; % m, Inner pipe, outer diameter
    if(codedtest == 1) % If using coded tests, matrix is referenced
        scwpipediaout = testinnerpipedim(enterinnerpipedim);
    end

    scwpipethick = 0.00391; % m, Thickness of inner pipe
    if(codedtest == 1) % If using coded tests, matrix is referenced
        scwpipethick  = testinnerpipethi(enterinnerpipedim);
    end

    scwpipediain = scwpipediaout-2*scwpipethick; % m, Inner pipe, inner diameter
    scwflowarea = (pi/4)*(scwpipediain)^2; % m2, Flow area of inner pipe

    disp('HX 1 Inner Tube Dimensions in mm')
    disp([scwpipediaout*1000, scwpipethick*1000, scwpipediain*1000])

    scwmassflux = 500; % kg/m2s, Mass flux of SCW, (lower limit of 200 kg/m2s based on Mokry et al.
correlation)
    if(codedtest == 1) % If using coded tests, matrix is referenced
        scwmassflux = testscwmassflux(enterscwmassflux);
```

```
    end

    scwtubemassflow = scwmassflux * scwflowarea; % kg/s, Mass flow rate of SCW per pipe

%%%%%%%%%%%%%%%%%%%%%%%%%%%%%%%%%%%%%%%%%%%%%%%%%%%%%%%%%%%%%%%%%%%%%%%%%%%%%%%
% HX Operating and Physical Parameters on SHS Side
%%%%%%%%%%%%%%%%%%%%%%%%%%%%%%%%%%%%%%%%%%%%%%%%%%%%%%%%%%%%%%%%%%%%%%%%%%%%%%%

    shspress = 5000; % kPa, Assume no Pressure Drop for this Analysis
    if(codedtest == 1)
        shspress = testpressure(entershspressure);
    end

    shslowlimit = refpropm('T', 'P', shspress, 'Q', 1, fluid); % K, Introduce saturation temperature of SHS
at operating pressure
    shstempin = shslowlimit + 25; % K, Inlet temperature of SHS into HX, account for a 25 K buffer to
saturation point
    shstempout = 873.15; % K, Outlet SHS temperature

    shspipediaout = 0.0334; % m, Outer pipe, outer diameter
    if(codedtest == 1)
        shspipediaout = testouterpipedim(enterouterpipedim);
    end

    shspipethick = 0.00165; % m, Thickness of outer pipe
    if(codedtest == 1)
        shspipethick = testouterpipethi(enterouterpipedim);
    end

    shspipediain = shspipediaout - 2*shspipethick; % m, Outer pipe, inner diameter
    shsflowarea = (pi/4)*((shspipediain)^2 - (scwpipediaout)^2); % m2, Flow area of annulus gap
    shswetperimeter = pi*(scwpipediaout + shspipediain); % m, Wetted perimeter for the annulus gap; inner
pipe OD and outer pipe ID
    shshyddia = (4*(pi/4)*(shspipediain^2 - scwpipediaout^2))/ shswetperimeter; % m, Hydraulic diameter

    disp('HX1 Outer Tube Dimensions in mm')
```

```
    disp([shspipediaout*1000, shspipethick*1000, shspipediain*1000])

    shstubemassflow = 0.09; % kg/s, Mass flow rate of SHS per pipe
    if(codedtest == 1)
        shstubemassflow = testshspipeflow(entershspipeflow);
    end
    shsmassflux = shstubemassflow/shsflowarea; % kg/m2s, Mass flux of SHS

    pipegap = shspipediain - scwpipediaout; % m, Annulus gap thickness

%%%%%%%%%%%%%%%%%%%%%%%%%%%%%%%%%%%%%%%%%%%%%%%%%%%%%%%%%%%%%%%%%%%%%%%%%%%%%%%
% Iterative Calculation for HX A/HX B
%%%%%%%%%%%%%%%%%%%%%%%%%%%%%%%%%%%%%%%%%%%%%%%%%%%%%%%%%%%%%%%%%%%%%%%%%%%%%%%

calculate = 1;
if (calculate == 1) % If "calculate" equals "1" enter into iterative process

inc = 0.05; % m, Increment to be used for each step calculation - steps are at 0.05 m (5 cm)
iternumber = 2000; % User defined maximum number of control volumes (HX positions/nodes)
hxlength = iternumber*inc; % m, Maximum length of HX based on defined number of positions/nodes
incarea = inc*pi*scwpipediaout; % m2, Incremental HX inner pipe outer wall area for

% In this counter flow application, the calculation will proceed from the
% HX inlet of the SCW and outlet of the SHS. For the SCW, the outlet
% temperature for a given control volume becomes the inlet temperature for the next one.
% For the SHS, the inlet temperature for a given control volume becomes the
% outlet temperature for the next one.

% Create empty matrices with the same number of cells as the number of
% control volumes
% SCW Bulk Parameters
    scwdensity   = zeros(iternumber, 1); % kg/m3, Local density parameter
    scwthermcond = zeros(iternumber, 1); % W/mK, Local thermal conductivity parameter
    scwviscosity = zeros(iternumber, 1); % Pa s, Local viscosity parameter
    scwenthalpy  = zeros(iternumber, 1); % J/kg, Local enthalpy parameter
    scwreynolds  = zeros(iternumber, 1); % Local Reynolds parameter
```

```
% SCW Wall Parameters
    scwdensitywall   = zeros(iternumber, 1); % kg/m3, Local wall density parameter
    scwviscositywall = zeros(iternumber, 1); % Pa s, Local wall viscosity parameter
    scwenthalpywall  = zeros(iternumber, 1); % J/kg, Local wall enthalpy parameter

% SCW Global Parameters
    scwcpavg         = zeros(iternumber, 1); % J/kgK, global average cp parameter
    scwprandtl       = zeros(iternumber, 1); % Global Prandtl parameter
    scwnusselt       = zeros(iternumber, 1); % Global Nusselt parameter
    scwhtc           = zeros(iternumber, 1); % W/m2K, Global HTC coefficient
    scwoutlettemp    = zeros(iternumber, 1); % K, Outlet temperature for a given control volume
    scwoutlettemp(1,1) = scwtempin;          % K, Known temperature of SCW entering HX, consider inlet of
HX the outlet of SCWR piping
    scwmcp           = zeros(iternumber, 1); % W/K, Heat capacity rate for SCW
    scwmcpdt         = zeros(iternumber, 1); % W, Heat transfer rate for SCW
    scwpressure      = zeros(iternumber, 1); % kPa, SCW Pressure
    scwpressure(1,1) = scwpress;             % kPa, Inlet pressure of SCW
    scwtubespeed     = zeros(iternumber, 1); % m/s, Fluid velocity across the HX
    scwdeltap        = zeros(iternumber, 1); % kPa, Pressure difference experienced across a control volume
    scwdeltap(1)     = 0;                    % kPa, Initialize pressure loss parameter

% For description of parameters see SCW definitions above
% SHS Bulk Parameters
    shsdensity       = zeros(iternumber, 1);
    shsthermcond     = zeros(iternumber, 1);
    shsviscosity     = zeros(iternumber, 1);
    shsenthalpy      = zeros(iternumber, 1);
    shsreynolds      = zeros(iternumber, 1);

% SHS Wall Parameters
    shsdensitywall   = zeros(iternumber, 1);
    shsviscositywall = zeros(iternumber, 1);
    shsenthalpywall  = zeros(iternumber, 1);

    % SHS Global Parameters
    shscpavg        = zeros(iternumber, 1);
```

```
    shsprandtl      = zeros(iternumber, 1);
    shsnusselt      = zeros(iternumber, 1);
    shshtc          = zeros(iternumber, 1);
    shsinlettemp    = zeros(iternumber, 1); % K, SHS inlet temperature into a given control volume
    shsinlettemp(1,1) = shstempout;         % K, Fixed temperature of SHS exiting HX, consider outlet of HX
the re-entry point to the SCWR
    shsmcp          = zeros(iternumber, 1);
    shsmcpdt        = zeros(iternumber, 1);
    shspressure     = zeros(iternumber, 1);
    shspressure(1,1) = shspress;
    shstubespeed    = zeros(iternumber, 1);
    shsdeltap       = zeros(iternumber, 1);
    shsdeltap(1,1)  = 0;

% Wall conditions
    walltemp      = zeros(iternumber, 1); % K, Temperature of wall, assume constant across
    wallthermcond = zeros(iternumber, 1); % W/mk, Thermal conductivity of the wall, calculated by
iterations
    position      = zeros(iternumber, 1); % m, Position along pipe
    position(1,1) = 0;                    % First position in the HX is 0
    counterwall1  = zeros(iternumber, 1); % Tracks number of iterations required to find wall temperature
for each control volume
    counterwall2  = zeros(iternumber, 1); % Tracks number of iterations to find each wall temperature
    countertemp1  = zeros(iternumber, 1); % Tracks number of iterations to find each control volume
temperature
    countertemp2  = zeros(iternumber, 1); % Tracks number of iterations to find each control volume
temperature

% Overall Conditions
    resistscw     = zeros(iternumber, 1); % K m2/W, SCW thermal resistance
    resistshs     = zeros(iternumber, 1); % K m2/W, SHS thermal resistance
    resistwall    = zeros(iternumber, 1); % K m2/W, Wall thermal resistance
    U  = zeros(iternumber, 1); % W/m2K, Overall HTC
    UA = zeros(iternumber, 1); % W/K
    scwheattrans = zeros(iternumber, 1); % W, Total heat transfer rate based on SCW thermal energy loss
    shsheatrec   = zeros(iternumber, 1); % W, Total heat transfer rate based on SHS thermal energy gain
```

```
% Pipe Material Conditions
    pipetenstrin      = zeros(iternumber, 1); % MPa, Tensile Strength of SS-304 inner pipe
    pipemodelasin     = zeros(iternumber, 1); % MPa, Modulus of Elasticity of SS-304 outer pipe
    pipetenstrout     = zeros(iternumber, 1); % MPa, Tensile Strength of SS-304 inner pipe
    pipemodelasout    = zeros(iternumber, 1); % MPa, Modulus of Elasticity of SS-304 outer pipe
    pipepoisson       = zeros(iternumber, 1); % Poissons Ratio, based on interpretation of graphical data
    pipeburstin       = zeros(iternumber, 1); % MPa, Burst pressure for inner pipe
    pipecollapsein    = zeros(iternumber, 1); % MPa, Collapse pressure for inner pipe
    pipeburstout      = zeros(iternumber, 1); % MPa, Burst pressure for outer pipe
    pipecollapseout   = zeros(iternumber, 1); % MPa, Collapse pressure for outer pipe

% General Tracking Parameters
    track = zeros(iternumber, 1);
    track2 = zeros(iternumber, 1);
    track3 = zeros(iternumber, 1);
    trackwall = zeros(iternumber, 1);
    trackinter = zeros(iternumber, 1);

%%%%%%%%%%%%%%%%%%%%%%%%%%%%%%%%%%%%%%%%%%%%%%%%%%%%%%%%%%%%%%%%%%%%%%%%%%%%%%%
% Create "for loop" to calculate inlet (SHS) and outlet (SCW) temperatures
% for each control volume along the length of the HX. First must calculate
% wall temperature to find overall HTC, followed by energy balance
% calculations to find operating fluid temperatures.
%%%%%%%%%%%%%%%%%%%%%%%%%%%%%%%%%%%%%%%%%%%%%%%%%%%%%%%%%%%%%%%%%%%%%%%%%%%%%%%

    for i = 2:1:iternumber
    position(i) = inc*i-inc; % m, Subtract increment to correct calculation

   % Bulk Fluid Parameters - Remain constant within a given control volume
   % SCW
   scwdensity(i,1)   = refpropm('D', 'T', scwoutlettemp(i-1,1),'P', scwpressure(i-1,1), fluid);
   scwthermcond(i,1) = refpropm('L', 'T', scwoutlettemp(i-1,1),'P', scwpressure(i-1,1), fluid);
   scwviscosity(i,1) = refpropm('V', 'T', scwoutlettemp(i-1,1),'P', scwpressure(i-1,1), fluid);
   scwenthalpy(i,1)  = refpropm('H', 'T', scwoutlettemp(i-1,1),'P', scwpressure(i-1,1), fluid);
   scwreynolds(i,1)  = (4*scwtubemassflow)/(pi*scwpipediain*scwviscosity(i,1));
```

```
 % SHS
   shsdensity(i,1)    = refpropm('D', 'T', shsinlettemp(i-1,1),'P', shspressure(i-1,1), fluid);
   shsthermcond(i,1) = refpropm('L', 'T', shsinlettemp(i-1,1),'P', shspressure(i-1,1), fluid);
   shsviscosity(i,1) = refpropm('V', 'T', shsinlettemp(i-1,1),'P', shspressure(i-1,1), fluid);
   shsenthalpy(i,1)   = refpropm('H', 'T', shsinlettemp(i-1,1),'P', shspressure(i-1,1), fluid);
   shsreynolds(i,1)   = (4*shstubemassflow)/(pi*(shspipediain + scwpipediaout)*shsviscosity(i,1));

%%%%%%%%%%%%%%%%%%%%%%%%%%%%%%%%%%%%%%%%%%%%%%%%%%%%%%%%%%%%%%%%%%%%%%%%%%%%
% Create "while loop" to calculate wall temperature for use in the Mokry et
% al. correlation. Calculation procedure: Assume a wall temperature;
% calculate relevant wall fluid thermophysical parameters; calculate new wall
% temperature using SCW and SHS thermal resistances; compare assumed and calculated
% values and if not equal then recalculate using modified wall temperature.
%%%%%%%%%%%%%%%%%%%%%%%%%%%%%%%%%%%%%%%%%%%%%%%%%%%%%%%%%%%%%%%%%%%%%%%%%%%%

        diffwalltemp  = 1;
        walltempguess = scwoutlettemp(i-1,1)-0.08; % K, Assume an initial value of wall temperature to
enable iterative calculation
        walltemp(i,1) = walltempguess;
        counterwall1(i,1) = 1;
        counterwall2(i,1) = 1;
        criteria1 = 0.001; % Used in while loop and if statement to define acceptance criteria

    while (abs(diffwalltemp) > criteria1)

% SCW Wall Calculations
        scwdensitywall(i,1) = refpropm('D', 'T', walltemp(i,1),'P', scwpressure(i-1,1), fluid);
        scwviscositywall(i,1) = refpropm('V', 'T', walltemp(i,1),'P', scwpressure(i-1,1), fluid);
        scwenthalpywall(i,1) = refpropm('H', 'T', walltemp(i,1),'P', scwpressure(i-1,1), fluid);

        scwcpavg(i,1) = (scwenthalpywall(i,1) - scwenthalpy(i,1)) / (walltemp(i,1) - scwoutlettemp(i-1,1));
        scwprandtl(i,1) = (scwcpavg(i,1)*scwviscosity(i,1))/scwthermcond(i,1) ;
        scwnusselt(i,1) =
enhancement*0.0061*((scwreynolds(i,1))^(0.904))*((scwprandtl(i,1))^0.684)*((scwdensitywall(i,1)/scwdensity(
i,1))^0.564); % Nusselt Number based on Mokry et al. correlation
        scwhtc(i,1) = (scwnusselt(i,1)*scwthermcond(i,1))/(scwpipediain);
```

```
% SHS Wall Calculations
        shsdensitywall(i,1) = refpropm('D', 'T', walltemp(i,1),'P', shspressure(i-1,1), fluid);
        shsviscositywall(i,1) = refpropm('V', 'T', walltemp(i,1),'P', shspressure(i-1,1), fluid);
        shsenthalpywall(i,1) = refpropm('H', 'T', walltemp(i,1),'P', shspressure(i-1,1), fluid);

        shscpavg(i,1) = (shsenthalpywall(i,1) - shsenthalpy(i,1)) / (walltemp(i,1) - shsinlettemp(i-1,1));
        shsprandtl(i,1) = (shscpavg(i,1)*shsviscosity(i,1))/shsthermcond(i,1) ;
        shsnusselt(i,1) =
htcenhancement*0.0061*((shsreynolds(i,1))^(0.904))*((shsprandtl(i,1))^0.684)*((shsdensitywall(i,1)/shsdensi
ty(i,1))^0.564); % Nusselt Number based on Mokry et al. correlation
        shshtc(i,1) = (shsnusselt(i,1)*shsthermcond(i,1))/(shshyddia);

% HTC Properties Calculations
        walltherмcond(i,1) = 0.00000002*(walltemp(i,1))^3 - 0.00004*(walltemp(i,1))^2 +
0.0398*(walltemp(i,1))+ 5.728; % Using equation from curve fit for known values
        resistscw(i,1) = scwpipediaout/(scwpipediain*scwhtc(i,1)); % Thermal resistance at inner surface of
inner pipe
        resistwall(i,1) = (scwpipediaout*log(scwpipediaout/scwpipediain))/(2*wallthermcond(i,1)); % Thermal
resistance across wall
        resistshs(i,1) = 1/shshtc(i,1); % Thermal resistance at outer surface of inner pipe

        interwalltemp = walltemp(i,1); % Assign assumed wall temperature to intermediate "interwalltemp"
parameter
        walltemp(i,1) = ((scwoutlettemp(i-1,1)/resistscw(i,1)) + (shsinlettemp(i-
1,1)/resistshs(i,1)))/(1/resistscw(i,1) + 1/resistshs(i,1)); % K, Calculation of wall temperature

        diffwalltemp = walltemp(i,1)-interwalltemp; % Find difference between calculated and assumed wall
temperature

                track(i,1) = diffwalltemp;
                trackwall(i,1) = walltemp(i,1);
                trackinter(i,1) = interwalltemp;

% The following "if statements" are used obtain a converging wall temperature
            if (diffwalltemp == criteria1 || diffwalltemp > criteria1)
```

```
                walltemp(i,1) = walltemp(i,1) - abs(diffwalltemp)/2;
                counterwall1(i,1) = counterwall1(i,1) + 1;
            end

            if (diffwalltemp < -criteria1)
                walltemp(i,1) = walltemp(i,1) + abs(diffwalltemp)/2;
                counterwall2(i,1) = counterwall2(i,1) + 1;
            end

        if(counterwall1(i,1) == 1000 || counterwall2(i,1) == 1000) % If the number of iterations reaches
defined maximum, stop iteration process
            disp('Temperature Error - Iteration Maximum (1000) reached'), disp(position(i))
            break
        end
    end  % Part of "while" loop

% Calculations related to the Overall HTC
        U(i,1) = 1/(resistscw(i,1) + resistshs(i,1) + resistwall(i,1)); % Calculated overall HTC using
values from wall temperature results from "while" loop
        U(1) = U(2,1) - 1; % Define overall HTC at HX inlet - value is assumed for data completion purposes
only
        walltemp(1) = walltemp(2,1) + 0.5; % Define wall temperature at HX inlet - value is assumed for
data completion purposes only
        UA(i,1) = U(i,1)*incarea;

%%%%%%%%%%%%%%%%%%%%%%%%%%%%%%%%%%%%%%%%%%%%%%%%%%%%%%%%%%%%%%%%%%%%%%%%%%%%%%%
% Create a second "while loop" to calculate control volume SCW outlet
% temperature and SHS inlet temperature. Calculation procedure: assume
% SHS inlet temperature to calculate SCW outlet temperature. Using
% calculated SCW outlet temperature to calculate a new SHS inlet temperature.
% Calculate heat transfer rate on the SCW and SHS side, compare values.
% If not equal, decrease/increase SHS inlet temperature accordingly and
% repeat the process. Exit process when values are approximately equal.
%%%%%%%%%%%%%%%%%%%%%%%%%%%%%%%%%%%%%%%%%%%%%%%%%%%%%%%%%%%%%%%%%%%%%%%%%%%%%%%

        diffmcpdt  = 1;
```

```
        shsinlettempguess = shsinlettemp(i-1,1)-0.08; % K, Assume an initial value of inlet temperature for
SHS to enable iterative calculation
        shsinlettemp(i,1) = shsinlettempguess;
        countertemp(i,1) = 1;
        criteria2 = 0.001; % Used in while loop and if statement to define acceptance criteria

        scwmcp(i,1) = scwtubemassflow*refpropm('C', 'T', scwoutlettemp(i-1,1),'P', scwpressure(i-1,1),
fluid); % W/K, Heat capacity rate on SCW side
        shsmcp(i,1) = shstubemassflow*refpropm('C', 'T', shsinlettemp(i-1,1),'P', shspressure(i-1,1),
fluid); % W/K, Heat capacity rate on SHS side

   while (abs(diffmcpdt) > criteria2)

        scwoutlettemp(i,1) = ((scwmcp(i,1)-0.5*UA(i,1))*scwoutlettemp(i-1,1) +
0.5*UA(i,1)*(shsinlettemp(i,1)...
        + shsinlettemp(i-1,1))) / (scwmcp(i,1) + 0.5*UA(i,1)); % Calculate SCW outlet temperature based on
SHS test value

        intershsinlettemp = shsinlettemp(i,1); % Assign assumed SHS inlet temperature to intermediate
variable to compare with calculated value

        shsinlettemp(i,1) = (shsinlettemp(i-1,1)*(shsmcp(i,1)+0.5*UA(i,1))-0.5*UA(i,1)*(scwoutlettemp(i-
1,1)...
        + scwoutlettemp(i,1))) / (shsmcp(i,1) - 0.5*UA(i,1)); % Calculate SHS inlet temperature based on
calculated SCW temperature

        scwmcpdt(i,1) = scwmcp(i,1)*(scwoutlettemp(i-1,1) - scwoutlettemp(i,1)); % Calculate Heat Transfer
Rate on the SCW side
        shsmcpdt(i,1) = shsmcp(i,1)*(shsinlettemp(i,1) - shsinlettemp(i-1,1)); % Calculate Heat Transfer
Rate on the SHS side

        diffmcpdt = scwmcpdt(i,1) + shsmcpdt(i,1); % Calculate the difference in heat transfer rates
        diffshsinlettemp = intershsinlettemp - shsinlettemp(i,1); % Calculate the difference in SHS
temperatures
        track2(i,1) = diffshsinlettemp;
        track3(i,1) = diffmcpdt;
```

```
% The following "if statements" are used obtain a converging SHS control
% volume inlet temperatures which balance the overall heat transfer rate
                if (diffmcpdt == criteria2 || diffmcpdt > criteria2)
                      shsinlettemp(i,1) = shsinlettemp(i,1) - diffshsinlettemp/2;
                      countertemp1(i,1) = countertemp1(i,1) + 1;
                end

                if (diffmcpdt < -criteria2)
                      shsinlettemp(i,1) = shsinlettemp(i,1) + abs(diffshsinlettemp)/2;
                      countertemp2(i,1) = countertemp2(i,1) + 1;
                end

        if(countertemp1(i,1) == 1000 || countertemp2(i,1) == 1000) % If number of iterations reaches
defined maximum, exit process
            disp('Heat Balance Error - Iteration Maximum (1000) reached'), disp(position(i))
            break
        end

   end % Part of "while loop" to balance heat transfer rates

    scwheattrans(i,1) = sum(scwmcpdt); % Total heat transfer rate taken on SCW side (loss to SHS)
    shsheatrec(i,1)   = sum(shsmcpdt); % Total heat transfer rate taken on SHS side (gained from SCW)
    shstubespeed(i,1) = shstubemassflow/(shsflowarea*refpropm('D', 'T', shsinlettemp(i-1,1), 'P',
shspressure(i-1,1), fluid));  % m/s, maximum SHS velocity
    scwtubespeed(i,1) = scwtubemassflow/(scwflowarea*refpropm('D', 'T', scwoutlettemp(i-1,1), 'P',
scwpressure(i-1,1), fluid)); % m/s, maximum SCW velocity

%%%%%%%%%%%%%%%%%%%%%%%%%%%%%%%%%%%%%%%%%%%%%%%%%%%%%%%%%%%%%%%%%%%%%%%%%%%%%%%
% Pressure Drop Calculations - Only account for frictional losses
%%%%%%%%%%%%%%%%%%%%%%%%%%%%%%%%%%%%%%%%%%%%%%%%%%%%%%%%%%%%%%%%%%%%%%%%%%%%%%%

    scwpressure(i) = scwpress; % Set SCW pressure for next control volume to initial pressure (no-pressure
losses)
    shspressure(i) = shspress; % Set SHS pressure for next control volume to initial pressure (no-pressure
losses)
```

```
% For SCW Flow
    if(pressurelosses == 1)
     scwfricfactor = (1/(0.790*log(scwreynolds(i,1))-1.64)^2);
     scwdeltap(i) = 0.001*scwfricfactor*scwdensity(i,1)*inc*(1/(2*scwpipediain))*...
         (scwtubemassflow/(scwflowarea*refpropm('D', 'T', scwoutlettemp(i-1,1), 'P', scwpressure(i-1,1),
fluid)))^2; % kPa, Pressure drop
     scwpressure(i) = (scwpressure(i-1,1)-scwdeltap(i)); % New SCW pressure for iterations
    end

% For SHS Flow
    if(pressurelosses == 1)
     shspressure(1) = shspress-447; % Assumed SHS pressure drop across HX - ONLY VALID FOR HX A CODE 13122,
other codes must be re-evaluated
     shsfricfactor = (1/((0.790*log(shsreynolds(i,1))-1.64)^2));
     shsdeltap(i) = 0.001*shsfricfactor*shsdensity(i,1)*inc*(1/(2*shshyddia))*...
         (shstubemassflow/(shsflowarea*refpropm('D', 'T', shsinlettemp(i-1,1), 'P', shspressure(i-1,1),
fluid)))^2; % kPa, Pressure drop
     shspressure(i) = (shspressure(i-1) + shsdeltap(i)); % New SHS pressure for iterations
    end

%%%%%%%%%%%%%%%%%%%%%%%%%%%%%%%%%%%%%%%%%%%%%%%%%%%%%%%%%%%%%%%%%%%%%%%%%%%%%%%
% Pipe Material Calculations
% Piping is contructed from Stainless Steel 304
%%%%%%%%%%%%%%%%%%%%%%%%%%%%%%%%%%%%%%%%%%%%%%%%%%%%%%%%%%%%%%%%%%%%%%%%%%%%%%%
    pipetenstrin(i) = -0.0004*(walltemp(i,1)-273.15)^2 - 0.2034*(walltemp(i,1)-273.15) + 605.14; % MPa,
Tensile strength of inner pipe
    pipetenstrout(i) = -0.0004*(shsinlettemp(i,1)-273.15)^2 - 0.2034*(shsinlettemp(i,1)-273.15) + 605.14; %
MPa, Tensile strength of outer pipe

    pipeburstin(i) = (2*pipetenstrin(i)*scwpipethick)/scwpipediain; % MPa, Burst pressure for inner pipe
        pipeburstout(i) = (2*pipetenstrout(i)*shspipethick)/shspipediain; % MPa, Burst pressure for outer
pipe

%%%%%%%%%%%%%%%%%%%%%%%%%%%%%%%%%%%%%%%%%%%%%%%%%%%%%%%%%%%%%%%%%%%%%%%%%%%%%%%
```

```
% Ensure that the SHS temperature entering the HX is well above saturation
        if(shsinlettemp(i,1)< shstempin)  % If SHS temperature falls below lower limit or the maximem
iterations are reached, end the calculation
            break
        end

    end % Part of 'for loop' to run iterations across the HX

end % Part of the if statement to conduct iterations

% Final calculation is to calculate the number of pipes required to
% transfer the entire thermal energy load.
reqtubes = ceil((hx1req*1000)/scwheattrans(i,1));
shsflowtot = reqtubes*shstubemassflow;
scwflowtot = reqtubes*scwtubemassflow;

%%%%%%%%%%%%%%%%%%%%%%%%%%%%%%%%%%%%%%%%%%%%%%%%%%%%%%%%%%%%%%%%%%%%%%%%%%%%
% Plotting and Printing of values into EXCEL
%%%%%%%%%%%%%%%%%%%%%%%%%%%%%%%%%%%%%%%%%%%%%%%%%%%%%%%%%%%%%%%%%%%%%%%%%%%%

graphscwoutlettemp = scwoutlettemp(1:i,:) - 273.15; % Graph SCW temperatures in Celsius
graphshsinlettemp = shsinlettemp(1:i,:) - 273.15; % Graph SHS temperatures in Celsius
graphwalltemp = walltemp(1:i,:) - 273.15; % Graph Wall temperatures in Celsius

mcps = [scwmcpdt(1:i,:), shsmcpdt(1:i,:)]; mcs = [scwmcp(1:i,:), shsmcp(1:i,:)];
plot(position(1:i,:), graphscwoutlettemp,'-r', position(1:i,:), graphshsinlettemp, '-.b',position(1:i,:),
U(1:i,:), '--g', position(1:i,:), graphwalltemp, ':b')
title('HX Temperatures'), xlabel('Position, m'), ylabel('Temperature, C')
location = 'NorthEast'; leg= legend('SCW Temp.', 'SHS Temp.',2, 'Location', location);

disp('The SCW outlet temperature is: '), disp(scwoutlettemp(i,1)-273.15)
disp('The maximum SHS and SCW flow velocities are (respectively): '), disp(max(shstubespeed)),
disp(max(scwtubespeed))
disp('The number of tubes required for the HX is: '), disp(reqtubes)
disp('The length of a single pipe is: '), disp(max(position))
disp('The total mass flow of SCW (kg/s) is: '), disp(scwflowtot)
```

```
disp('The total mass flow of SHS (kg/s) is: '), disp(shsflowtot)

% Print Thermal Energy Transferred
disp('The total energy transferred (SCW/SHS flows) in kJ is: '), disp(scwheattrans(i,1)/1000),
disp(shsheatrec(i,1)/1000)

disp('SHS max speed: '), disp(max(shstubespeed(1:i,1)));
if(heatexcalc == 1) % Print values for HX A to Excel spreadsheet
    printvaluessingle = printresults;
        if(printvaluessingle == 1)

% The following are parameters with single entries (not involved in
% iterative calculations)
        excelnamessingle = { 'Maximum Energy Requirement, kJ', 'Maximum Energy for Recycling, kJ',
'Fraction of Energy Recycled', 'Actual Energy Required, kJ', 'Fraction of Energy Transferred by HX1',
'Energy Transferred by HX1, kJ', 'Number of Tubes Required',...
                    ...
                    'SCW Pressure, MPa', 'SCW Total Flow, kg/s', 'Inner Tube Outer Diameter, m', 'Inner Tube
Pipe Thickness, m', 'Inner Tube Inner Diameter, m',...
                    'Inner Tube Flow Area, m2', 'SCW Mass Flux, kg/m2s', 'Maximum SCW Speed, m/s', 'SCW Tube
Mass Flow Rate, kg/s',...
                    ...
                    'SHS Pressure, MPa', 'SHS Total Flow, kg/s', 'Outer Tube Outer Diameter, m', 'Outer Tube
Pipe Thickness, m', 'Outer Tube Inner Diameter, m',...
                    'Annulus Flow Area, m2', 'SHS Mass Flux, kg/m2s', 'Maximum SHS Speed, m/s', 'Annulus
Wetted Perimeter, m', 'Annulus Hydraulic Diameter, m', 'SHS Tube Mass Flow Rate, kg/s', 'Pipegap, m'};

        excelvaluessingle = horzcat(h2maxreq, h2maxrecyc, h2fracrecyc, h2energyreq, frachx1, hx1req,
reqtubes,...
                    ...
                    scwpressure(i,1), scwflowtot, scwpipediaout, scwpipethick,scwpipediain,...
                    scwflowarea, scwmassflux, max(scwtubespeed), scwtubemassflow,...
                    ...
                    shspressure(i,1), shsflowtot, shspipediaout, shspipethick, shspipediain,...
                    shsflowarea, shsmassflux, max(shstubespeed), shswetperimeter, shshyddia,
shstubemassflow, pipegap);
```

```
        writefilenamessingle = xlswrite('tempdata.xls',excelnamessingle, 'HXA-HXB General','A1');
        writefilevaluessingle= xlswrite('tempdata.xls',excelvaluessingle, 'HXA-HXB General','A2');

    printvalues = printresults;
        if(printvalues == 1)

% The following parameters are involved in the iterative calculation
% process
        excelnames = {'position, m', 'SCW Outlet Temperatures, C', 'SCW Heat Capacity Rate, W/K', 'SCW Heat
Transfer Rate, W', 'SCW Total Heat Transfer Rate', ...
                    'SHS Inlet Temperatures, C', 'SHS Heat Capacity Rate, W/K', 'SHS Heat Transfer Rate, W',
'SHS Total Heat Transfer Rate', ...
                    ...
                    'Wall Temperatures, C', 'Overall Heat Transfer Coefficient, W/m2K', 'UA-Value, W/K',
'Thermal Resistance (Inner Wall), K/W', ...
                    'Thermal Resistance (Wall), K/W', 'Thermal Resistance (Outer Wall), K/W', 'Wall Thermal
Conductivity, W/mK', ...
                    ...
                    'SCW Density, kg/m3', 'SCW Thermal Conductivity, W/mK', 'SCW Viscosity, Pa s', 'SCW
Enthalpy, J/kg', ...
                    'SCW Reynolds Number', 'SCW Density (Wall), kg/m3', 'SCW Viscosity (Wall), Pa s', 'SCW
Enthalpy (Wall), J/kg', ...
                    'SCW Average Cp, J/kgK', 'SCW Prandtl', 'SCW Nusselt Number', 'SCW Heat Transfer
Coefficient, W/m2K', ...
                    ...
                    'SHS Density, kg/m3', 'SHS Thermal Conductivity, W/mK', 'SHS Viscosity, Pa s', 'SHS
Enthalpy, J/kg', ...
                    'SHS Reynolds Number', 'SHS Density (Wall), kg/m3', 'SHS Viscosity (Wall), Pa s', 'SHS
Enthalpy (Wall), J/kg', ...
                    'SHS Average Cp, J/kgK', 'SHS Prandtl', 'SHS Nusselt Number', 'SHS Heat Transfer
Coefficient, W/m2K',...
                    ...
                    'Inner Pipe Tensile Strength, MPa', 'Inner Pipe Burst Pressure, MPa',...
                    'Outer Pipe Tensile Strength, MPa', 'Outer Pipe Burst Pressure, MPa',...
                    ...
                    'SCW Pressure, kPa', 'SHS Pressure kPa'};
```

```
        excelvalues = horzcat(position(1:i,:), scwoutlettemp(1:i,:)-273.15, scwmcp(1:i,:), scwmcpdt(1:i,:),
scwheattrans(1:i,:), shsinlettemp(1:i,:)-273.15, shsmcp(1:i,:), shsmcpdt(1:i,:), shsheatrec(1:i,:),...
                    walltemp(1:i,:)-273.15, U(1:i,:), UA(1:i,:), resistscw(1:i,:), resistwall(1:i,:),
resistshs(1:i,:), wallthermcond(1:i,:),...
                    ...
                    scwdensity(1:i,:), scwthermcond(1:i,:), scwviscosity(1:i,:), scwenthalpy(1:i,:),
scwreynolds(1:i,:), scwdensitywall(1:i,:),...
                    scwviscositywall(1:i,:), scwenthalpywall(1:i,:), scwcpavg(1:i,:), scwprandtl(1:i,:),
scwnusselt(1:i,:), scwhtc(1:i,:),...
                    ...
                    shsdensity(1:i,:), shsthermcond(1:i,:), shsviscosity(1:i,:), shsenthalpy(1:i,:),
shsreynolds(1:i,:), shsdensitywall(1:i,:),...
                    shsviscositywall(1:i,:), shsenthalpywall(1:i,:), shscpavg(1:i,:), shsprandtl(1:i,:),
shsnusselt(1:i,:), shshtc(1:i,:),...
                    ...
                    pipetenstrin(1:i,:), pipeburstin(1:i,:), pipetenstrout(1:i,:), pipeburstout(1:i,:),...
                    ...
                    scwpressure(1:i,:), shspressure(1:i,:));

        writefilenames  = xlswrite('tempdata.xls',excelnames, 'HXA-HXB Detail','A1');
        writefilevalues = xlswrite('tempdata.xls',excelvalues, 'HXA-HXB Detail','A2');
        end % Part of if statement for SCW/SHS variable printing
        end % Part of if statement for SCW/SHS variable printing
end

%%%%%%%%%%%%%%%%%%%%%%%%%%%%%%%%%%%%%%%%%%%%%%%%%%%%%%%%%%%%%%%%%%%%%%%%%%%%%%%
if(heatexcalc == 2) % Print values for the HX B to Excel Spreadsheet
    printvaluessingle = printresults;
        if(printvaluessingle == 1)

% The following are parameters with single entries (not involved in
% iterative calculations)
        excelnamessingle = { 'Maximum Energy Requirement, kJ', 'Maximum Energy for Recycling, kJ',
'Fraction of Energy Recycled', 'Actual Energy Required, kJ', 'Fraction of Energy Transferred by HX1',
'Energy Transferred by HX1, kJ', 'Number of Tubes Required',...
                    ...
```

```
                    'Inlet HP SHS Pressure, MPa', 'HP SHS Total Flow, kg/s', 'Inner Tube Outer Diameter, m',
'Inner Tube Pipe Thickness, m', 'Inner Tube Inner Diameter, m',...
                    'Inner Tube Flow Area, m2', 'HP SHS Mass Flux, kg/m2s', 'Maximum HP SHS Speed, m/s', 'HP
SHS Tube Mass Flow Rate, kg/s',...
                    ...
                    'Inlet LP SHS Pressure, MPa', 'LP SHS Total Flow, kg/s', 'Outer Tube Outer Diameter, m',
'Outer Tube Pipe Thickness, m', 'Outer Tube Inner Diameter, m',...
                    'Annulus Flow Area, m2', 'LP SHS Mass Flux, kg/m2s', 'Maximum LP SHS Speed, m/s',
'Annulus Wetted Perimeter, m', 'Annulus Hydraulic Diameter, m', 'LP SHS Tube Mass Flow Rate, kg/s',
'Pipegap, m'};

        excelvaluessingle = horzcat(h2maxreq, h2maxrecyc, h2fracrecyc, h2energyreq, frachx1, hx1req,
reqtubes,...
                    ...
                    scwpressure(1,1), scwtubemassflow*reqtubes, scwpipediaout, scwpipethick,scwpipediain,...
                    scwflowarea, scwmassflux, max(scwtubespeed), scwtubemassflow,...
                    ...
                    shspressure(i,1), shsflowtot, shspipediaout, shspipethick, shspipediain,...
                    shsflowarea, shsmassflux, max(shstubespeed), shswetperimeter, shshyddia,
shstubemassflow, pipegap);

        writefilenamessingle = xlswrite('tempdata.xls',excelnamessingle, 'HXA-HXB General','A1');
        writefilevaluessingle= xlswrite('tempdata.xls',excelvaluessingle, 'HXA-HXB General','A2');

    printvalues = printresults;
        if(printvalues == 1)

% The following parameters are involved in the iterative calculation
% process
        excelnames = {'position, m', 'HP SHS Outlet Temperatures, C', 'HP SHS Heat Capacity Rate, W/K', 'HP
SHS Heat Transfer Rate, W', 'HP SHS Total Heat Transfer Rate', ...
                    'LP SHS Inlet Temperatures, C', 'LP SHS Heat Capacity Rate, W/K', 'LP SHS Heat Transfer
Rate, W', 'LP SHS Total Heat Transfer Rate', ...
                    ...
                    'Wall Temperatures, C', 'Overall Heat Transfer Coefficient, W/m2K', 'UA-Value, W/K',
'Thermal Resistance (Inner Wall), K/W', ...
```

```
                    'Thermal Resistance (Wall), K/W', 'Thermal Resistance (Outer Wall), K/W', 'Wall Thermal
Conductivity, W/mK', ...
                    ...
                    'HP SHS Density, kg/m3', 'HP SHS Thermal Conductivity, W/mK', 'HP SHS Viscosity, Pa s',
'HP SHS Enthalpy, J/kg', ...
                    'HP SHS Reynolds Number', 'HP SHS Density (Wall), kg/m3', 'HP SHS Viscosity (Wall), Pa
s', 'HP SHS Enthalpy (Wall), J/kg', ...
                    'HP SHS Average Cp, J/kgK', 'HP SHS Prandtl', 'HP SHS Nusselt Number', 'HP SHS Heat
Transfer Coefficient, W/m2K', ...
                    ...
                    'LP SHS Density, kg/m3', 'LP SHS Thermal Conductivity, W/mK', 'LP SHS Viscosity, Pa s',
'LP SHS Enthalpy, J/kg', ...
                    'LP SHS Reynolds Number', 'LP SHS Density (Wall), kg/m3', 'LP SHS Viscosity (Wall), Pa
s', 'LP SHS Enthalpy (Wall), J/kg', ...
                    'LP SHS Average Cp, J/kgK', 'LP SHS Prandtl', 'LP SHS Nusselt Number', 'LP SHS Heat
Transfer Coefficient, W/m2K',...
                    ...
                    'Inner Pipe Tensile Strength, MPa', 'Inner Pipe Burst Pressure, MPa', 'Outer Pipe
Tensile Strength, MPa', 'Outer Pipe Burst Pressure, MPa',...
                    ...
                    'HP SHS Pressure, MPa', 'LP SHS Pressure MPa'};

        excelvalues = horzcat(position(1:i,:), scwoutlettemp(1:i,:)-273.15, scwmcp(1:i,:), scwmcpdt(1:i,:),
scwheattrans(1:i,:), shsinlettemp(1:i,:)-273.15, shsmcp(1:i,:), shsmcpdt(1:i,:), shsheatrec(1:i,:),...
                    walltemp(1:i,:)-273.15, U(1:i,:), UA(1:i,:), resistscw(1:i,:), resistwall(1:i,:),
resistshs(1:i,:), wallthermcond(1:i,:),...
                    ...
                    scwdensity(1:i,:), scwthermcond(1:i,:), scwviscosity(1:i,:), scwenthalpy(1:i,:),
scwreynolds(1:i,:), scwdensitywall(1:i,:),...
                    scwviscositywall(1:i,:), scwenthalpywall(1:i,:), scwcpavg(1:i,:), scwprandtl(1:i,:),
scwnusselt(1:i,:), scwhtc(1:i,:),...
                    ...
                    shsdensity(1:i,:), shsthermcond(1:i,:), shsviscosity(1:i,:), shsenthalpy(1:i,:),
shsreynolds(1:i,:), shsdensitywall(1:i,:),...
                    shsviscositywall(1:i,:), shsenthalpywall(1:i,:), shscpavg(1:i,:), shsprandtl(1:i,:),
shsnusselt(1:i,:), shshtc(1:i,:),...
                    ...
```

```
                    pipetenstrin(1:i,:), pipeburstin(1:i,:), pipetenstrout(1:i,:), pipeburstout(1:i,:),...
                    ...
                    scwpressure(1:i,:), shspressure(1:i,:));

        writefilenames  = xlswrite('tempdata.xls',excelnames, 'HXA-HXB Detail','A1');
        writefilevalues = xlswrite('tempdata.xls',excelvalues, 'HXA-HXB Detail','A2');
        end % Part of if statement for SCW/SHS variable printing
        end % Part of if statement for SCW/SHS variable printing
end % Part of if statement for printing of HX A parameters
end % Part of if statement for iterative calculations for HX A and HX B

%%%%%%%%%%%%%%%%%%%%%%%%%%%%%%%%%%%%%%%%%%%%%%%%%%%%%%%%%%%%%%%%%%%%%%%%%%%%
%           HX B - Log Mean Temperature Difference Method
%               Verification Calculation Procedure
%%%%%%%%%%%%%%%%%%%%%%%%%%%%%%%%%%%%%%%%%%%%%%%%%%%%%%%%%%%%%%%%%%%%%%%%%%%%

% Note: Although coolant flow on the primary side (SCWR) at this location
% is no longer supercritical (SCW) water, variables on the primary flow side
% still include 'scw' to distinguish between the SHS flows on the HX sides.
% SCW is actually High Pressure SHS.

if (heatexcalc == 3)

rxreheatflow = 780 ; % Steam flow at the reheater outlet

hx2req = h2energyreq;
disp('The energy transferred by via HX2 is: '), disp(hx2req)

% HX Operating and Physical Parameters on HP SHS Side
scwpressure2 = 5700; % kPa, assume no pressure drop

scwtempin2 = 898.15; % K, inlet temperature of HP SHS
scwenthalpyin2 = refpropm('H', 'T', scwtempin2, 'P', scwpressure2, fluid)/1000; % inlet enthapy, kJ/kg
scwtempout2 = 613.15; % K, outlet temperature of HP SHS
scwenthalpyout2 = refpropm('H', 'T', scwtempout2, 'P', scwpressure2, fluid)/1000; % outlet enthapy, kJ/kg
scwflowtot2 = hx2req / (scwenthalpyin2 - scwenthalpyout2);  % kg/s, SCW required flow for HX
```

```
scwpipediaout2 = 0.0267; % m, inner pipe, outer diameter
scwpipethick2 = 0.00391; % m, thickness of inner pipe
scwpipediain2 = scwpipediaout2-2*scwpipethick2; % m, inner pipe, inner diameter
scwflowarea2 = (pi/4)*(scwpipediain2)^2; % m2, flow area of inner pipe
disp('HX B Inner tube dimensions in mm')
disp([scwpipediaout2*1000, scwpipethick2*1000, scwpipediain2*1000])

scwmassflux2 = 400; % kg/m2s, mass flux of HP SHS, lower limit of 200 kg/m2s based on Mokry et al.
correlation

scwtubemassflow2 = scwmassflux2 * scwflowarea2; % kg/s, mass flow rate of HP SHS per pipe
scwtubespeed2 = scwtubemassflow2 / (scwflowarea2*refpropm('D', 'T', scwtempin2, 'P', scwpressure2, fluid));
% m/s, HP SHS velocity HX entry point

reqtubes2 = ceil(scwflowtot2/scwtubemassflow2); % Number of HX pipe units tubes required for the HX based
on HP SHS flowrate requirements

% HX Operating and Physical Parameters on LP SHS Side

shspressure2 = 5000; % kPa, assume no pressure drop
shslowlimit2 = refpropm('T', 'P', shspressure2, 'Q', 1, fluid); % K, Introduce saturation temperature of LP
SHS at operating pressure

shstempin2 = shslowlimit2 + 25; % K, Inlet temperature of SHS into HX, account for a 25 K buffer to
saturation point
shsenthalpyin2 = refpropm('H', 'T', shstempin2, 'P', shspressure2, fluid)/1000; % kJ/kg, Inlet enthalpy

shstempout2 = 873.15; % K, Outlet temperature of SHS
shsenthalpyout2 = refpropm('H', 'T', shstempout2, 'P', shspressure2, fluid)/1000; % kJ/kg, Outlet enthalpy

shsflowtot2 = hx2req / (shsenthalpyout2 - shsenthalpyin2); % kg/s, Required SHS mass flow rate for HX

shspipediaout2 = 0.0334; % m, Outer pipe, outer diameter
shspipethick2 = 0.00165; % m, Thickness of outer pipe
shspipediain2 = shspipediaout2 - 2*shspipethick2; % m, Annulus pipe, inner diameter
```

```
shsflowarea2 = (pi/4)*((shspipediain2)^2 - (scwpipediaout2)^2); % m2, Flow area of inner pipe
shswetperimeter2 = pi*(scwpipediaout2 + shspipediain2); % m, Wetted perimeter for the annulus gap; inner
pipe OD and outer pipe ID
shshyddia2 = (4*(pi/4)*(shspipediain2^2 - scwpipediaout2^2))/ shswetperimeter2; % m, Hydraulic diameter
disp('HX2 Outer tube dimensions in mm'), disp([shspipediaout2*1000, shspipethick2*1000,
shspipediain2*1000])

shstubemassflow2 = 0.1; % kg/s, Mass flow rate of SHS per pipe
shsmassflux2 = shstubemassflow2/shsflowarea2; % kg/m2s, Mass flux of SHS, lower limit of 200 kg/m2s based
on Mokry et al. correlation

shstubespeed2 = shstubemassflow2 / (shsflowarea2*refpropm('D', 'T', shstempout2, 'P', shspressure2,
fluid));  % m/s, SHS speed at arbitrary point at 700 K

pipegap2 = shspipediain2 - scwpipediaout2; % Annulus gap between the pipes

%%%%%%%%%%%%%%%%%%%%%%%%%%%%%%%%%%%%%%%%%%%%%%%%%%%%%%%%%%%%%%%%%%%%%%%%%%%%%%%
% Pipe Material Calculations
% Piping is contructed from Stainless Steel 304
%%%%%%%%%%%%%%%%%%%%%%%%%%%%%%%%%%%%%%%%%%%%%%%%%%%%%%%%%%%%%%%%%%%%%%%%%%%%%%%

avgtemphx2 = (shstempin2 + shstempout2 + scwtempin2 + scwtempout2)/4; % K, average of all inlet/outlet
temperatures
pipetenstr2 = -0.0004*(avgtemphx2-273.15)^2 - 0.2034*(avgtemphx2-273.15) + 605.14; % MPa, Tensile strength
of SS-304 at average temperature
pipemodelas2 = -81.544*(avgtemphx2-273.15) + 198075; % MPa, Modulus of Elasticity of SS-304
pipepoisson2 = 0.28; % based on interpretation of graphical data

pipeburstin2 = (2*pipetenstr2*scwpipethick2)/scwpipediaout2; % MPa, burst pressure for inner pipe
pipecollapsein2 = ((2*pipemodelas2)/(1-pipepoisson2^2))*(scwpipethick2/scwpipediaout2)^3; % MPa, collapse
pressure for inner pipe

pipeburstout2 = (2*pipetenstr2*shspipethick2)/shspipediaout2; % MPa, burst pressure for outer pipe
pipecollapseout2 = ((2*pipemodelas2)/(1-pipepoisson2^2))*(shspipethick2/shspipediaout2)^3; % MPa, collapse
pressure for outer pipe
```

```
%%%%%%%%%%%%%%%%%%%%%%%%%%%%%%%%%%%%%%%%%%%%%%%%%%%%%%%%%%%%%%%%%%%%%%%%%%%%
% HP/LP SHS Thermophysical Parameters
% Bulk Fluid
scwtempavg2   = (scwtempin2 + scwtempout2)/2;
scwdensity2   = refpropm('D', 'T', scwtempavg2,'P', scwpressure2, fluid);
scwthermcond2 = refpropm('L', 'T', scwtempavg2,'P', scwpressure2, fluid);
scwviscosity2 = refpropm('V', 'T', scwtempavg2,'P', scwpressure2, fluid);
scwenthalpy2  = refpropm('H', 'T', scwtempavg2,'P', scwpressure2, fluid);
scwreynolds2  = (4*scwtubemassflow2)/(pi*scwpipediain2*scwviscosity2);

shstempavg2   = (shstempin2 + shstempout2)/2;
shsdensity2   = refpropm('D', 'T', shstempavg2,'P', shspressure2, fluid);
shsthermcond2 = refpropm('L', 'T', shstempavg2,'P', shspressure2, fluid);
shsviscosity2 = refpropm('V', 'T', shstempavg2,'P', shspressure2, fluid);
shsenthalpy2  = refpropm('H', 'T', shstempavg2,'P', shspressure2, fluid);
shsreynolds2  = (4*shstubemassflow2)/(pi*(shspipediain2 + scwpipediaout2)*shsviscosity2);

% Calculate logarithmic temperature difference for a counterflow HX design
deltaT1 = scwtempin2 - shstempout2;
deltaT2 = scwtempout2 - shstempin2;
tlog = (deltaT1 - deltaT2)/log(deltaT1/deltaT2);

%%%%%%%%%%%%%%%%%%%%%%%%%%%%%%%%%%%%%%%%%%%%%%%%%%%%%%%%%%%%%%%%%%%%%%%%%%%%
% Iterative calculation to find the HX wall temperature. See process for HX
% A for procedure used.
%%%%%%%%%%%%%%%%%%%%%%%%%%%%%%%%%%%%%%%%%%%%%%%%%%%%%%%%%%%%%%%%%%%%%%%%%%%%

    diffwalltemp2 = 1;
    walltempguess = scwtempavg2-0.08;
    walltemp2 = walltempguess;
    counterwall2 = 1;
    criteria3 = 0.001;

        while (abs(diffwalltemp2) > criteria3)
```

```
% SCW Wall Fluid Rough Calculations
        scwdensitywall2 = refpropm('D', 'T', walltemp2,'P', scwpressure2, fluid);
        scwviscositywall2 = refpropm('V', 'T', walltemp2,'P', scwpressure2, fluid);
        scwenthalpywall2 = refpropm('H', 'T', walltemp2,'P', scwpressure2, fluid);

        % SCW Overall Fluid Rough Calculations
        scwcpavg2 = (scwenthalpywall2 - scwenthalpy2) / (walltemp2 - scwtempavg2);
        scwprandtl2 = (scwcpavg2*scwviscosity2)/scwthermcond2;
        scwnusselt2 =
0.0061*((scwreynolds2)^(0.904))*((scwprandtl2)^0.684)*((scwdensitywall2/scwdensity2)^0.564); % Nusselt
Number based on Mokry et al. correlation
        scwhtc2 = (scwnusselt2*scwthermcond2)/(scwpipediain2);

        % SHS Wall Fluid Rough Calculations
        shsdensitywall2 = refpropm('D', 'T', walltemp2,'P', shspressure2, fluid);
        shsviscositywall2 = refpropm('V', 'T', walltemp2,'P', shspressure2, fluid);
        shsenthalpywall2 = refpropm('H', 'T', walltemp2,'P', shspressure2, fluid);

        % SHS Overall Fluid Rough Calculations
        shscpavg2 = (shsenthalpywall2 - shsenthalpy2) / (walltemp2 - shstempavg2);
        shsprandtl2 = (shscpavg2*shsviscosity2)/shsthermcond2;
        shsnusselt2 =
0.0061*((shsreynolds2)^(0.904))*((shsprandtl2)^0.684)*((shsdensitywall2/shsdensity2)^0.564); % Nusselt
Number based on Mokry et al. correlation
        shshtc2 = (shsnusselt2*shsthermcond2)/(shshyddia2);

        % HTC Properties Rough Calculations
        wallthermcond2 = 0.00000002*(walltemp2)^3 - 0.00004*(walltemp2)^2 + 0.0398*(walltemp2)+ 5.728; %
using equation from curve fit for known values
        resistscw2 = scwpipediaout2/(scwpipediain2*scwhtc2); % K m2/ W, thermal resistance at inner surface
        resistwall2 = (scwpipediaout2*log(scwpipediaout2/scwpipediain2))/(2*wallthermcond2); % K m2/ W, %
thermal resistance across wall
        resistshs2 = 1/shshtc2; % K m2/ W, % thermal resistance at outer surface

        interwalltemp2 = walltemp2;
```

```
        walltemp2 = ((scwtempavg2/resistscw2) + (shstempavg2/resistshs2))/(1/resistscw2 + 1/resistshs2); %
K, Calculation of wall temperature

        diffwalltemp2 = interwalltemp2 - walltemp2; % Calculate difference in assumed and calculated wall
temperatures

% The following "if statements" are used obtain a converging wall temperature

              if (diffwalltemp2 == criteria3 || diffwalltemp2 > criteria3)
              walltemp2 = walltemp2 - diffwalltemp2/2;
              counterwall2 = counterwall2 + 1;
              end

              if (diffwalltemp2 < -criteria3)
              walltemp2 = walltemp2 + diffwalltemp2/2;
              counterwall2 = counterwall2 + 1;
              end

            if(counterwall2 == 1000)  % If the number of iterations reaches defined maximum, stop iteration
process
                disp('Error - Iteration Maximum (1000) reached')
                break
            end

        end

        U2 = 1/(resistscw2 + resistshs2 + resistwall2); % Overall HTC
        As2= (hx2req*1000/reqtubes2)/(U2*tlog); % Required HX heat transfer surface area
        L2 = As2/(pi*scwpipediaout2); % Required length for an individual pipe

disp('The Heat Transfer Surface Area (m2) per tube would be: '), disp(As2)
disp('The length of each tube (m) within the HX would be: '), disp(L2)
disp('The total HP SHS/LP SHS flow (kg/s) would be: '), disp(scwflowtot2), disp(shsflowtot2)
disp('The number of tubes required would be: '), disp(reqtubes2)
disp('The maximum HP SHS speed (m/s) would be: '), disp(scwtubespeed2)
disp('The maximum LP SHS speed (m/s) would be: '), disp(shstubespeed2)
```

```
%%%%%%%%%%%%%%%%%%%%%%%%%%%%%%%%%%%%%%%%%%%%%%%%%%%%%%%%%%%%%%%%%%%%%%%%%%%%%%%
% Printing of values into EXCEL
%%%%%%%%%%%%%%%%%%%%%%%%%%%%%%%%%%%%%%%%%%%%%%%%%%%%%%%%%%%%%%%%%%%%%%%%%%%%%%%

printvalues2 = printresults;
if(printvalues2 == 1)

% The following are parameters with single entries (not involved in
% iterative calculations)
excelvaluessingle2 = horzcat(rxreheatflow, h2maxreq, h2maxrecyc, h2fracrecyc, h2energyreq, hx2req,
reqtubes2,...
                    ...
                    scwpressure2, scwtempin2-273.15, scwenthalpyin2, scwtempout2-273.15, scwenthalpyout2,
scwflowtot2, scwpipediaout2, scwpipethick2, scwpipediain2,...
                    scwflowarea2, scwmassflux2, scwtubespeed2, scwtubemassflow2,...
                    ...
                    shspressure2, shstempin2-273.15, shsenthalpyin2, shstempout2-273.15, shsenthalpyout2,
shsflowtot2, shspipediaout2, shspipethick2, shspipediain2,...
                    shsflowarea2, shsmassflux2, shstubespeed2, shswetperimeter2, shshyddia2,
shstubemassflow2, pipegap2,...
                    ...
                    avgtemphx2, pipetenstr2, pipeburstin2, pipeburstout2);
%
excelnamessingle2 = { 'Reactor Primary Side SHS Flow, kg/s', 'Maximum Energy Requirement, kJ', 'Maximum
Energy for Recycling, kJ', 'Fraction of Energy Recycled', 'Actual Energy Required, kJ', 'Energy Transferred
by HX2, kJ', 'Number of Tubes Required',...
                    ...
                    'HP SHS Pressure, MPa', 'HP SHS Inlet Temperature, C', 'HP SHS Inlet Enthalpy, kJ/kg',
'HP SHS Outlet Temperature, C', 'HP SHS Outlet Enthalpy, kJ/kg', 'HP SHS Total Flow, kg/s', 'Inner Tube
Outer Diameter, m', 'Inner Tube Pipe Thickness, m', 'Inner Tube Inner Diameter, m',...
                    'Inner Tube Flow Area, m2', 'HP SHS Mass Flux, kg/m2s', 'Average HP SHS Speed, m/s', 'HP
SHS Tube Mass Flow Rate, kg/s',...
                    ...
                    'LP SHS Pressure, MPa', 'LP SHS Inlet Temperature, C', 'LP SHS Inlet Enthalpy, kJ/kg',
'LP SHS Outlet Temperature, C', 'LP SHS Outlet Enthalpy, kJ/kg', 'LP SHS Total Flow, kg/s', 'Outer Tube
Outer Diameter, m', 'Outer Tube Pipe Thickness, m', 'Outer Tube Inner Diameter, m',...
```

```
                    'Annulus Flow Area, m2', 'LP SHS Mass Flux, kg/m2s', 'LP SHS Speed, m/s', 'Annulus
Wetted Perimeter, m', 'Annulus Hydraulic Diameter, m', 'LP SHS Mass Flow Rate, kg/s', 'Pipegap, m',...
                    ...
                    'Average HX Temperature, K', 'Pipe Tensile Strength, MPa', 'Inner Pipe Burst Pressure,
MPa', 'Outer Pipe Burst Pressure, MPa'};

% Select following parameters were involved in the iterative calculation
% process
excelvaluessingle22 = horzcat(deltaT1, deltaT2, tlog, walltemp2-273.15, U2, As2, L2, wallthermcond2,
resistscw2, resistwall2, resistshs2,...
                              ...
                              scwtempavg2-273.15, scwdensity2, scwthermcond2, scwviscosity2, scwenthalpy2,
scwreynolds2,...
                              scwdensitywall2, scwviscositywall2, scwenthalpywall2, scwcpavg2, scwprandtl2,
scwnusselt2, scwhtc2,...
                              ...
                              shstempavg2-273.15, shsdensity2, shsthermcond2, shsviscosity2, shsenthalpy2,
shsreynolds2,...
                              shsdensitywall2, shsviscositywall2, shsenthalpywall2, shscpavg2, shsprandtl2,
shsnusselt2, shshtc2);

excelnamessingle22 = { 'Delta T1', 'Delta T2', 'TLog', 'Avg. Wall Temperature, C', 'Avg. Overall HTC,
W/m2K', 'Heat Transfer Area, m2', 'Tube Length, m', 'Wall Thermal Conductivity, W/mK', 'Thermal Resistance
- HP SHS, K/W', 'Thermal Resistance - Wall, K/W', 'Thermal Resistance - LP SHS, K/W'...
                         ...
                         'HP SHS Avg. Temperature, C', 'HP SHS Density, kg/m3', 'HP SHS Thermal
Conductivity, W/mK', 'HP SHS Viscosity, Pa s', 'HP SHS Enthalpy, J/kg', 'HP SHS Reynolds Number',...
                         'HP SHS Density (Wall), kg/m3', 'HP SHS Viscosity (Wall), Pa s', 'HP SHS Enthalpy
(Wall), J/kg', 'HP SHS Average Cp, J/kgK', 'HP SHS Prandtl', 'HP SHS Nusselt Number', 'HP SHS Heat Transfer
Coefficient, W/m2K',...
                         ...
                         'LP SHS Avg. Temperature, C', 'LP SHS Density, kg/m3', 'LP SHS Thermal
Conductivity, W/mK', 'LP SHS Viscosity, Pa s', 'LP SHS Enthalpy, J/kg', 'LP SHS Reynolds Number',...
                         'LP SHS Density (Wall), kg/m3', 'LP SHS Viscosity (Wall), Pa s', 'LP SHS Enthalpy
(Wall), J/kg', 'LP SHS Average Cp, J/kgK', 'LP SHS Prandtl', 'LP SHS Nusselt Number', 'LP SHS Heat Transfer
Coefficient, W/m2K'};
```

```
writefilenamessingle2  = xlswrite('tempdata.xls',excelnamessingle2, 'HXB-LogMean','A1');
writefilevaluessingle2 = xlswrite('tempdata.xls',excelvaluessingle2, 'HXB-LogMean','A2');
writefilenamessingle22 = xlswrite('tempdata.xls',excelnamessingle22, 'HXB-LogMean','A4');
writefilevaluessingle22= xlswrite('tempdata.xls',excelvaluessingle22, 'HXB-LogMean','A5');

end
end % Applies to "if statement" for HX B LMTD analysis selection
```

APPENDIX E – PUBLICATIONS

In total, 6 papers have been prepared for participation in international conferences.

Lukomski, **A**., Gabriel, K., Pioro, I. and Naterer, G., 2011. Use of a Supercritical Water Cooled Reactor for Process Heat to Support Thermochemical Hydrogen Production, Proceedings of the 14th International Topical Meeting on Nuclear Reactor Thermalhydraulics (NURETH-14), Toronto, Ontario, Sept. 25-30, 2011. 12 Pages.

Mokry, S., **Lukomski**, **A**., Gabriel, K., Pioro, I., Naterer, G., 2011. Thermalhydraulic and heat transfer correlations for an intermediate heat exchanger linking a supercritical water-cooled reactor and a copper-chlorine cycle of hydrogen production, Proceedings of the 2nd International Conference on Hydrogen Production, Thessaloniki, Greece, June 19-22, 2011. 17 Pages.

Lukomski, **A**., Gabriel, K., Pioro, I. and Naterer, G., 2011. Intermediate Double-Pipe Heat Exchanger for Thermochemical Hydrogen Co-Generation with SCW NPP, Proceedings of the 19th International Conference on Nuclear Engineering, Makuhari, Chiba, Japan. Paper No. 43640. 9 Pages.

Lukomski, **A**., Pioro, I. and Gabriel, K., 2011. Hydrogen Production Using Process Heat from a Supercritical Water-cooled Nuclear Power Plant via a Double-pipe Heat Exchanger, Proceedings of the 5th International Symposium on SCWRs, Vancouver, British Columbia, Canada, March 13-16, 2011. Paper #71. 12 Pages.

Lukomski, **A**., Pioro, I. and Gabriel, K., 2010. Aspects of Hydrogen Production Using a Supercritical Water-Cooled Nuclear Reactor, Proceedings of the 34th Student Conference of the Canadian Nuclear Sciety and Canadian Nuclear Association, Montreal Quebec, Canada, May 24-27, 2010. 10 Pages.

Lukomski, **A**., Pioro, I. and Gabriel, K., 2010. Aspects of Hydrogen Co-Generation Using a Thermochemical Cycle Linked to a Supercritical Water-Cooled Nuclear Reactor, Proceedings of the 5th Canada-China Joint Workshop on Supercritical Water-Cooled Nuclear Reactors, Toronto, Ontario, Canada, April 25-28, 2010. 12 Pages.

APPENDIX F – CONFERENCES

In addition to conference paper preparation, three conferences have been attended and attendance is planned at a fourth:

19th International Conference on Nuclear Engineering, October 24-25, 2011. Osaka, Japan: ASME/JSME.

14th International Topical Meeting on Nuclear Reactor Thermalhydraulics, Sept. 25-30, 2011. Toronto, Canada: CNS.

34th CNS/CNA Student Conference, May 24-27th, 2010. Montreal, Canada: CNS.

2nd Canada-China Joint Workshop on SuperCritical Water-cooled Reactors (CCSC 2010). Toronto, Canada: CNS.